



Cardiac functions of the cellular oxygen sensors prolyl-4-hydroxylase domain enzymes 2 and 3

Kumulative Dissertation

zur Erlangung des mathematisch-naturwissenschaftlichen Doktorgrades

“Doctor rerum naturalium”

der Georg-August-Universität zu Göttingen

vorgelegt von

Marion Hölscher

aus Paderborn

Göttingen 2012

Mitglieder des Betreuungsausschusses:

Referentin: Prof. Dr. S. Pöggeler

Koreferentin: Prof. Dr. F. Alves

Koreferentin: Prof. Dr. D. M. Katschinski

Tag der mündlichen Prüfung: 06.06.2012

Statutory Declaration

I declare that I have authored this thesis independently, that I have not used other than the declared sources / resources, and that I have explicitly marked all material which has been quoted either literally or by content from the used sources.

Marion Hölscher

Contents

Abbreviations	1
List of publications	2
1. Summary	3
2. Introduction	5
2.1 Hypoxia.....	5
2.2 Hypoxia-Inducible Factor.....	6
2.3 Prolyl-4-hydroxylase domain enzymes.....	9
2.4 Mouse models.....	11
2.4.1 PHD knock-out mice.....	11
2.4.2 HIF transgenic mice.....	11
2.5 Cardiovascular diseases.....	13
2.5.1 Cardiomyopathies.....	13
2.5.2 Mechanical load: preload versus afterload.....	13
2.5.2 Myocardial infarction.....	14
3. Original publications	15
3.1 Cardiomyocyte-specific Prolyl-4-hydroxylase Domain 2 Knock Out Protects from Acute Myocardial Ischemic Injury.....	16
3.2 Unfavourable consequences of chronic cardiac HIF-1 α stabilization.....	28
4. Unpublished Data	47
4.1 Detrimental consequences of a cardiomyocyte-specific knock-out of PHD2.....	47
4.2 Cardiac-specific double knock-out of PHD2 and PHD3 leads to dilated cardiomyopathy and a premature death.....	50
5. Discussion	60
5.1 Beneficial effects of PHD2 knock-out, respectively HIF-1 α stabilization.....	61
5.2 Detrimental effects of PHD2 knock-out, respectively HIF-1 α stabilization.....	62
5.3 Cardiomyocyte-specific PHD2/PHD3 double knock-out mice.....	64
5.4 PHD inhibitors as a therapeutic approach in acute myocardial infarction.....	65
5.5 Summary and outlook.....	67
6. References	70
Acknowledgements	77
Curriculum vitae	78

Abbreviations

2-OG	2-oxoglutarate
α MHC	α -myosin heavy chain
AAR	area at risk
AMPK	5'-adenosine monophosphate-activated protein kinase
AON	area of necrosis
ARNT	aryl hydrocarbon nuclear translocator
bHLH	basic helix-loop-helix
Ca^{2+}	calcium
CA IX	carbonic anhydrase 9
CSQ	calsequestrin
C-TAD	C-terminal transactivation domain
DCM	dilated cardiomyopathy
DMOG	dimethylloxaloylglycine
E	embryonic day
<i>e.g.</i>	<i>exempli gratia</i> (for example)
EGLN	egg-laying deficiency protein nine-like protein
Fig	figure
FIH-1	factor inhibiting HIF-1
FAS	fractional area shortening
FDG	fluorodesoxyglucose
Fe^{2+}	iron
FS	fractional shortening
FTHA	fluoro-6-thia-heptadecanoic acid
Glut1	glucose transporter 1
H9c2	rat heart cell-line
HCM	hypertrophic cardiomyopathy
HIF	hypoxia-inducible factor
HRE	hypoxia responsive element
ICM	ischemic cardiomyopathy
<i>i.e.</i>	<i>id est</i> (that is)
LAD	left anterior descending artery
LVEDD	left ventricular end-diastolic diameter
LVESD	left ventricular end-systolic diameter
MI	myocardial infarction
O_2	oxygen
ODDD	oxygen-dependent degradation domain
PAS	PER-ARNT-SIM
PET	positron emission tomography
Pfkl	phosphofructokinase I
PHD	prolyl -4-hydroxylase domain enzyme
PLB	phospholamban
RyR2	type-2 ryanodine receptor
SEM	standard error of the mean
SERCA	sarcoplasmic/endoplasmic reticulum calcium ATPase
SUV	standard uptake volume
TAC	transverse aortic constriction
TTC	triphenyltetrazolium chloride
pVHL	von Hippel-Lindau protein
qRT-PCR	quantitative real-time polymerase chain reaction
wt	wild-type

List of Publications

Marion Hölscher, Monique Silter, Sabine Krull, Melanie von Ahlen, Amke Hesse, Peter Schwartz, Ben Wielockx, Georg Breier, Dörthe M. Katschinski, Anke Zieseniss (2011)

Cardiomyocyte-specific Prolyl-4-hydroxylase Domain 2 Knock Out Protects from Acute Myocardial Ischaemic Injury

J Biol Chem 286:11185-11194

Marion Hölscher, Katrin Schäfer, Sabine Krull, Katja Farhat, Amke Hesse, Monique Silter, Yun Lin, Bernd Pichler, Patricia Thistlethwaite, Ali El-Armouche, Lars S. Maier, Dörthe M. Katschinski, Anke Zieseniss (2012)

Unfavourable consequences of chronic cardiac HIF-1 α stabilization

Cardiovasc Res. 94:77-86

1. Summary

1. Summary

Cardiovascular diseases are the major cause of death in the western world and produce furthermore the highest medical costs among all diseases. About 41% of all deaths in Germany in the year 2010 can be attributed to cardiovascular diseases ("Statistisches Bundesamt Deutschland", press release no. 354, 23.09.2011). About 17% of these deaths were caused by myocardial infarction (men: 56%, women: 44%). Cardiac tissue protection in case of acute ischemia could therefore result in better short and long term survival of these patients.

In 2003 it was described for the first time that the Hypoxia-inducible factor (HIF), a heterodimeric transcription factor, which is stabilized under hypoxic conditions, *e.g.* in myocardial infarction, can mediate cardioprotection (Cai *et al.*, 2003). It was shown that the cardioprotective effect of intermittent hypoxia, which is defined as repeated episodes of hypoxia interspersed with episodes of normoxia, is dependent on the HIF-1 α gene dosage. This was shown by a better ventricular contractile function and a significantly smaller infarct size following ischemia-reperfusion in mice pretreated with intermittent hypoxia. This preconditioning effect was lost in HIF-1 α ^{+/-} mice. Since then a lot of subsequent papers have been published that demonstrate the crucial role for HIF-1 in various modalities of cardioprotection (*e.g.* Kido *et al.*, 2005; Date *et al.* 2005). With the discovery of the HIF regulating proly-4 hydroxylase domain (PHD) enzymes 1-3 potential therapeutic targets to modulate HIF-1 α stability and thus possibilities to improve ischemic diseases have been discovered. Despite these findings a lot of open questions remain that will be addressed in my PhD thesis.

- Are there any effects of long-term stabilization of HIF-1 α in the heart?
- Are there any PHD-dependent but HIF-independent effects that need to be considered if PHD inhibiting drugs are being developed in order to stabilize HIF-1 α ?
- Is HIF-1 α stabilization also beneficial after elevated mechanical load?
- Are there isoform specific functions of the three PHDs that need to be taken into account when designing PHD inhibitors?
- Which cell parameters like calcium handling or metabolism are modulated by HIF-1 α stabilization that could be beneficial or detrimental for the heart?

1. Summary

To answer some of the above mentioned questions I have analyzed several genetically modified mouse strains during my thesis:

- cardiomyocyte-specific PHD2 knock-out mice (*cPhd2^{-/-}*)
- cardiac-specific transgenic HIF-1 α mice (*Hif-1 α ^{tg}*)
- cardiomyocyte-specific PHD2/PHD3 double knock-out mice (*cPhd2/3^{-/-}*)

In summary, I was able to generate cardiomyocyte-specific PHD2 knock-out mice (*cPhd2^{-/-}*) with subsequent mild stabilization of HIF-1 α . These mice are protected from acute myocardial infarction as shown by a smaller area at risk (AAR) and a smaller area of necrosis (AON) six hours after ligation of the *left anterior descending artery* (LAD). Three weeks after the ligation these mice show a better preserved heart function compared to *wt* littermates. This phenomenon is at least in part due to an increased capillary area in the hearts of *cPhd2^{-/-}* mice. When challenged by elevated mechanical load by performing *transverse aortic constriction* (TAC) surgery these mice show a comparable degree of hypertrophy with a similar decline in heart function. Aging *cPhd2^{-/-}* mice develop a mild hypertrophy which does not occur in *wt* mice.

Furthermore I could show in a cardiac-specific HIF-1 α transgenic mouse model (*Hif-1 α ^{tg}*) that the constitutive expression of HIF-1 α leads to changes in capillary area and shifts the cardiac metabolism towards glycolysis. Furthermore, calcium- (Ca^{2+}) handling of the cells is altered, which leads to increased Ca^{2+} transients and a faster intracellular Ca^{2+} decline. After TAC surgery *Hif-1 α ^{tg}* mice show a strong cardiac decompensation. Moreover, cardiomyopathy was also seen in aging *Hif-1 α ^{tg}* mice.

Preliminary data of cardiomyocyte-specific PHD2/PHD3 double knock-out mice (*cPhd2/3^{-/-}*) illustrate detrimental effects with severe dilated cardiomyopathy that lead to a premature death at the age of 4.5 to 6 months.

Summing up, I could show that a short-term stabilization of HIF-1 α seems to have beneficial effects on the heart whereas long-term stabilization seems to be detrimental.

2. Introduction

2. Introduction

2.1 Hypoxia

The maintenance of cellular oxygen homeostasis is critical to all aerobic organisms in order to *e.g.* produce energy for cell survival, motility or reproduction. In case of reduced oxygen availability hypoxia develops. Hypoxia is a condition in which the whole body (generalized hypoxia) or parts of the body (tissue hypoxia) are deprived of an adequate oxygen supply. This is due to an imbalance of oxygen availability and oxygen consumption. Anoxia is defined by a complete lack of oxygen. Hypoxia occurs physiologically during embryonic development (3-5% O₂) when hypoxia is required for vascular growth, which is in turn important for successful development (Asikainen and White, 2007), or when ascending to higher altitudes (Hackett and Roach, 2001). This can cause high-altitude sickness leading to life-threatening conditions (Paralihar and Paralihar, 2010).

Tissue hypoxia occurs when there is a local restriction of the blood flow to otherwise well-oxygenated tissues. The reduced oxygen supply is then insufficient to satisfy the tissue's oxygen demand. This pathophysiological hypoxia occurs for example in ischemic diseases or in solid tumors.

The master regulator of the cellular hypoxia response pathway is the transcription factor hypoxia-inducible factor (HIF). HIF was discovered by the identification of a hypoxia response element (HRE) (5'-RCGTG-3') in the enhancer of the erythropoietin gene (Goldberg *et al.*, 1988; Semenza, 1998), a glycoprotein hormone that controls erythropoiesis. In following studies HIF was identified as a heterodimeric transcription factor consisting of an oxygen-sensitive α -subunit and a constitutively expressed β -subunit, which was beforehand identified as the aryl hydrocarbon nuclear translocator (ARNT), a binding partner of the aryl hydrocarbon receptor (Reyes *et al.*, 1992).

Among the critical physiological processes regulated by HIF-1 are erythropoiesis, angiogenesis, and glycolysis, which are examples of systemic, local tissue, and intracellular adaptive responses to hypoxia. So far, more than 200 genes were identified to be HIF-dependently regulated (Benita *et al.*, 2009; Ortiz-Barahona *et al.*, 2010), but it is assumed that in total about 2% of the human genome is hypoxia-inducible.

2. Introduction

2.2 Hypoxia-inducible factor

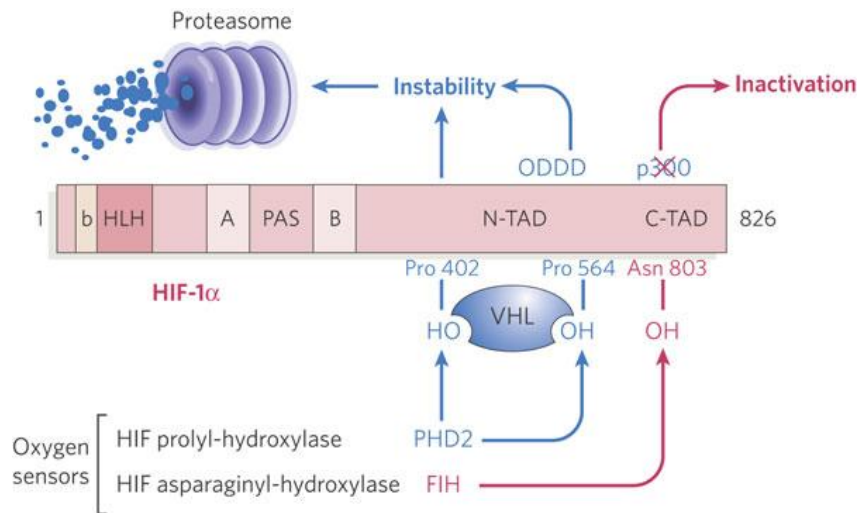
HIFs are heterodimeric transcription factors consisting of one out of three oxygen-sensitive α -subunits (HIF-1 α , HIF-2 α or HIF-3 α) and the common oxygen-insensitive HIF- β subunit. Both subunits belong to the PER-ARNT-SIM (PAS) subfamily of the basic helix-loop-helix (bHLH) family of transcription factors. The N-terminal domain contains the bHLH and the PAS domains which facilitate the dimerization of the HIF- α and the HIF- β subunit and allows the binding to hypoxia responsive elements (HREs) of HIF target genes (Erbel *et al.*, 2003).

The N- and the C-terminal oxygen-dependent degradation domains (ODDD) are located within the N-terminal transactivation domain. The O₂⁻, Fe²⁺⁻, 2-oxoglutarate- (2-OG) and ascorbate-dependent proly-4-hydroxylase domain (PHD) proteins, PHD1, PHD2 and PHD3, can hydroxylate two proline residues (Pro⁴⁰² and Pro⁵⁶⁴) within this domain and thereby influence the stability of HIF- α . The hydroxylation initiates the binding of an E3 ubiquitin ligase, the von Hippel-Lindau (pVHL) protein. pVHL is a component of a protein-ubiquitin ligase complex that targets the α -subunit for rapid degradation by the proteasome (Maxwell *et al.*, 1999).

Besides the HIF- α stability also the HIF- α activity is determined by hydroxylation. In 2001 the factor inhibiting HIF (FIH-1) was first described (Mahon *et al.*, 2001). It can hydroxylate an asparagine residue (Asn⁸⁰³) in the C-terminal transactivation domain (C-TAD) of HIF-1 α . Through this hydroxylation the binding of necessary co-factors, such as p300, is blocked and so the transcriptional activation of HIF-1 is restricted (Lando *et al.*, 2002).

In figure 1 a schematic drawing of HIF-1 α and the oxygen-dependent regulation of HIF-1 α protein stabilization and activation are shown.

2. Introduction

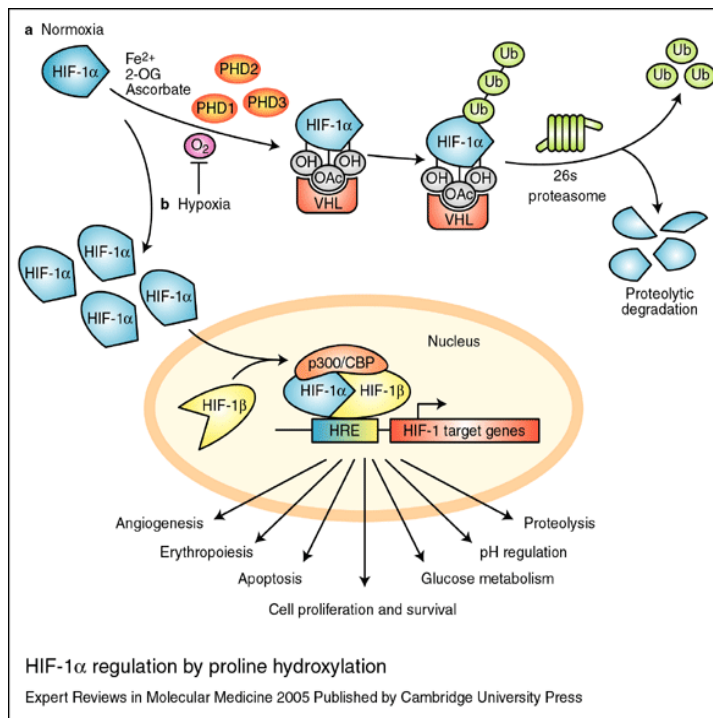


Taken from Pouyssegur *et al.* (2006)

Fig.1 Schematic drawing of HIF-1 α and the oxygen-dependent regulation of HIF-1 α protein stabilization and activation. The basic helix-loop-helix (bHLH) domain, involved in DNA-binding, and the Per-Arnt-Sim (PAS) A and B domains, which are responsible for heterodimerization with HIF-1 β , are located in the N-terminal region of HIF-1 α . The proline residues Pro⁴⁰² and Pro⁵⁶⁴ that are hydroxylated by the PHD enzymes are located in the oxygen-dependent degradation domain (ODDD). The factor inhibiting HIF (FIH) can hydroxylate an asparagine residue (Asn⁸⁰³) in the C-terminal transcriptional activation domain (C-TAD) of HIF-1 α and inhibits thereby the binding of cofactors, such as p300, that are required for the transcription of HIF-dependent genes. The N-TAD, a second transcriptional activation domain, overlapping with the ODDD, is FIH-independent and may be involved in distinct gene expression.

In normoxia the transcriptionally inactive HIF-1 α subunit is quickly degraded with a half-life of less than five minutes. In hypoxia on the contrary, the oxygen dependent PHDs and FIH are enzymatically inactive and hence cannot hydroxylate the proline and the asparagine residues of the HIF-1 α subunit. Thereupon, the non-degraded, stabilized HIF-1 α accumulates into the nucleus where it dimerizes with the constitutively expressed HIF-1 β subunit. Subsequently HIF-1 binds to HREs of HIF target genes, *e.g.* Glut1 or VEGF, which are then transcriptionally activated (see fig. 2).

2. Introduction



Taken from Carroll *et al.* (2005)

Fig.2 HIF-1 α in hypoxia and normoxia. Under normoxic conditions HIF-1 α is hydroxylated by the PHDs. This hydroxylation triggers its association with the pVHL E3 ligase complex which leads to rapid proteasomal degradation of HIF-1 α . In hypoxia the oxygen-dependent PHDs cannot hydroxylate the HIF-1 α subunit. HIF-1 α is consequently stabilized and translocates into the nucleus where it dimerizes with HIF-1 β . After binding to p300/CBP the transcription of HIF-target genes, like Glut1 or VEGF, is induced.

HIF-1 has been detected in all metazoan species that have been analyzed from *Trichoplax adhaerens* (Loernaz *et al.*, 2011) to *Homo sapiens*, suggesting that the appearance of HIF-1 represented an adaptation that was essential to metazoan evolution.

After the discovery of HIF-1 α two additional HIF- α isoforms were identified - HIF-2 α and HIF-3 α (Ema *et al.*, 1997; Flamme *et al.*, 1997). Both HIF-2 α and HIF-3 α display close sequence similarity to HIF-1 α in the N-terminal part of the 22 polypeptide containing the bHLH and PAS domains, but HIF-3 α lacks the C-TAD (Ema *et al.*, 1997; Flamme *et al.*, 1997; Gu *et al.*, 1998; Hogenesch *et al.*, 1997; Tian *et al.*, 1997.)

HIF-1 α and HIF-2 α have a number of structural and biochemical similarities and both bind to HREs. But in contrast to the ubiquitously expressed HIF-1 α , HIF-2 α is mainly expressed in the lung, endothelium and carotid body (Ema *et al.*, 1997; Tian *et al.*, 1998). Furthermore there is evidence that HIF-1 α preferentially activates genes that are important for glycolysis, while HIF-2 α appears to favor the activation of genes involved in angiogenesis (Hu *et al.*, 2003). The importance of HIF-1 α and HIF-2 α can be demonstrated by the fact that knock-out of HIF-

2. Introduction

1 α as well as HIF-2 α leads to embryonic lethality in mice (Compernelle *et al.*, 2002; Iver *et al.*, 1998).

Although less is known about HIF-3 α , it could be shown that HIF-3 α can also dimerize with HIF-1 β and bind to HREs thereby preventing the binding of HIF-1 and HIF-2. There are splice variants of HIF-3 α without transactivation domains. These variants instead bind to HIF-1 α and prevent its DNA-binding. So in general HIF-3 α acts as a negative regulator of HIF-1 α and HIF-2 α (Hara *et al.*, 2001).

2.3 Prolyl-4-hydroxylase domain enzymes

The prolyl-4-hydroxylase domain enzymes (PHDs) have been first described in 2001-2002 as a subfamily of 2-oxoglutarate-dependent dioxygenases that are responsible for the hydroxylation of HIF-1 α (Bruick *et al.*, 2001; Epstein *et al.*, 2002). In lower animals, like nematodes, only a single PHD isoform exists whereas in higher animals, like in mammals, three PHDs (PHD1, PHD2 and PHD3) have been discovered. Another isoform, prolyl-4-hydroxylase transmembrane (P4H-TM) was detected but so far the function of this transmembrane protein remains unclear (Oehme *et al.*, 2002; Koivunen *et al.*, 2007).

The PHD enzymes are given several names: prolyl-4-hydroxylase domain enzymes (PHD1, PHD2 and PHD3), HIF-prolyl hydroxylases (HIF-P4H-3, HIF-P4H-2 and HIF-P4H-1) and EGLNs (EGLN-2, EGLN-1 and EGLN-3, respectively). The EGLN terminology refers to the relationship of these proteins to the protein egg-laying-deficient 9 of the nematode worm *Caenorhabditis elegans* and the term prolyl-hydroxylase domain (PHD) reflects the functionality as hydroxylases but avoids it to consider the PHDs to be HIF-specific as HIF-independent functions of the PHDs have been described (Cummins *et al.*, 2006).

The ability of the PHDs to function as oxygen sensors can be revealed by their K_m values (230- 250 μM) which are slightly above the atmospheric partial oxygen pressure at sea level (Hirsilä *et al.*, 2003). Therefore even small changes in atmospheric oxygen concentration affect the enzymatic function of the PHDs and consequently the transcriptional activity of HIF is induced.

As mentioned before, PHDs hydroxylate two proline residues in HIF's Leu-Xaa-Xaa-Leu-Ala-Pro motif. It was shown that the hydroxylation activity of PHD2 and PHD3 is similar whereas that of PHD1 is lower (Tuckerman *et al.*, 2004). In this hydroxylation reaction one oxygen atom of the molecular oxygen is added to a peptidyl proline to form hydroxyproline and the

2. Introduction

other oxygen atom is used in a coupled decarboxylation reaction that converts 2-oxoglutarate to succinate; thus, PHDs require 2-oxoglutarate as a co-substrate (McDonough *et al.*, 2006).

PHD2 is clearly the most abundant of the three mammalian isoenzymes and it is also responsible for setting the normoxic steady-state levels of HIF- α (Appelhoff *et al.*, 2004; Berra *et al.*, 2003). Furthermore, PHD2 knock-out mice die between embryonic day (E) 12.5 and 14.5, whereas PHD1 and PHD3 knock-out mice are viable.

The *phd2* and *phd3* genes contain HREs which makes these two isoforms inducible by HIF-1 under hypoxia (Metzen *et al.*, 2005; Pescador *et al.*, 2005). This is to guarantee a quick degradation of HIF-1 α after reoxygenation.

Although the PHDs have many features in common, they show some differences in their expression pattern, catalytic properties and physiological role. In table 1 alternative names, the tissue distribution, intracellular localization, substrate preference, hypoxia inducibility, chromosome localization, protein size and the K_m values are listed.

Table 1 Overview of some features of PHD1, PHD2 and PHD3

	PHD1	PHD2	PHD3
alternative names	EGLN2, HPH3 [1]	EGLN1, HPH2 [1]	EGLN3, HPH1 [1]
tissue of expression (in mice)	testis, liver, kidney, brain, (heart) [2]	heart, liver, brain, kidney, skeletal muscle, lung [2]	heart, liver, brain, kidney, skeletal muscle, lung [2]
intracellular localization	nucleus [5]	cytoplasm [5]	cytoplasm and nucleus [5]
relative substrate preference	HIF-2 α >HIF-1 α [3] C-ODD>N-ODD [4]	HIF-1 α >HIF-2 α [3] C-ODD>N-ODD [4]	HIF-2 α >HIF-1 α [3] C-ODD only [4]
hypoxia-inducibility	no	yes	yes
chromosomal localization (in mice)	7	8	12
protein size [kDa]	44	46	27
K_m values for O₂ [μM]	230	250	230

[1] Sharp and Bernaudin, 2004 [2] Lieb *et al.*, 2002 [3] Appellhoff *et al.*, 2004 [4] Hirsilä *et al.*, 2003 [5] Metzen *et al.*, 2003

2. Introduction

2.4 Mouse models

2.4.1 PHD knock-out mice

To gain insight into the *in vivo* functions of the PHDs several PHD knock-out mouse models have been established.

Takeda *et al.* (2006) created constitutive PHD1 (targeted Exon: 3), PHD2 (targeted Exon: 2) and PHD3 (targeted Exon: 2) knock-out mice (PHD1^{-/-}, PHD2^{-/-}, PHD3^{-/-}). While PHD1^{-/-} and PHD3^{-/-} mice seem apparently normal, PHD2^{-/-} mice die between E12.5 and E14.5. These embryos display severe symptoms like retardation in heart development, an open interventricular septum, thinner compact layer of ventricles, enlarged atria (which were congested with fetal erythrocytes), a malformed placenta and a pale yolk sac.

To further study the function of PHD2 *in vivo*, two groups created two independent conditional PHD2 knock-out mouse models (Minamishima *et al.*, 2007; Takeda *et al.*, 2007). The tamoxifen-inducible PHD2 knock-out mouse model created by Minamishima *et al.* (targeted Exons: 2 and 3) is restricted viable as these mice die suddenly at the age of about ten weeks. The knock-out mice are significantly smaller than their *wt* littermates and exhibit profound increases in red blood cell production which goes along with increased serum erythropoietin levels. Histological examination reveals venous congestion and occasional retroperitoneal hemorrhage. It has also been shown that these mice develop a dilated cardiomyopathy with enlarged cardiomyocytes. Furthermore signs of early cardiac ischemia were shown by an increased contraction band necrosis. But it was not analyzed whether these symptoms are an indirect consequence of polycythemia and hyperviscosity or if it is a direct consequence of chronic high-level HIF activation in cardiomyocytes.

The PHD2 knock-out mouse model created by Takeda *et al.* (targeted Exon: 2) is viable. These mice showed a hyperactive angiogenesis and angiectasia in multiple organs, including lung, liver and the heart.

2.4.2 Transgenic HIF-1 α mice

To study the function of HIF, which is normally only active in a hypoxic environment, in normoxia, HIF-1 α transgenic mice were created. Bkeredjian *et al.* (2010) created a transgenic mouse model carrying the human HIF-1 α cDNA under the control of the α MHC promoter with alanine substitutions at Pro⁴⁰², Pro⁵⁶⁴ and Asn⁸⁰³ which makes HIF-1 α oxygen-insensitive. A doxycycline-inducible construct (tet-off system) was used to obtain tight

2. Introduction

exogenous regulation of transgene expression. Echocardiographic analysis showed a marked dilation of the left ventricle and a decrease in fractional shortening but only modest signs of cardiac hypertrophy after doxycycline withdrawal. After restoring doxycycline, the heart function returned to normal. Despite the worsened heart function the myocardium showed no obvious abnormalities. No increased apoptosis, no fibrosis, no hypertrophy, nor heterogeneity in myocyte size could be detected. Cardiac transcript array analysis revealed an up-regulation of 213 genes and a down-regulation of 100 genes three days after doxycycline removal. The most notably regulated genes fulfill functions in metabolism, especially in glycolysis. In addition, genes regarding the calcium handling of the cell were regulated. The sarcoplasmic/endoplasmic reticulum calcium ATPase (SERCA), phospholamban (PLB) and the type-2 ryanodine receptor (RyR2) were also reduced on mRNA level with an impaired Ca^{2+} uptake after one week of HIF transgene expression.

Kido *et al.* (2005) investigated whether constitutive expression of HIF-1 α influences infarct size and cardiac performance after myocardial infarction. To answer this question a transgenic mouse was created carrying the unmodified HIF-1 α coding sequence under the control of the α MHC promoter which restricts the expression of the transgene primarily to cardiomyocytes.

Transgenic (HIF-1 α (+)) and age matched *wt* mice (HIF-1 α (-)) underwent ligation of the *left anterior descending artery* (LAD) and were analyzed 24 hours and four weeks after ligation. 24 hours after the ligation HIF-1 α (+) and HIF-1 α (-) had comparable infarct sizes and areas at risk as determined by Evans Blue/ triphenyltetrazolium chloride (TTC) staining. However, it was shown that HIF-1 α (+) mice had a smaller infarct size than HIF-1 α (-) with a bigger viable left ventricle area four weeks after the ligation. The cardiac function was likewise better preserved in HIF-1 α (+) mice as indicated by a significantly higher fractional shortening and ejection fraction. A contributing factor could be the increased angiogenesis that could be detected in the infarct and the peri-infarct region four weeks after ligation. This mouse strain was further analyzed in this thesis.

2. Introduction

2.5 Cardiovascular diseases

In this thesis several cardiovascular diseases are mimicked and analyzed in the different mouse models. These are cardiomyopathies, myocardial infarction and an elevated mechanical load.

2.5.1 Cardiomyopathies

Cardiomyopathies, or generally spoken heart muscle diseases are diseases, in which the heart is abnormally enlarged, thickened and/or stiffened. There are several different types of cardiomyopathies. Some important ones are:

-Dilated cardiomyopathy (DCM) which is the most often occurring form. It is a condition in which the heart becomes weakened and enlarged so that the blood cannot be pumped efficiently anymore. The decreased heart function can affect the lung, liver, and other organs (Maron *et al.*, 2006).

-Ischemic cardiomyopathy (ICM) is defined as a state of the heart in which it cannot pump enough blood to supply the whole body. This is due to coronary artery disease, a buildup of a hard substance (plaque) in the coronary arteries (Maron *et al.*, 2006).

-Hypertrophic cardiomyopathy (HCM) is a condition in which the heart muscle thickens. This thickening can appear asymmetrical so that one part of the heart is thicker than others. Through the hardening it is more difficult for the blood to leave the heart which forces the heart to pump even harder. HCM is caused by a variety of mutations encoding contractile proteins of the cardiac sarcomere (Maron *et al.*, 2006).

2.5.2 Mechanical load: preload versus afterload

Load is a critical factor of myocardial function. The two types of load are preload and afterload. Preload builds up during diastolic filling and stretches the cardiomyocytes. Afterload is the tension or stress developed in the wall of the left ventricle during ejection. In a mouse model an elevated afterload is achieved through *transverse aortic constriction* (TAC) (Toischer *et al.*, 2010). In this surgery a ligation with a defined diameter is placed around the *aorta transversa* (Laufs *et al.*, 2008). This surgery mimics another important heart disease- an aortic valve stenosis in which the opening of the aortic valve is narrowed. This narrowing hinders the blood from easily flowing into the aorta and then into the body. The heart can initially compensate this by thickening of its walls which leads to cardiac hypertrophy. But in

2. Introduction

later stages of the disease progress the left ventricle dilates, the wall becomes thinner and in addition the systolic function decreases.

2.5.3 Myocardial Infarction

Myocardial infarction is the irreversible necrosis of the heart muscle secondary to prolonged ischemia. This usually results from an imbalance between oxygen supply and demand, which is most often caused by blood clots in a coronary vessel, resulting in an acute reduction of blood and oxygen supply to a portion of the myocardium.

To mimic this disease pattern in a mouse model the *left anterior descending artery* can be surgically ligated (Patten *et al.*, 1998). Afterwards the area at risk and the area of necrosis can be determined by Evan's Blue/TTC staining (Bohl *et al.*, 2009). Furthermore, the cardiac remodeling can be analyzed by echocardiography over time.

3. Original Publications

3. Original Publications

This chapter contains the following original articles which are published at the submission date of this thesis:

3.1. Marion Hölscher, Monique Silter, Sabine Krull, Melanie von Ahlen, Amke Hesse, Peter Schwartz, Ben Wielockx, Georg Breier, Dörthe M. Katschinski, Anke Zieseniss (2011)

Cardiomyocyte-specific Prolyl-4-hydroxylase Domain 2 Knock Out Protects from Acute Myocardial Ischaemic Injury

J Biol Chem 286:11185-11194

3.2. Marion Hölscher, Katrin Schäfer, Sabine Krull, Katja Farhat, Amke Hesse, Monique Silter, Yun Lin, Bernd Pichler, Patricia Thistlethwaite, Ali El-Armouche, Lars S. Maier, Dörthe M. Katschinski, Anke Zieseniss (2012)

Unfavourable consequences of chronic cardiac HIF-1 α stabilization

Cardiovasc Res 94:77-86

3. Original Publications

3.1. Cardiomyocyte-specific Prolyl-4-hydroxylase Domain 2 Knock Out Protects from Acute Myocardial Ischemic Injury

The prolyl-4-hydroxylase domain enzyme 2 (PHD2) is the most important isoform of the PHDs based on its ubiquitous expression pattern and its dominant effect on HIF-1 α in normoxia. PHD2 knock-out embryos die between E12.5 and E14.5 which coincides with increased levels of PHD2 in *wt* animals (Takeda *et al.*, 2006). To further analyze the consequences of PHD2 loss *in vivo* two independent PHD2 knock-out mouse models have been created (Minamishima *et al.*, 2007; Takeda *et al.*, 2007). The phenotype of these mice is similar to the consequences of HIF-1 α overexpression with increased angiogenesis, erythropoiesis and extramedullary hematopoiesis. These mice also show signs of a cardiac phenotype with symptoms of a dilated cardiomyopathy. But as these mice also have an increased hematocrit, an indirect effect via the increased blood viscosity cannot be excluded.

To gain deeper insight into the direct functions of PHD2 in the heart, we created a cardiomyocyte-specific PHD2 knock-out mouse model (*cPhd2*^{-/-}) and analyzed these mice in comparison to *wt* littermates.

In the following publication the successful generation of these cardiomyocyte-specific PHD2 knock-out mice is described. The mice were analyzed with regard to HIF-1 α stabilization, heart function, capillaries and ultrastructure in the heart. Furthermore, these mice underwent *transverse aortic constriction* and permanent ligation of the *left anterior descending artery*.

In summary, I was able to show that these mice show elevated HIF-1 α protein levels with subsequent up-regulation of HIF target genes. *cPhd2*^{-/-} mice do not respond differently to an increased mechanical load by *transverse aortic constriction* compared to their *wt* littermates. After ligation of the *left anterior descending artery*, however, the area at risk and area of necrosis were significantly smaller in *cPhd2*^{-/-} mice compared with *Phd2 wt* mice. This is most likely due to an increased capillary area as a consequence of pro-vasodilatory pathways induced by HIF.

Cardiomyocyte-specific Prolyl-4-hydroxylase Domain 2 Knock Out Protects from Acute Myocardial Ischemic Injury^{*S}

Received for publication, September 20, 2010, and in revised form, January 15, 2011. Published, JBC Papers in Press, January 26, 2011, DOI 10.1074/jbc.M110.186809

Marion Hölscher[‡], Monique Silter[‡], Sabine Krull[‡], Melanie von Ahlen[‡], Amke Hesse[‡], Peter Schwartz[§], Ben Wielockx[¶], Georg Breier[¶], Dörthe M. Katschinski^{†1}, and Anke Ziesenis[‡]

From the [‡]Department of Cardiovascular Physiology, Universitätsmedizin Göttingen, Georg-August University Göttingen, D-37073 Göttingen, Germany, the [§]Department of Anatomy and Embryology, Universitätsmedizin Göttingen, Georg August University Göttingen, D-37075 Göttingen, Germany, and the [¶]Department of Pathology, TU Dresden, D-01307 Dresden, Germany

Prolylhydroxylase domain proteins (PHD) are cellular oxygen-sensing molecules that regulate the stability of the α -subunit of the transcription factor hypoxia inducible factor (HIF)-1. HIF-1 affects cardiac development as well as adaptation of the heart toward increased pressure overload or myocardial infarction. We have disrupted PHD2 in cardiomyocytes (*cPhd2*^{-/-}) using *Phd2*^{lox/lox} mice in combination with MLCvCre mice, which resulted in HIF-1 α stabilization and activation of HIF target genes in the heart. Although *cPhd2*^{-/-} mice showed no gross abnormalities in cardiac filament structure or function, we observed a significant increased cardiac capillary area in those mice. *cPhd2*^{-/-} mice did not respond differently to increased mechanical load by transverse aortic constriction compared with their wild-type (*wt*) littermates. After ligation of the left anterior descending artery, however, the area at risk and area of necrosis were significantly smaller in the *cPhd2*^{-/-} mice compared with *Phd2* *wt* mice in line with the described pivotal role of HIF-1 α for tissue protection in case of myocardial infarction. This correlated with a decreased number of apoptotic cells in the infarcted myocardium in the *cPhd2*^{-/-} mice and significantly improved cardiac function 3 weeks after myocardial infarction.

When oxygen availability is impaired, the resulting hypoxia activates homeostatic mechanisms at the systemic and cellular level (1). Hypoxia-inducible factors (HIFs)² are essential players in these responses because they regulate the transcription of a

large number of genes that affect a myriad of cellular processes, including angiogenesis, metabolism, cell survival, and oxygen delivery (2). HIF is a heterodimeric protein comprising the oxygen-sensitive α -subunit HIF-1 α or the more cell type-specifically expressed HIF-2 α or HIF-3 α and the oxygen-insensitive β -subunit (3). In the presence of oxygen, HIF α becomes hydroxylated at two critical proline residues by prolylhydroxylase domain (PHD) enzymes (4, 5). The PHD protein family responsible for HIF α regulation consists of three members called prolylhydroxylase domain (PHD)1, PHD2, and PHD3 (6, 7). Following prolyl-4-hydroxylation of the critical prolyl residues under normoxic conditions, the ubiquitin ligase von Hippel-Lindau tumor suppressor protein recognizes HIF-1 α subunits and targets them for rapid ubiquitination and proteasomal degradation (8–10).

Based on the ubiquitous expression pattern and its dominant effect in normoxia, it had to be assumed that PHD2 is the most critical HIF-1 α -regulating PHD isoform in most tissues (11–13). This notion, learned from *in vitro* studies, was confirmed by the up to now available genetically modified *Phd2* mouse models (14). *Phd2* knock-out embryos die between embryonic day (E) 12.5 and E14.5 (15). This time point coincides with the increased levels of PHD2 in wild-type (*wt*) mice starting from E9.0. A major role of PHD2 in regulating the HIF system is further underscored by mouse models with a somatic *Phd2*^{-/-} knock out, which enable to analyze the *in vivo* function of PHD2 in the adult mice. Two independent inducible *Phd2*^{-/-} mouse models were developed by Takeda *et al.* (16) and Minamishima *et al.* (17). The phenotype of these mice most obviously resembles the consequences of HIF α overexpression with increased angiogenesis, erythropoiesis, and extramedullary hematopoiesis (17, 18). Most interestingly, these mice also develop a cardiac phenotype with symptoms of dilated cardiomyopathy. In the heart, HIF-1 α and thereby also the PHDs are known to influence key components of heart development, morphogenesis, and function (19, 20). Long term activation of HIF-1 α in the heart seems to activate detrimental pathways resulting in the development of heart failure (21). Thus, it is tempting to speculate that loss of PHD2 in the heart is responsible for the dilated cardiomyopathy as observed in the inducible *Phd2*^{-/-} mice. However, because these mice also develop an increased hematocrit, secondary blood hyperviscosity-dependent cardiac changes cannot be ruled out.

Therefore we have generated cardiomyocyte-specific PHD2 knock-out mice (*cPhd2*^{-/-}) by crossing *MLCvCre* mice with

^{*} This work was supported by Kröner Fresenius Stiftung Grant P25/10//A12/10 (to A. Z.) and Deutsche Forschungsgemeinschaft Grants Ka1269/11-1 (to D. M. K.), Br 1336/2-3 and SFB 655 A8 (to G. B.), and Wi 3291/1-1 (to B. W.). The work was performed as collaborative project within the COST Action TD0901 "HypoxiaNet."

^S The on-line version of this article (available at <http://www.jbc.org>) contains supplemental Figs. 1 and 2.

¹ To whom correspondence should be addressed: Dept. of Cardiovascular Physiology, Georg-August University Göttingen, Humboldtallee 23, D-37073 Göttingen, Germany. Tel: 49 551 39 5648; Fax: 49 551 39 5895; E-mail: katschinski@physiol.med.uni-goettingen.de.

² The abbreviations used are: HIF, hypoxia-inducible factor; AAR, area at risk; Ang, angiotensin; AON, area of necrosis; Bnip3, BCL2/adenovirus E1B 19-kDa protein-interacting protein 3; BNP, brain natriuretic peptide; *cPhd2*^{-/-}, cardiac-specific PHD2 knock out; E, embryonic day; FS, fractional shortening; Glut-1, glucose transporter-1; Hox-1, homeobox gene; iNOS, inducible nitric oxide synthase; LAD, left anterior descending artery; PDK1, pyruvate dehydrogenase kinase 1; pfk1, phosphofruktokinase 1; PGK, phosphoglycerate kinase; PHD, prolylhydroxylase domain; TAC, transverse aortic constriction; TTC, 2,3,5-triphenyltetrazolium chloride; wt, wild type.



3. Original Publications

PHD2 and Myocardial Ischemia

Phd2^{fllox/fllox} mice. While this work was ongoing Moslehi *et al.* have recently reported the generation of cardiac-specific PHD2 knock-out mice using α MHCCre expressing mice as deleter mice in combination with *Phd2^{fllox/fllox}* mice (22). In line with our observation, Moslehi *et al.* observed no striking differences in morphology or function of resting young *cPhd2^{-/-}* mice. Moslehi *et al.* additionally analyzed older mice and demonstrated that with increasing age cardiomyocyte-specific PHD2 knock-out mice developed changes, which phenocopy ischemic cardiomyopathy. At a young age these animals responded to increased afterload with fortified heart failure despite the successful development of cardiac hypertrophy.

In contrast to the results of Moslehi *et al.*, we did not observe significant changes in the development of hypertrophy and heart failure of young PHD2-deficient mice toward increased afterload in our animal model. Moreover, we observed cardioprotective effects in the PHD2-lacking mice in a model of myocardial ischemia. Challenging the mice with permanent ligation of the left anterior descending artery (LAD) resulted in cardiac tissue protection and decreased myocardial infarct size in the *cPhd2^{-/-}* mice compared with *Phd2 wt* littermates. Taken together, our results show for the first time that lack of PHD2 in cardiomyocytes protects the heart from an acute ischemic insult. This phenomenon is at least in part most likely due to an increased capillary area in the *cPhd2^{-/-}* mice.

EXPERIMENTAL PROCEDURES

Mice—The generation and detailed characterization of *Phd2^{fllox/fllox}* mice will be reported elsewhere.³ In brief, LoxP sites were cloned into the *Phd2* gene via Red/ET recombination (23) flanking exons 2 and 3. To characterize the *Phd2^{fllox/fllox}* mice, full inactivation of the *Phd2* gene was achieved via an intercross with *PGKCre* mice. Consistent with earlier reports, no viable *PHD2^{-/-}* mice were obtained (15, 17).

Cre-mediated excision of exons 2 and 3 results in a frameshift mutation from exon 1 to 4 leading to an early translational stop and subsequent *Phd2* knock out. Exons 2 and 3 encode for almost the entire catalytic domain of *Phd2*. The successful deletion of *Phd2* in the floxed mice was verified by Western blotting on protein extracts of embryonic hearts (E14.5) from *PGKCre* \times *Phd2^{fllox/fllox}* mice using a homemade *Phd2* antibody against a C-terminal peptide (supplemental Fig. 1). No PHD2 protein could be detected in *Phd2^{-/-}* hearts. Moreover, the fact that HIF-1 α protein is stabilized in these samples verifies the loss of functionality of *Phd2*. To analyze, if a shorter PHD2 protein encoded by exon 1 is formed, we performed Western blotting using an antibody, which detects the N-terminal part of PHD2 (supplemental Fig. 2). There is indeed a shorter *Phd2* protein detectable in the *Phd2^{+/-}* and *Phd2^{-/-}* mice, which in its apparent molecular mass matches the predicted number of 31.5 kDa. The putatively exon 1-encoded protein, however, was expressed compared with the wt PHD2 protein in *wt* or *Phd2^{+/-}* embryos only at very low levels. Whether this shorter protein would have a dominant negative character and therefore would bind to its interaction partner (e.g. HIF α) and block

its normal function has not been studied. However, it was suggested that in human PHD2 both Arg³⁷¹ and Pro³¹⁷ (in mice Arg³⁴⁸ and Pro²⁹⁴ located in exons 3 and 2, respectively) contribute to the HIF-1 α or HIF-2 α binding (24). In our mice these sites are not present anymore, and a dominant negative interaction with HIF-1 α is therefore unlikely.

All animals in this study were backcrossed to C57BL/6 mice at least five times. *Phd2^{fllox/fllox}* mice were crossed with *MLCvCre^{+/-}* mice (25) to generate *Phd2^{fllox/fllox}* \times *MLCvCre^{+/-}* mice within two generations. *Phd2^{fllox/fllox}* \times *MLCvCre^{+/-}* mice were then crossed with *Phd2^{fllox/fllox}* mice to obtain *cPhd2^{-/-}* (*Phd2^{fllox/fllox}* \times *MLCvCre^{+/-}*) mice and littermate control wild-type mice (*Phd2^{fllox/fllox}*).

Mice were genotyped by PCR using the following primers: Cre forward, 5'-CGTACTGACGGTGGGAGAAT-3' and Cre reverse, 5'-CGGCAAAACAGGTAGTTA-3'; PHD2 forward, 5'-CTCACTGACCTACGCCGTGT-3' and PHD2 reverse, 5'-CGCATCTTCCATCTCCATTT-3'.

The deletion of floxed exons in cDNAs isolated from ventricles or atria by PCRs was shown with the following primers: PHD2 forward, 5'-TACAGGATAAACGGCCGAAC-3' and PHD2 reverse, 5'-GGCAACTGAGAGGCTGTAGG-3'. The forward primer binds in exon 1, the reverse primer binds in exon 5.

Animal Experimentation and Echocardiography—Animal experimentation was performed with *cPhd2^{-/-}* mice and littermate *Phd2 wt* control mice. All protocols regarding animal experimentation were conducted according to the German animal protection laws and approved by the responsible governmental authority (Niedersächsisches Landesamt für Verbraucherschutz und Lebensmittelsicherheit in Oldenburg; animal experimentation numbers 33.942502-04-10/0024 and 33.9-42502-04-10/0069). Pressure overload was induced by transverse aortic constriction (TAC) and performed essentially as described previously by our group with blunted 27-gauge needles as placeholders in 10-week-old female mice (26).

LAD ligations were performed by an investigator who was blinded regarding the genotypes of the mice. The measurement of infarct size was performed by an additional investigator, who was likewise blinded.

LAD ligation was performed on female mice having a minimum weight of 21 g (8–12 weeks of age). Mice were anesthetized (2% isoflurane). The trachea was surgically exposed, and tracheal intubation was performed. A blunt intubation cannula (intubation cannula, stainless steel with Y-adaptor, 1.2-mm outer diameter, 30-mm length; Hugo Sachs Elektronik, Harvard Apparatus GmbH) was inserted into the trachea. Correct tube placement was confirmed by direct visualization of the cannula within the previously exposed trachea. The tracheal tube was connected to a mechanical ventilator (MiniVent; Hugo Sachs Elektronik, Harvard Apparatus GmbH), and the animals were ventilated by using a pressure-controlled ventilation mode (stroke volume 150 μ l, 150 strokes/min fractional inspired O₂ = 0.3). After exposing the heart, the pericardium was removed, and a 9-0 polyamide suture with a U-shaped needle was passed under the left anterior descending artery. The

³ B. Wielockx, K. Anastasiadis, A. F. Stewart, and G. Breier, unpublished observations.

3. Original Publications

PHD2 and Myocardial Ischemia

suture was tied to occlude the artery. The chest was closed and the mouse recovered.

Echocardiography and measurement of posterior wall thickness, septum thickness, left ventricular end systolic diameter, left ventricular end diastolic diameter, and fractional shortening (FS) were performed as described by Silter *et al.* (26).

Measurement of Infarct Size—Six hours after LAD ligation the mice were given heparin (250 units) and anesthetized, and the hearts were excised. Myocardial infarct size was determined by using Evans blue/2,3,5-triphenyltetrazolium chloride (TTC) staining as described by Bohl *et al.* (27). Briefly, the ascending aorta was cannulated with a 20-gauge tubing adapter, and 1% Evans blue was perfused into the aorta and coronary arteries to delineate the “area at risk” (AAR). The Evans blue dye was distributed uniformly to those areas of the myocardium, which were well perfused; hence, the area of the myocardium that was not stained with Evans blue was defined as the AAR. The left ventricle was separated from the rest of the heart and sectioned into three transverse slices. Sections were incubated in 2% TTC for 20 min at 37 °C to identify viable tissue. Infarct quantification was performed on digital photographs (SMZ 100; Nikon, Tokyo, Japan) using ImageJ (National Institutes of Health). The area of necrosis (AON) and AAR were determined as the average percent area per slice from the middle section and the lowest section. Also, myocardial samples were collected for cyrosectioning and assessment of apoptosis.

Protein Extraction and Immunoblot Analyses—Heart tissue was rapidly homogenized in a buffer containing 4 M urea, 140 mM Tris (pH 6.8), 1% SDS, 2% Nonidet P-40, and protease inhibitors (Roche Applied Science). Protein concentrations were quantified (DC Protein Assay; Bio-Rad). For immunoblot analysis protein samples were resolved by SDS-PAGE and transferred onto nitrocellulose membranes (Amersham Biosciences) by semidry blotting (PeqLab). Primary antibodies used were: anti-PHD2 (NB100-2219; Novus), anti-HIF-1 α (NB100-479; Novus), and anti-vinculin (hVin-1, V9264; Sigma).

For detection of immunocomplexes, horseradish peroxidase-conjugated secondary goat anti-rabbit or goat anti-mouse antibodies (Santa Cruz Biotechnology) were used, and membranes were incubated with 100 mM Tris-HCl (pH 8.5), 2.65 mM H₂O₂, 0.45 mM luminol, and 0.625 mM coumaric acid for 1 min. Chemiluminescence signals were detected with the LAS3000 camera system (Fuji Film Europe, Düsseldorf, Germany).

RT-PCR Analyses—After RNA extraction reverse transcription (RT) was performed with 2 μ g of RNA and a first strand cDNA synthesis kit (Fermentas, St. Leon-Rot). mRNA levels were quantified by using 1 μ l of the cDNA reaction and a SYBR Green qPCR reaction kit (Clontech) in combination with a MX3000P light cycler (Stratagene). The initial template concentration of each sample was calculated by comparison with serial dilutions of a calibrated standard. Primers were as follows: glucose transporter-1 (Glut-1) forward, 5'-TGGCCTTGCTGGAACGGCTG and Glut-1 reverse, 5'-TCCTTGGGCTGCAGGGAGCA-3'; mS12 forward, 5'-GAAGCTGCCAAGGCCTTAGA-3 and mS12 reverse, 5'-AACTGCAACCAACCACTTC-3'; PHD2 forward, 5'-TTGCTGACATTGAACCCAAA-3' and PHD2 reverse, 5'-GGCAACTGAGAGGCTGTAGG-3'; PHD1 forward, 5'-GCTAGGCTGAGGGAGG-

AAGT-3' and PHD1 reverse, 5'-TCTACCCAGGCAATCTGTGC-3'; PHD3 forward, 5'-GGCCGCTGTATCACCTGTAT-3 and PHD3 reverse, 5'-TTCTGCCCTTCTTCAGCAT-3'; brain natriuretic peptide (BNP) forward, 5'-AAGTCCTAGCCAGTCTCCAGA-3' and BNP reverse, 5'-GAGCTGTCTCTGGGCCATTTC-3'; phosphofruktokinase 1 (Pfk1) forward, 5'-ACGAGGCCATCCAGCTCCGT-3' and Pfk1 reverse 5'-TGGGGCTTGGGCAGTGTCT-3'; pyruvate dehydrogenase kinase 1 (PDK-1) forward, 5'-GTTACGTCACGCTGGGCGA-3' and PDK-1 reverse, 5'-CCAGGCGTCCCATGTGCGTT-3'; phosphoglycerate kinase (PGK) forward, 5'-ACGTCTGCCGCGCTGTTCTC-3' and PGK reverse, 5'-ACCATGGA-GCTATGGGCTCGGT-3'; VEGF forward, 5'-CGAACGTACTGCCGATTGAGA-3 and VEGF reverse, 5'-TGGTGAGGT-TTGATCCGCATGATCTG-3'; angiotensin (Ang)-1 forward, 5'-CGCTCTCATGCTAACAGGAGGTTGG-3' and Ang-1 reverse, 5'-GCATTCTCTGGACCCAAGTGGCG-3'; Ang-2 forward, 5'-CACCCAACTCCAAGAGCTCGG-3' and Ang-2 reverse, 5'-CACGTAGCGGTGCTGACCGG-3'; BCL2/adenovirus E1B 19-kDa protein-interacting protein 3 (Bnip3) forward, 5'-GTCCAGTGTGCGCTGGCCTC-3' and Bnip3 reverse, 5'-TGGGAGCGAGGTGGGTGTC-3'; iNOS, inducible nitric-oxide synthase; (iNOS) forward, 5'-GCTGCC-TTCCTGCTGTCGCA-3' and iNOS reverse, 5'-GGAGCCGCTGCTGCCAGAAA-3; hemoxygenase (Hox)-1 forward, 5'-TGGTGCAAGATACTGCCCTGC-3' and Hox-1 reverse, 5'-TGGGGGACAGCAGTCGTGGT-3', apelin forward, 5'-TGCAGTTTGTGGAGTGCCACTG-3' and apelin reverse, 5'-GCACCGGGAGGCACT-3'; adrenomedullin forward, 5'-TGGCCCCCTACAAGCCAGCAAT-3' and adrenomedullin reverse, 5'-GCCAACGGGATACTGCCCG-3'. The sets of primers for adenosine receptor A2b and CD73 were according to previously published sequences (28).

BNP Enzyme Immunoassay—Plasma BNP levels were measured using a commercially available enzyme immunoassay kit (catalog number EK-011-23; Phoenix Pharmaceuticals) according to the manufacturer's instructions.

Histological Analyses—For Trichrome staining, heart tissue was fixed in 4% paraformaldehyde in phosphate-buffered saline (PBS) and embedded in paraffin before sectioning.

Cryosectioning and Immunofluorescence Labeling—Freshly isolated hearts were treated as described before (29). Briefly, hearts were sectioned (5–10 μ m) in a cryostat, mounted on glass slides, and dried for at least 30 min. After being washed with PBS, the sections were briefly incubated with 1% Triton X-100 and then fixed with 4% formaldehyde and permeabilized with 0.2% Triton X-100. Nonspecific binding of antibodies was blocked by incubation with 1% bovine serum albumin for 1 h. The sections were then incubated with the polyclonal anti-CD31 antibodies (DLA 310, diluted 1:20; Dianova) and anti-vinculin antibodies (hVin-1, diluted 1:100; Sigma) at room temperature for 1 h, washed three times in PBS, and then incubated with anti-mouse TR (diluted 1:200; Santa Cruz Biotechnology) and anti-rat FITC (1:200; Santa Cruz Biotechnology). Samples were counterstained for DNA (Hoechst). Finally, samples were washed extensively in PBS, mounted in Mowiol, and examined by fluorescence microscopy (Axio Observer D1; Carl Zeiss, Göttingen, Germany). The capillary area was determined by



3. Original Publications

PHD2 and Myocardial Ischemia

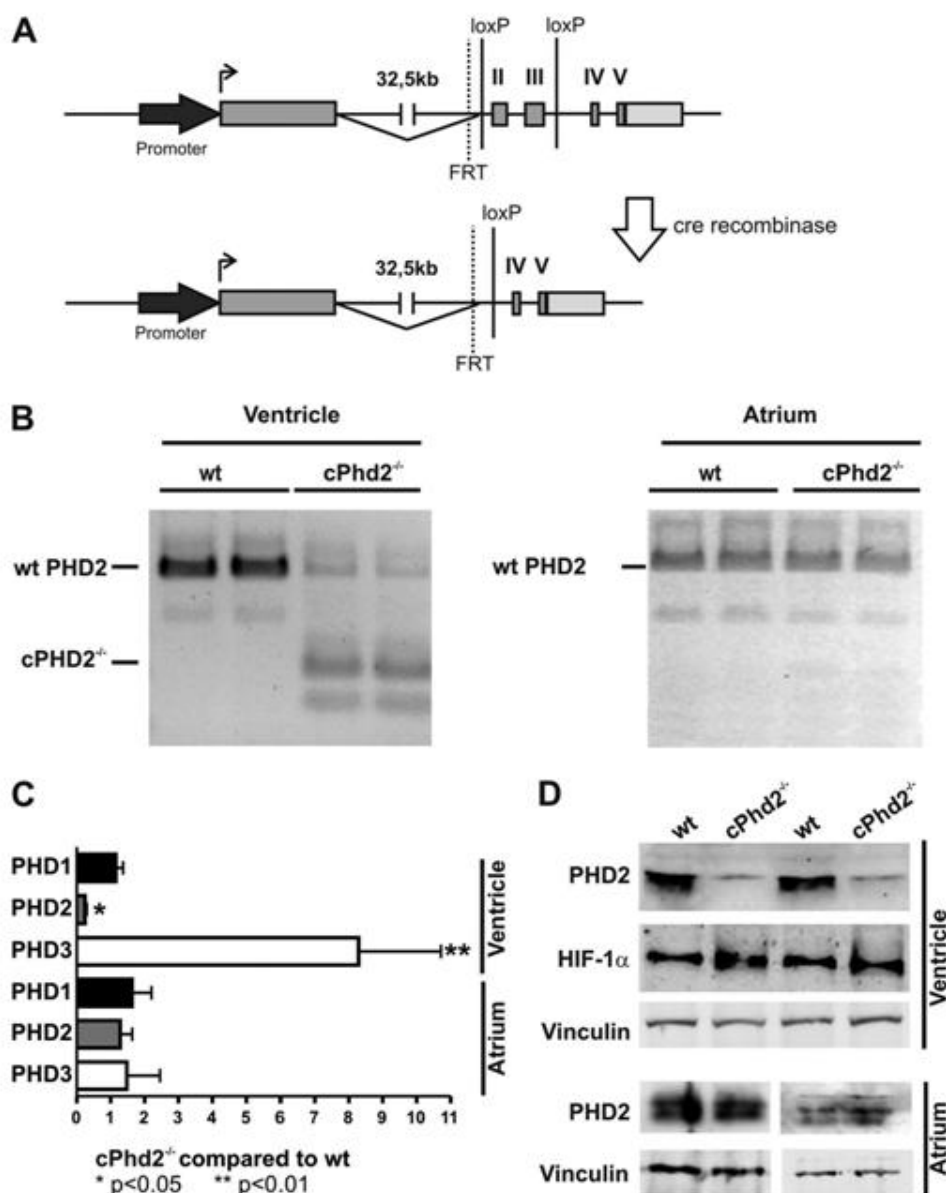


FIGURE 1. Generation and analyses of *cPhd2*^{-/-} mice. *A*, schematic description of the gene targeting strategy is shown. In the targeted *Phd2* locus, exons 2 and 3 are flanked by two *loxP* sites. Exons 2 and 3 are deleted by Cre-mediated recombination by crossing *Phd2*^{loxP/loxP} mice with MLCvCre mice. *B*, PCRs were performed with cDNAs isolated from left ventricles or atria of *cPhd2*^{-/-} or *Phd2* wt control mice to demonstrate the deletion of floxed exons in the ventricles but not the atria. Incomplete recombination in the ventricles is most likely due to the presence of noncardiomyocytes in the tissue samples. Additional bands resemble splice variants. *C*, RT-PCR analysis confirmed the significant reduction of PHD2 mRNA transcripts in the left ventricles but not the atria of 8-week-old *cPhd2*^{-/-} mice compared with wt littermates. Transcripts of the HIF-target PHD3 were increased whereas PHD2 mRNA was unchanged. In total, 11 wild-type mice and 7 *cPhd2*^{-/-} were analyzed. *, *p* < 0.05; **, *p* < 0.01. Data represent mean values ± S.E. (error bars). *D*, PHD2 protein was detected by Western blot analysis. Protein extracts prepared from left ventricles and atria of 8-week-old *Phd2* wt and *cPhd2*^{-/-} mice were analyzed with anti-PHD2, anti-HIF-1α, and anti-vinculin antibodies, confirming that PHD2 was successfully knocked out in the left ventricles but not in the atria.

analyzing CD31-positive pixels using ImageJ). In addition, the number of capillaries were counted per view of field.

Immunohistochemistry—Paraffin-embedded sections were immunostained as described by others (22). The anti-HIF-1α primary antibody (Novus NB100-123) was used at a 1:1000 dilution.

Electron Microscopy—Standard procedures were applied for fixation (1.5% glutaraldehyde and 1.5% paraformaldehyde in phosphate buffer) of hearts of *cPhd2*^{-/-} and *Phd2* wt mice. The hearts were then washed in PBS and fixed in 2% osmium tetroxide. The samples were dehydrated in a graded series of alcohol and embedded in Araldite. Ultrathin sections were

stained with 2% methanolic uranyl acetate. Samples were then examined in a transmission electron microscope equipped with photodocumentation.

TUNEL Assay—Apoptotic cells were detected with a TUNEL assay according to the manufacturer's protocol (In Situ Cell Death Detection kit, catalog number 11 684 795 001; Roche Applied Science). Three hearts of each genotype were analyzed, and five random high power fields from each heart sample were quantified.

Statistical Analyses—Data were analyzed by two-tailed Student's *t* test or (in case of repeated echocardiography analysis after TAC treatment) as paired *t* test and presented

3. Original Publications

PHD2 and Myocardial Ischemia

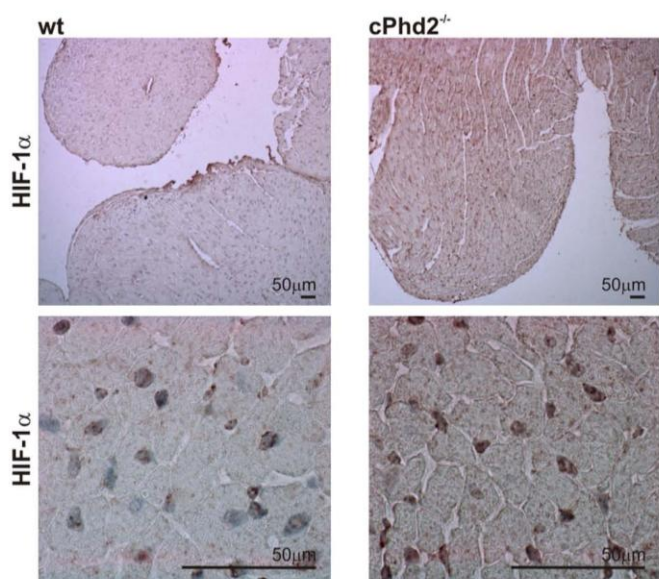


FIGURE 2. HIF-1 α protein accumulates in *cPhd2*^{-/-} hearts. Immunohistochemical analyses of hearts from 8-week-old *cPhd2*^{-/-} and *Phd2* wt mice are shown. HIF-1 α protein accumulates in the nuclei of *cPhd2*^{-/-} ventricles.

as mean \pm S.E. A *p* value < 0.05 was considered statistically significant.

RESULTS

Generation of Cardiac-specific PHD2 Knock-out Mice—For generating *cPhd2*^{-/-} mice, we crossed *Phd2*^{lox/lox} mice with mice that express the Cre recombinase under the control of the MLCv promoter (25). The MLCv-driven Cre permits recombination of the floxed *Phd2* exons 2 and 3 in ventricular cardiomyocytes (Fig. 1A). Isolation and PCR analysis of cDNAs from atria and ventricles of *cPhd2*^{-/-} and littermate *Phd2* wt control mice verified successful recombination in the ventricles but not in the atria of the *cPhd2*^{-/-} mice (Fig. 1B). The additional bands seen in the PCR analysis of *Phd2* wt mice most likely are the result of described PHD2 splice variants (30).

Quantification of PHD2 RNA levels in the left ventricles and atria of *cPhd2*^{-/-} mice compared with *Phd2* wt mice revealed a roughly 5-fold reduction in the knock-out ventricles but not the atria, confirming the MLCvCre-mediated knock out in the ventricular cardiomyocytes (Fig. 1C). Considering that the RNA was isolated from the whole left ventricles, which besides the cardiomyocytes also contain especially cardiac fibroblasts but also endothelial cells, smooth muscle cells etc., this reduction in PHD2 expression is in accordance with a successful recombination in the Cre-expressing cardiomyocytes. In line, cardiac PHD2 expression was also reduced at the protein level in left ventricles but not the atria of *cPhd2*^{-/-} mice as determined by immunoblot analysis (Fig. 1D). As a consequence of the PHD2 knock out, HIF-1 α protein levels were slightly increased (Fig. 1D). Immunohistochemical analysis confirmed the accumulation of HIF-1 α protein in cell nuclei of the cardiomyocytes (Fig. 2). Detection of HIF-2 α by immunohistochemistry was hampered by varying qualities of the batches of the commercially available polyclonal anti-HIF-2 α antibodies. At least *in vitro* it was described that in contrast to PHD3, PHD2 seems to have

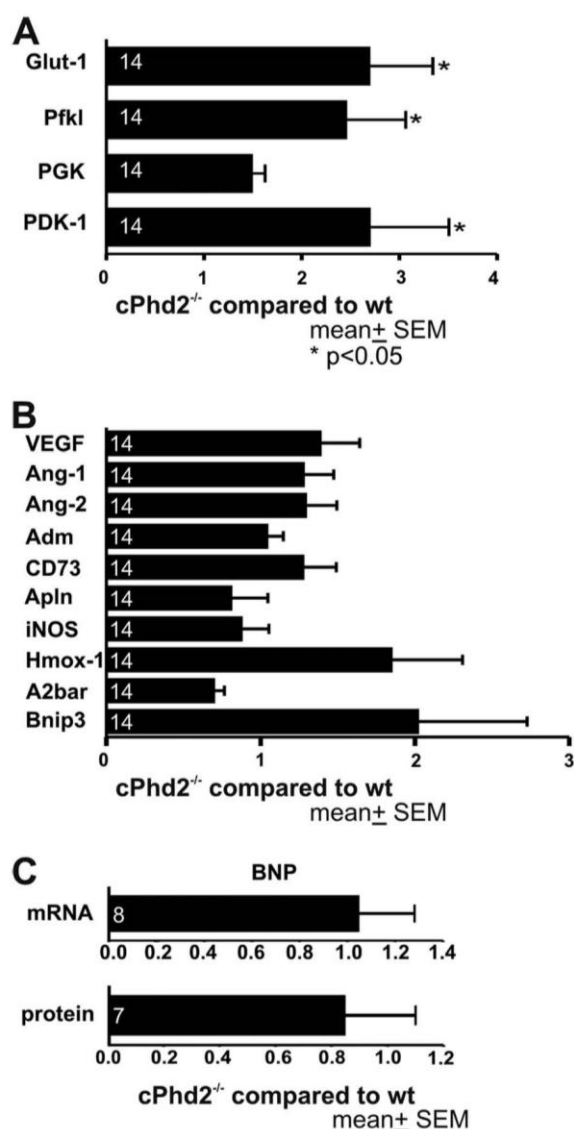


FIGURE 3. PHD2-deficient ventricles exhibit increased expression of HIF target genes. A and B, quantitative real-time RT-PCR (qPCR) analysis of left ventricles from 8-week-old *cPhd2*^{-/-} or *Phd2* wt mice was performed. Transcript levels of genes involved in glucose transport and glucose metabolism (A) as well as HIF-target genes related to angiogenesis, vasotonus regulation, and apoptosis (B) were analyzed. The numbers in the bars indicate the number of animals analyzed. *, *p* < 0.05. Data represent mean values \pm S.E. (error bars). C, changes of BNP mRNA in the left ventricles or in serum protein levels of *cPhd2*^{-/-} compared with *Phd2* wt mice were not detectable by qPCR and ELISA, respectively. Data represent mean values \pm S.E.

higher activity toward HIF-1 α compared with HIF-2 α (30). Therefore the increased levels of HIF-1 α in the cardiomyocytes are in line with an effective PHD2 knock out in our mouse model. A moderate activation of the HIF-signaling pathway in the hearts of *cPhd2*^{-/-} mice was likewise detected by analyzing the expression of the HIF target genes PHD3 (Fig. 1C), Glut-1, Pfk1, and PDK1 (Fig. 3A). Whereas increased levels of Glut-1, Pfk1, and PDK1 reflect the impact of HIF on glucose transport and glucose metabolism, respectively (31), the elevated levels of PHD3 are indicative of the described negative HIF/PHD feedback loop, which involves the HIF-dependent transcription of PHD3 (32). In contrast, PHD1 RNA levels, which are not induc-



3. Original Publications

PHD2 and Myocardial Ischemia

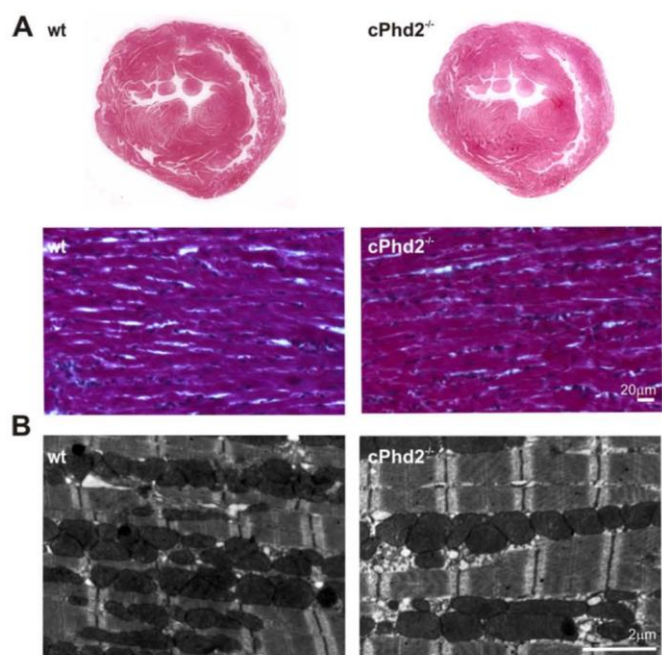


FIGURE 4. *cPhd2*^{-/-} hearts show no gross structural abnormalities. *A*, paraffin-embedded tissue sections of *Phd2* wt and *cPhd2*^{-/-} hearts stained with Trichrome. *B*, transmission electron microscopy of the *Phd2* wt and *cPhd2*^{-/-} hearts.

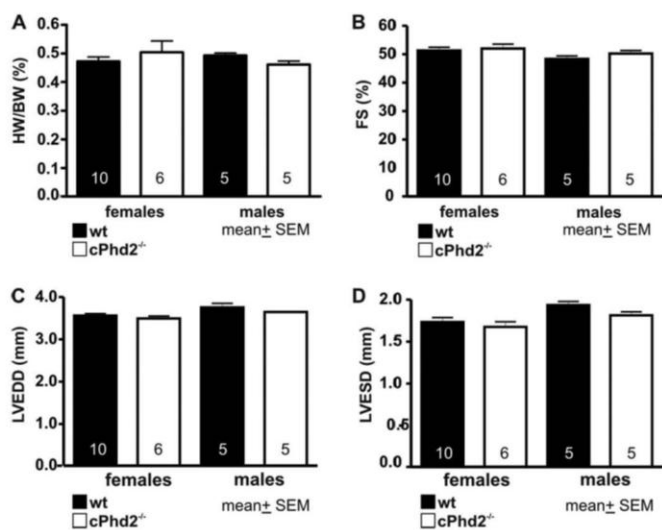


FIGURE 5. Cardiac PHD2 deficiency does not affect heart function in 8-week-old mice. *A*, hearts of *Phd2* wt or *cPhd2*^{-/-} mice were excised, and the ratios of heart weight (HW) compared with body weight (BW) were determined. Data represent mean values \pm S.E. (error bars). The numbers in the bars indicate the number of animals analyzed. *B–D*, fractional shortening (FS) (*B*), left ventricular end diastolic diameter (LVEDD) (*C*), and left ventricular end systolic diameter (LVESD) (*D*) were analyzed by echocardiography and showed no differences between indicated genotypes. The numbers in the bars indicate the number of animals analyzed. Data represent mean values \pm S.E.

ible by hypoxia (13), were not affected in the hearts of *cPhd2*^{-/-} mice (Fig. 1C). HIF target genes involved in angiogenesis (VEGF, Ang-1, Ang-2), vasotonus regulation (adrenomedullin, apelin, iNOS, and Hox-1), purinergic signaling (CD73, and adenosine receptor A2b), and apoptosis (Bnip3) were found to be unchanged (Fig. 3B). BNP is produced in the ventricles and is regarded as surrogate marker for heart failure (33). Analyzing

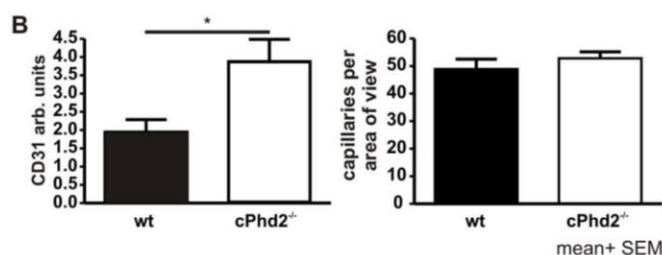
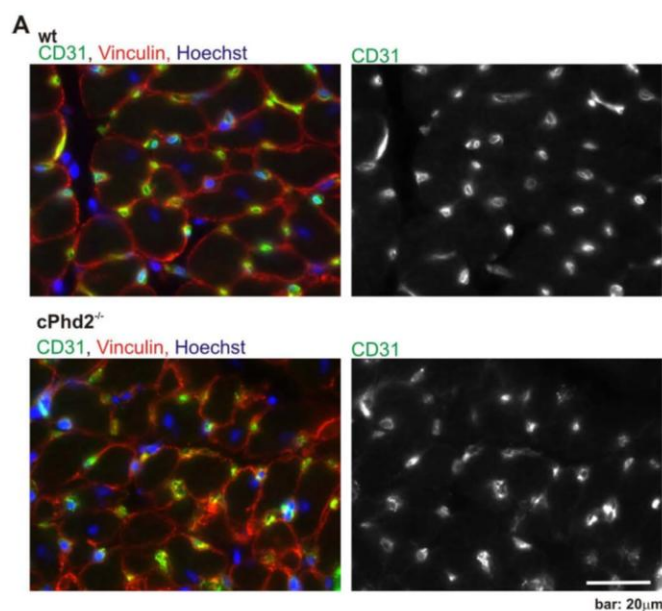


FIGURE 6. Increased capillary area in PHD2-deficient hearts. *A*, hearts of *cPhd2*^{-/-} mice ($n = 4$) and *Phd2* wt ($n = 4$) littermates were excised and analyzed for angiogenesis as determined by anti-CD31 staining. Sections were co-stained for vinculin and DNA (Hoechst). *B*, the area of capillaries, which were determined in *A*, were quantified by determining the extent of CD31-positive staining, and the number of capillaries were counted. *, $p < 0.05$. Data represent mean values \pm S.E. (error bars).

BNP RNA levels in the left ventricles or BNP plasma levels of *Phd2* wt and *cPhd2*^{-/-} mice revealed no significant differences, indicating that there were no obvious signs for heart failure in the *cPhd2*^{-/-} mice (Fig. 3C).

Histological assessment of the heart revealed no gross abnormalities in the *cPhd2*^{-/-} mice (Fig. 4A). Furthermore, electron microscopy analysis displayed no significant changes in ultrastructure or filament architecture (Fig. 4B). Heart weight (Fig. 5A) and heart function as determined by echocardiography of the *cPhd2*^{-/-} mice were found to be not different compared with *Phd2* wt mice (Fig. 5, B–D). Interestingly, a significant difference between *Phd2* wt and *cPhd2*^{-/-} mice, however, could be observed when analyzing capillaries in the heart via CD31 immunostaining (Fig. 6). In the *cPhd2*^{-/-} hearts significantly more CD31-positive staining was detected. This was due to an increased capillary area but not to an increase in the number of capillaries (Fig. 6B). Taken together, basal heart structure and function are, besides an increased diameter of the capillaries, not changed in 8 weeks old mice as a consequence of a lack of PHD2 in ventricular cardiomyocytes. In this regard it should be noted that *MLCvCre* \times *HIF-1 α* ^{lox/lox} mice similarly do not present obvious changes in resting heart function (34). In contrast to resting conditions, however, HIF-1 α indeed seems to

3. Original Publications

PHD2 and Myocardial Ischemia

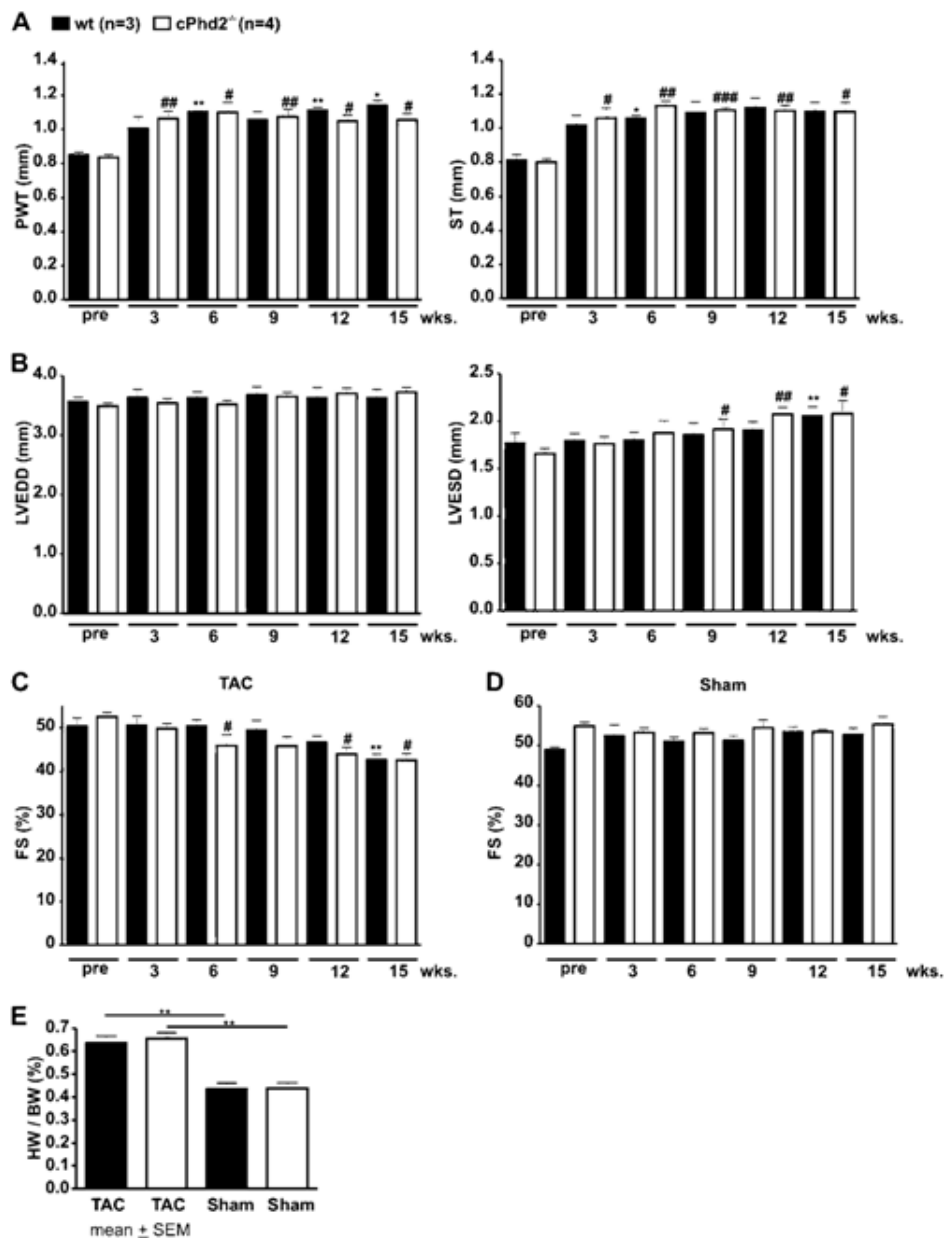


FIGURE 7. PHD2 does not affect cardiac hypertrophy and cardiac function after TAC in female mice. Sustained pressure overload was induced in 10-week-old female *Phd2* wt and *cPhd2*^{-/-} mice by TAC. Subsequently (A) posterior wall thickness (PWT) and septum thickness (ST) as well as (B) left ventricular end diastolic diameter (LVEDD) and left ventricular end systolic diameter (LVESD) were analyzed before (pre) and up to 15 weeks after TAC by echocardiography. Based on the left ventricular end diastolic diameter and left ventricular end systolic diameter, fractional shortenings (FS) of TAC-treated (C) and sham-operated animals (D) were determined. In addition, heart weight (HW) to body weight (BW) ratios were determined 15 weeks after TAC (E). *, $p < 0.05$ TAC-treated *Phd2* wt versus nontreated/pre *Phd2* wt mice; **, $p < 0.01$ TAC-treated *Phd2* wt versus nontreated/pre *Phd2* wt mice; #, $p < 0.05$ TAC-treated *cPhd2*^{-/-} versus nontreated/pre *cPhd2*^{-/-} mice; ##, $p < 0.01$ TAC-treated *cPhd2*^{-/-} versus nontreated/pre *cPhd2*^{-/-} mice; ###, $p < 0.001$ TAC-treated *cPhd2*^{-/-} versus nontreated/pre *cPhd2*^{-/-} mice. Data represent mean values ± S.E. (error bars).

play a role in the adaptation of the heart to increased mechanical load or ischemia (20, 26). Therefore, we analyzed the *cPhd2*^{-/-} mice under stressed conditions, i.e. TAC or LAD.

Lack of PHD2 in the Heart Does Not Affect the Cardiac Response to Increased Afterload—Increased mechanical load by TAC stimulates an adaptation program, which results in hypertrophy and if the load sustains in cardiac failure. We applied the aortic constriction between the branches of the truncus brachiocephalicus and the arteria carotis communis and followed the mice up to 15 weeks by echocardiography. As expected

TAC-treated *Phd2* wt and *cPhd2*^{-/-} mice developed cardiac hypertrophy as a consequence of the aortic constriction (Fig. 7A) whereas sham-treated animal did not (data not shown). The load-induced increase in posterior wall thickness and septum thickness, however, was not different in *Phd2* wt compared with *cPhd2*^{-/-} mice. Likewise, both, i.e. TAC-treated *Phd2* wt and *cPhd2*^{-/-} mice, but not the sham-treated animals (Fig. 7D), developed an increased left ventricular end systolic diameter (Fig. 7B) and a drop in FS (Fig. 7C) to a similar extent at around 12–15 weeks after the intervention. Furthermore, no change in

3. Original Publications

PHD2 and Myocardial Ischemia

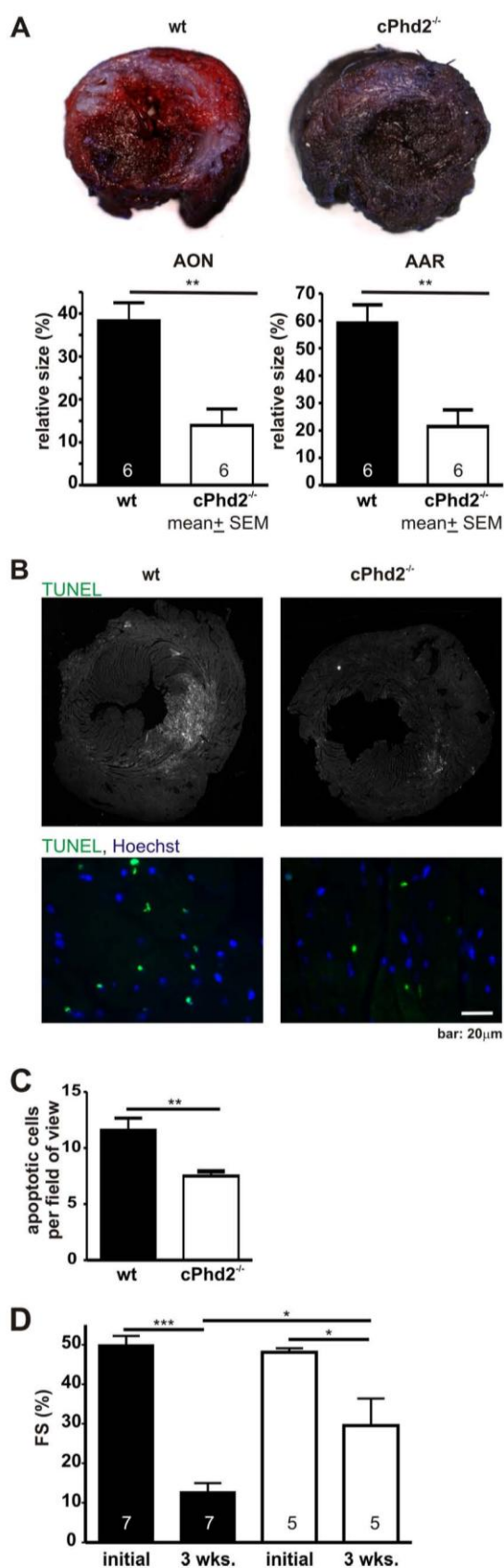


FIGURE 8. *cPHD2*^{-/-} mice are protected from myocardial infarction. *A*, hearts of female *Phd2* wt and *cPhd2*^{-/-} mice were harvested 6 h after LAD ligation, and the AON (white area) and the AAR (non-blue red area) were

the heart to body weight ratio was seen in TAC-treated *Phd2* wt mice compared with *cPhd2*^{-/-} mice (Fig. 7E).

Cardiac PHD2 Knock-out Mice Are Protected from Acute Myocardial Ischemia—Ligation of the LAD allows studying the acute and chronic pathophysiological processes in myocardial ischemia and was applied to *Phd2* wt and *cPhd2*^{-/-} mice. The extent of tissue, which was well supplied by blood 6 h after the intervention, was analyzed by Evans blue perfusion. Myocardial slices were additionally stained with TTC to discriminate between nonperfused dead and vital tissue. This technique relies on the ability of dehydrogenase enzymes and co-factors in the vital tissue to react with tetrazolium salts to form a formazan pigment. Vital tissue appears red and reflects the AAR, whereas dead/nonvital tissue appears white, indicating the AON. The AAR and the AON were significantly smaller in the *cPhd2*^{-/-} mice compared with littermate *Phd2* wt control mice (Fig. 8A). This correlated with a significantly smaller number of apoptotic cardiomyocytes in the infarcted area in the *cPhd2*^{-/-} mice as determined by TUNEL assays (Fig. 8, B and C).

Echocardiography was performed at base line and 3 weeks after myocardial infarction in *cPhd2*^{-/-} mice compared with *Phd2* wt control mice (Fig. 8D). Before LAD ligation the FS was not different between *cPhd2*^{-/-} and control mice and was reduced in both groups after myocardial infarction. In line with the smaller AAR and AON, myocardial function was better preserved in the *cPhd2*^{-/-} mice as indicated by a significant higher FS 3 weeks after surgery in *cPhd2*^{-/-} mice than in *Phd2* wt control mice.

DISCUSSION

Small molecule PHD inhibitors have been demonstrated to be promising in strategies for treating diseases related to hypoxic adaptation like anemia, stroke, or myocardial infarction (14, 35, 36). The concept of cardiac tissue protection is delineated from several recent preclinical studies. Intramyocardial injection of small hairpin RNA targeting PHD2 following LAD ligation results in improved neovascularization in the peri-infarct region and improved cardiac function as indicated by determining FS (37). Treatment of mice with the PHD inhibitors dimethylxaloylglycine or GSK60 had similar protective effects in mouse or rat myocardial infarction models (28, 38). Furthermore, a recent report by Hyvärinen *et al.* has underscored the cardiac protective effect of HIF-1 α in a PHD2 hypomorphic mouse model (39). Taken collectively, these studies point to a cardiac tissue protective mechanism by inhibiting

determined with Evans blue perfusion and TTC staining. Representative mid-myocardial cross-sections of stained hearts are shown. AAR and AON were significantly smaller in *cPHD2*^{-/-} hearts. The numbers in the bars indicate the number of animals analyzed. **, $p < 0.01$. Data represent mean values \pm S.E. (error bars). *B*, heart sections of *cPhd2*^{-/-} mice ($n = 3$) and wt mice ($n = 3$) were analyzed for apoptotic cells by TUNEL assay after LAD ligation. Nuclei were stained with Hoechst (blue), apoptotic nuclei were stained green by the TUNEL assay. Representative images are shown. *C*, apoptotic cells per field of view within the AAR after myocardial infarction of *cPhd2*^{-/-} and *Phd2* wt mice were quantified. **, $p < 0.01$. Data represent mean values \pm S.E. (error bars). *D*, cardiac function is preserved in *cPHD2*^{-/-} mice 3 weeks after myocardial infarction. FS was analyzed before (initial) and 3 weeks after LAD ligation by echocardiography. *, $p < 0.05$; ***, $p < 0.001$. Data represent mean values \pm S.E. The numbers in the bars represent the number of animals analyzed.

3. Original Publications

PHD2 and Myocardial Ischemia

PHD activity in ischemia; however, they do not explicitly answer whether inhibiting the activities of PHDs in cardiomyocytes is involved in this process. In our study, in which the surgeon and the investigator analyzing the myocardial infarct size were blinded, both, *i.e.* AAR and AON, were significantly decreased after LAD ligation in *cPhd2*^{-/-} mice, which lack PHD2 just in ventricular cardiomyocytes compared with *Phd2* *wt* littermates. This correlated with a decreased number of apoptotic cells. Moreover, 3 weeks after LAD ligation *cPhd2*^{-/-} mice demonstrated better heart function compared with *Phd2* *wt* control animals. To this end the present study adds to the understanding of the consequences of loss of PHD2 specifically in cardiomyocytes.

In line with recently published results obtained with a mouse model similar to the one developed in our study, filament structure and cardiac function were not affected by the cardiomyocyte-specific loss of PHD2 in young mice (22). However, we did not observe any change in the response of *cPhd2*^{-/-} mice compared with *Phd2* *wt* mice to sustained pressure overload in regard to cardiac hypertrophy or development of heart failure. This is in contrast to the results of Moselehi *et al.* (22), who have described a decompensation in PHD2-deficient hearts in response to increased afterload. TAC in the mouse is a commonly used experimental model for pressure overload-induced cardiac hypertrophy and heart failure. The discrepancy in the TAC model comparing the study by Moselehi *et al.* and our study may be in part explained by the different deleter Cre mice applied. Furthermore, the development of cardiac failure after TAC intervention is highly depending on the severity of aortic constriction. The severity is mainly determined by the ratio of the basal diameter of the aorta and the diameter of the needle, which is used as placeholder during the constriction procedure. Whereas the needle size was the same in both studies, the severity of the constriction still seems to be more severe in the study of Moselehi *et al.* because the fractional shortening in the challenged mice was reduced already after 4–8 weeks, whereas our mice responded just after 12–15 weeks with a diminished FS.

Interestingly, we observed a significant increase in myocardial capillary size as defined by CD31 staining but not in the number of capillaries. This is consistent with the observation that genes involved in angiogenesis were not found to be up-regulated in the *cPhd2*^{-/-} mice presented in this study. Still, it is conceivable that the increased capillary diameter results in an improved cardiac blood supply which might contribute to the cardiac tissue protection in the *cPhd2*^{-/-} mice 6 h after ligation of the LAD.

A HIF-1 α -mediated cardioprotection has also been observed in cardiac-specific HIF-1 transgenic mice after myocardial infarction (40) and in ischemia-reperfusion in mice carrying a hypomorphic *Phd2* allele (39) and, very recently, in *Phd1*^{-/-} mice (41). The cause of cardioprotection is likely multifactorial and due to the activation of several HIF target genes and the subsequent modulation of pathways involved in, for example, β -catenin signaling (41), the purinergic signaling pathways (28), and the glucose metabolism (39). However, in the *cPhd2*^{-/-} mice presented in our study purinergic signaling was not affected as no significant changes in adenosine 2B receptor and CD73 transcriptional levels were observed. Yet, similar to

the study by Hyvärinen *et al.* (39), we noticed significantly increased mRNA levels for Glut-1 and several enzymes of glycolysis which are all known HIF targets (42). A shift from oxidative to glycolytic metabolism in the heart confers an advantage in surviving ischemic insults. This might, together with the increased capillary vessel area in *cPhd2*^{-/-} hearts, explain the cardioprotection after acute myocardial infarction.

Taken together, our data indicate that deficiency of PHD2 in the heart does not affect the response toward increased mechanical load but induces an acute tissue protective effect in case of myocardial ischemia. Long term inhibition of PHD2 as well as long term stabilization of HIF-1 α in the heart seem to impair heart function as demonstrated in old (8 months) *cPhd2*^{-/-} mice (22) (and own observations) and heart-specific HIF-1 α transgenic mice (21). Further studies, which clarify for how long and when in relation to the myocardial insult PHD activity needs to be diminished, are therefore needed to delineate whether the application of small molecule PHD inhibitors are feasible and useful for inducing tissue protective effects in case of myocardial infarction.

Acknowledgments—We thank Gudrun Federkeil for help with the cryosections and Annette Hillemann for expert technical assistance.

REFERENCES

1. Schofield, C. I., and Ratcliffe, P. I. (2005) *Biochem. Biophys. Res. Commun.* **30**, 617–626
2. Wenger, R. H. (2002) *FASEB J.* **16**, 1151–1162
3. Wang, G. L., and Semenza, G. L. (1995) *J. Biol. Chem.* **270**, 1230–1237
4. Ivan, M., Kondo, K., Yang, H., Kim, W., Valiando, I., Ohh, M., Salic, A., Asara, J. M., Lane, W. S., and Kaelin, W. G., Jr. (2001) *Science* **292**, 464–468
5. Jaakkola, P., Mole, D. R., Tian, Y. M., Wilson, M. I., Gielbert, I., Gaskell, S. J., von Kriegsheim, A., Hebestreit, H. F., Mukherji, M., Schofield, C. I., Maxwell, P. H., Pugh, C. W., and Ratcliffe, P. I. (2001) *Science* **292**, 468–472
6. Epstein, A. C., Gleadle, I. M., McNeill, L. A., Hewitson, K. S., O'Rourke, I., Mole, D. R., Mukherji, M., Metzzen, E., Wilson, M. I., Dhanda, A., Tian, Y. M., Masson, N., Hamilton, D. L., Jaakkola, P., Barstead, R., Hodgkin, I., Maxwell, P. H., Pugh, C. W., Schofield, C. I., and Ratcliffe, P. I. (2001) *Cell* **107**, 43–54
7. Bruck, R. K., and McKnight, S. L. (2001) *Science* **294**, 1337–1340
8. Hon, W. C., Wilson, M. I., Harlos, K., Claridge, T. D., Schofield, C. I., Pugh, C. W., Maxwell, P. H., Ratcliffe, P. I., Stuart, D. I., and Jones, E. Y. (2002) *Nature* **417**, 975–978
9. Min, J. H., Yang, H., Ivan, M., Gertler, F., Kaelin, W. G., Jr., and Pavletich, N. P. (2002) *Science* **296**, 1886–1889
10. Maxwell, P. H., Wiesener, M. S., Chang, G. W., Clifford, S. C., Vaux, E. C., Cockman, M. E., Wykoff, C. C., Pugh, C. W., Maher, E. R., and Ratcliffe, P. I. (1999) *Nature* **399**, 271–275
11. Berra, E., Benizri, E., Ginouvès, A., Volmat, V., Roux, D., and Pouyssegur, J. (2003) *EMBO J.* **22**, 4082–4090
12. Lieb, M. E., Menzies, K., Moschella, M. C., Ni, R., and Taubman, M. B. (2002) *Biochem. Cell Biol.* **80**, 421–426
13. Appelhoff, R. J., Tian, Y. M., Raval, R. R., Turley, H., Harris, A. L., Pugh, C. W., Ratcliffe, P. I., and Gleadle, I. M. (2004) *J. Biol. Chem.* **279**, 38458–38465
14. Katschinski, D. M. (2009) *Acta Physiol.* **195**, 407–414
15. Takeda, K., Ho, V. C., Takeda, H., Duan, L. I., Nagy, A., and Fong, G. H. (2006) *Mol. Cell Biol.* **26**, 8336–8346
16. Takeda, K., Cowan, A., and Fong, G. H. (2007) *Circulation* **116**, 774–781
17. Minamishima, Y. A., Moselehi, J., Bardeesy, N., Cullen, D., Bronson, R. T., and Kaelin, W. G., Jr. (2008) *Blood* **111**, 3236–3244



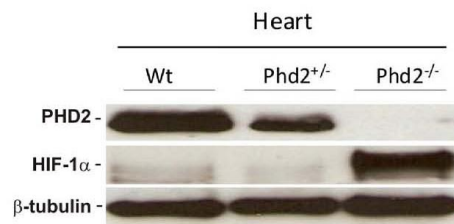
3. Original Publications

PHD2 and Myocardial Ischemia

18. Takeda, K., Aguila, H. L., Parikh, N. S., Li, X., Lamothe, K., Duan, L. J., Takeda, H., Lee, F. S., and Fong, G. H. (2008) *Blood* **111**, 3229–3235
19. Krishnan, J., Ahuja, P., Bodenmann, S., Knapik, D., Perriard, E., Krek, W., and Perriard, J. C. (2008) *Circ. Res.* **103**, 1139–1146
20. Krishnan, J., Suter, M., Windak, R., Krebs, T., Felley, A., Montessuit, C., Tokarska-Schlattner, M., Aasum, E., Bogdanova, A., Perriard, E., Perriard, J. C., Larsen, T., Pedrazzini, T., and Krek, W. (2009) *Cell Metab.* **9**, 512–524
21. Bekeredian, R., Walton, C. B., MacCannell, K. A., Ecker, J., Kruse, F., Outten, J. T., Sutcliffe, D., Gerard, R. D., Bruick, R. K., and Shohet, R. V. (2010) *PLoS One* **5**, e11693
22. Moslehi, J., Minamishima, Y. A., Shi, J., Neubergh, D., Charytan, D. M., Padera, R. F., Signoretti, S., Liao, R., and Kaelin, W. G., Jr. (2010) *Circulation* **122**, 1004–1016
23. Zhang, Y., Muylers, J. P., Testa, G., and Stewart, A. F. (2000) *Nat. Biotechnol.* **18**, 1314–1317
24. Percy, M. J., Furlow, P. W., Beer, P. A., Lappin, T. R., McMullin, M. F., and Lee, F. S. (2007) *Blood* **110**, 2193–2196
25. Minamisawa, S., Gu, Y., Ross, J., Jr., Chien, K. R., and Chen, J. (1999) *J. Biol. Chem.* **274**, 10066–10070
26. Silter, M., Kögler, H., Zieseniss, A., Wilting, J., Schafer, K., Toischer, K., Rokita, A. G., Breves, G., Maier, L. S., and Katschinski, D. M. (2010) *Eur. J. Physiol.* **459**, 569–577
27. Bohl, S., Medway, D. J., Schulz-Menger, J., Schneider, J. E., Neubauer, S., and Lygate, C. A. (2009) *Am. J. Physiol. Heart Circ. Physiol.* **297**, H2054–2058
28. Eckle, T., Köhler, D., Lehmann, R., El Kasmi, K., and Eltzschig, H. K. (2008) *Circulation* **118**, 166–175
29. Zieseniss, A., Schroeder, U., Buchmeier, S., Schoenenberger, C. A., van den Heuvel, J., Jockusch, B. M., and Illenberger, S. (2007) *Cell Tissue Res.* **327**, 583–594
30. Hirsilä, M., Koivunen, P., Günzler, V., Kivirikko, K. I., and Myllyharju, J. (2003) *J. Biol. Chem.* **278**, 30772–30780
31. Wenger, R. H., Stiehl, D. P., and Camenisch, G. (2005) *Sci. STKE* **2005**, re12
32. Stiehl, D. P., Wirthner, R., Köditz, J., Spielmann, P., Camenisch, G., and Wenger, R. H. (2006) *J. Biol. Chem.* **281**, 23482–23491
33. Palazzuoli, A., Gallotta, M., Quatrini, I., and Nuti, R. (2010) *Vasc. Health Risk Manag.* **6**, 411–418
34. Huang, Y., Hickey, R. P., Yeh, J. L., Liu, D., Dadak, A., Young, L. H., Johnson, R. S., and Giordano, F. J. (2004) *FASEB J.* **18**, 1138–1140
35. Myllyharju, J. (2009) *Curr. Pharm. Des.* **15**, 3878–3885
36. Yan, L., Colandrea, V. J., and Hale, J. J. (2010) *Expert Opin. Ther. Pat.* **20**, 1219–1245
37. Huang, M., Chan, D. A., Jia, F., Xie, X., Li, Z., Hoyt, G., Robbins, R. C., Chen, X., Giaccia, A. J., and Wu, J. C. (2008) *Circulation* **118**, S226–233
38. Bao, W., Qin, P., Needle, S., Erickson-Miller, C. L., Duffy, K. J., Ariazi, J. L., Zhao, S., Olzinski, A. R., Behm, D. J., Pipes, G. C., Jucker, B. M., Hu, E., Lepore, J. J., and Willette, R. N. (2010) *J. Cardiovasc. Pharmacol.* **56**, 147–155
39. Hyvärinen, J., Hassinen, I. E., Sormunen, R., Mäki, J. M., Kivirikko, K. I., Koivunen, P., and Myllyharju, J. (2010) *J. Biol. Chem.* **285**, 13646–13657
40. Kido, M., Du, L., Sullivan, C. C., Li, X., Deutsch, R., Jamieson, S. W., and Thistlethwaite, P. A. (2005) *J. Am. Coll. Cardiol.* **46**, 2116–2124
41. Adhuri, R. S., Thirunavukkarasu, M., Dunna, N. R., Zhan, L., Oriowo, B., Takeda, K., Sanchez, J., Otani, H., Maulik, G., Fong, G. H., and Maulik, N. (2010) *Antioxid. Redox Signal.*, in press
42. Semenza, G. L. (2007) *J. Bioenerg. Biomembr.* **39**, 231–234

Supplemental figures

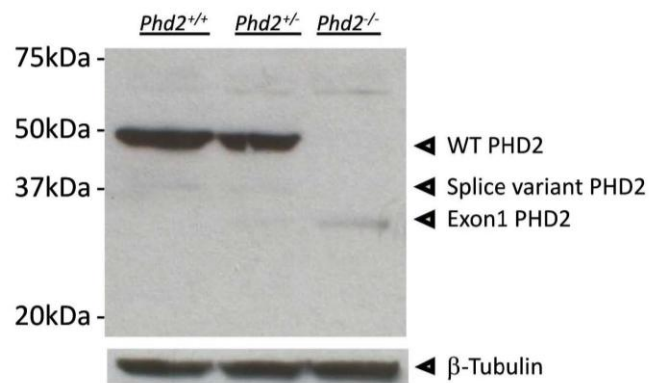
Fig.1



Supplementary Figure 1: Protein expression in the Phd 2 deficient heart. Hearts from mouse embryos (PGKCre x Phd2^{lox/lox}) were isolated at E14.5 and western blot analysis was performed on protein extracts (10 μg total protein). The anti mouse-Phd2 antibody targeted the C-terminal end of the protein (homemade). No PHD2 signal could be detected in the Phd2^{-/-} heart (as in the rest of the embryo (data not shown)) resulting in the protection of HIF-1α protein from degradation. β-tubulin served as loading control.

3. Original Publications

Fig.2



Supplementary Figure 2: Proteins were isolated from embryos (*PGKCre x Phd2^{fllox/fllox}*) at E12.5 and western blot analysis was performed on protein extracts (30 μ g total protein). The anti mouse-Phd2 antibody detects the N-terminal end of the protein (Cell Signaling). A truncated Phd2 protein (exon1) could be detected in the *Phd2*^{-/-} as well as in the *Phd2*^{+/-} embryos. β -tubulin served as loading control.

3. Original Publications

3.2 Unfavourable consequences of chronic cardiac HIF-1 α stabilization

Kido *et al.* created a mouse strain carrying the unmodified HIF-1 α gene under the control of the α MHC promoter (HIF-1 α (+)) (Kido *et al.*, 2005). By analyzing this mouse model it is possible to determine the effects of HIF-1 α , which is normally only stabilized and therefore active in hypoxic conditions, in a normoxic environment. Kido *et al.* could show that HIF-1 α (+) mice have a better outcome after myocardial infarction as indicated by a smaller infarct size and a better preserved heart function four weeks after the ligation of the *left anterior descending artery*.

Long-term consequences of HIF-1 α stabilization and the response of these mice to mechanical load, however, were not investigated. The following manuscript describes the investigations of these HIF-1 α transgenic mice (*Hif-1 α ^{tg}*) when challenged by *transverse aortic constriction*. Furthermore, a group of mice was followed over a time period of eight months to investigate long term consequences of HIF-1 α stabilization. In addition, the metabolism and the calcium handling of *Hif-1 α ^{tg}* mice in comparison to *wt* littermates were determined.

In summary, I was able to show that the metabolism of *Hif-1 α ^{tg}* mice is shifted towards glycolysis with a net increase in glucose uptake and that furthermore Ca²⁺-handling is altered with increased Ca²⁺-transients and a faster Ca²⁺ re-uptake. Subjected to *transverse aortic constriction* *Hif-1 α ^{tg}* mice exhibited profound cardiac decompensation. Moreover, cardiomyopathy was also seen in aging *Hif-1 α ^{tg}* mice.



Unfavourable consequences of chronic cardiac HIF-1 α stabilization

Marion Hölscher¹, Katrin Schäfer², Sabine Krull¹, Katja Farhat¹, Amke Hesse¹,
Monique Silter¹, Yun Lin³, Bernd J. Pichler³, Patricia Thistlethwaite⁴, Ali El-Armouche⁵,
Lars. S. Maier², Dörthe M. Katschinski^{1*†}, and Anke Ziesenis^{1†}

¹Department of Cardiovascular Physiology, Universitätsmedizin, Georg-August-University Göttingen, Humboldtallee 23, 37073 Göttingen, Germany; ²Department of Cardiology and Pneumology, Georg-August-University Göttingen, Germany; ³Department of Preclinical Imaging and Imaging Technology of the Werner Siemens-Foundation, University of Tübingen, Germany; ⁴Division of Cardiothoracic Surgery, University of California, San Diego, CA, USA; and ⁵Department of Pharmacology, Georg-August-University Göttingen, Germany

Received 19 October 2011; revised 19 December 2011; accepted 12 January 2012

Time for primary review: 25 days

Aims

The hypoxia-inducible factor-1 (HIF-1) is the master modulator of hypoxic gene expression. The effects of chronically stabilized cardiac HIF-1 α and its role in the diseased heart are not precisely known. The aims of this study were as follows: (i) to elucidate consequences of HIF-1 α stabilization in the heart; (ii) to analyse long-term effects of HIF-1 α stabilization with ageing and the ability of the HIF-1 α overexpressing hearts to respond to increased mechanical load; and (iii) to analyse HIF-1 α protein levels in failing heart samples.

Methods and results

In a cardiac-specific HIF-1 α transgenic mouse model, constitutive expression of HIF-1 α leads to changes in capillary area and shifts the cardiac metabolism towards glycolysis with a net increase in glucose uptake. Furthermore, Ca²⁺ handling is altered, with increased Ca²⁺ transients and faster intracellular [Ca²⁺] decline. These changes are associated with decreased expression of sarcoplasmic/endoplasmic reticulum calcium ATPase 2a but elevated phosphorylation of phospholamban. HIF-1 α transgenic mice subjected to transverse aortic constriction exhibited profound cardiac decompensation. Moreover, cardiomyopathy was also seen in ageing transgenic mice. In parallel, we found an increased stabilization of HIF-1 α in heart samples of patients with end-stage heart failure.

Conclusion

Changes induced with transgenic cardiac HIF-1 α possibly mediate beneficial effects in the short term; however, with increased mechanical load and ageing they become detrimental for cardiac function. Together with the finding of increased HIF-1 α protein levels in samples from human patients with cardiomyopathy, these data indicate that chronic HIF-1 α stabilization drives autonomous pathways that add to disease progression.

Keywords

Hypoxia • Prolyl-4-hydroxylase domain enzymes • Hypoxia-inducible factor-1 • Metabolism • Ischaemia • Cardiomyopathy

1. Introduction

Coronary artery disease and increased mechanical load are two major leading causes for cardiomyopathy.¹ Myocardial ischaemia, in the case of coronary artery disease, and cardiac hypertrophy, in the case of increased mechanical load, are both associated with a dysfunctional oxygen supply to the heart. This is due to vessel occlusion and capillary rarefaction, respectively.² Hypoxia is the initial trigger during myocardial ischaemia, and during increased mechanical load Hypoxia is the initial trigger during the process of myocardial remodelling.

The hypoxia-inducible factor (HIF) plays a pivotal role in the transcriptional response to changes in oxygen availability.³ HIF comprises two subunits, the α -subunit, which is regulated in an oxygen-dependent manner, and the constitutively expressed β -subunit. The HIF α subunit has an exceptionally short half-life and low steady-state levels in normoxic conditions.⁴ The regulation of HIF α half-life is mediated by three prolyl-4-hydroxylase domain (PHD) enzymes, which hydroxylate two prolyl residues by the use of molecular oxygen.^{5,6} Hydroxylation of HIF α allows binding of the von Hippel-Lindau tumour (pVHL) suppressor, which targets HIF α for

* Corresponding author. Tel: +49 551 39 9778; fax: +49 551 39 5895, Email: doerthe.katschinski@med.uni-goettingen.de

†These authors contributed equally to this work.

Published on behalf of the European Society of Cardiology. All rights reserved. © The Author 2012. For permissions please email: journals.permissions@oup.com.

proteasomal degradation.^{7,8} Hypoxia impairs the hydroxylation, which results in HIF α stabilization, nuclear accumulation, heterodimerization with HIF-1 β , and subsequent hypoxia-inducible gene expression. HIF-1 is known to control the expression of a myriad of genes that regulate cell survival, cell metabolism, and angiogenesis in hypoxic conditions.⁹ In line with these documented functions, increasing HIF-1 α stabilization has been reported to be protective against acute cardiac ischaemia.^{10–12} The consequences of HIF-1 α stabilization in the heart, which may form the basis for ischaemic cardioprotection, are not fully characterized.¹³

In particular, the consequences of long-term stabilization of HIF-1 α in the heart are yet to be described. To clarify the outcome of chronically increased HIF-1 α protein levels in the heart, we analysed the influence of cardiac transgenic overexpression of HIF-1 α in mice (*Hif-1 α ^{tg}*). It has been shown previously that cardiac HIF-1 α stabilization has tissue protective effects when these mice are challenged by myocardial infarction at a young age (12-week-old mice);¹⁴ however, the long-term consequences of HIF-1 α stabilization in older mice and their response to mechanical load are unknown.

2. Methods

2.1 Animals and surgical intervention

All protocols regarding animal experimentation were approved by the Niedersächsische Landesamt für Verbraucherschutz und Lebensmittelsicherheit (33.9.42502-04-10/0024 and 33.9.42502-04-10/0069) and conform with the Directive 2010/63/EU of the European Parliament. Surgical interventions were performed with littermate mice that were either wild-type (*Hif-1 α ^{wt}*) or heterozygous for the *HIF-1 α* transgene (*Hif-1 α ^{tg}*) as described previously;¹⁴ see Supplemental Methods for further details.

2.2 Echocardiography

Echocardiography and measurements of posterior wall thickness (PWT), septum thickness (ST), left ventricular end-systolic diameter (LVESD), left ventricular end-diastolic diameter (LVEDD), and fractional shortening (FS) of ageing mice were performed as described before by our group.¹⁵ Assessment of fractional area shortening (FAS), PWT, ST, LVESD, and LVEDD after transverse aortic constriction (TAC) was performed using a Vevo2100 system (VisualSonics, Toronto, ON, Canada). See Supplemental Methods for further details.

2.3 Positron emission tomography analysis

The [¹⁸F]FTHA and [¹⁸F]FDG positron emission tomography (PET) measurements were performed on a dedicated small animal Inveon PET scanner (Siemens Healthcare, Knoxville, TN, USA) with 2 days in between to monitor the energy alteration of fatty acid oxidation and glucose metabolism. Experimental details of the PET analysis and the radiotracer production can be found in the Supplemental Methods section.

2.4 Histology

For Masson's Trichrome and periodic acid-Schiff staining, heart tissue was fixed in 4% paraformaldehyde in phosphate-buffered saline (PBS) and embedded in paraffin before sectioning. To visualize triglycerides and lipids, 10- μ m-thick cryosections were prepared and stained with Sudan III. Nuclei were stained with Haematoxylin.

2.5 Immunohistochemistry

Paraffin-embedded sections were immunostained using the CSA II System (Dako, Carpinteria, CA, USA) as described previously by our group.¹¹ The anti-HIF-1 α primary antibody (Novus NB100-123) was used at a 1:1000 dilution.

2.6 Cryosections and immunofluorescence labelling

Freshly isolated hearts were treated and stained as described before.¹⁶ Details can be found in the Supplemental Methods section.

2.7 RNA extraction and RT-PCR analysis

After RNA extraction, reverse transcription was performed with 2 μ g of RNA and a first strand complementary DNA (cDNA) synthesis kit (Fermentas GmbH, St Leon-Rot, Germany). mRNA levels were quantified by using 0.5 μ L of the cDNA reaction and the SyBR Green qPCR reaction kit (Agilent, Santa Clara, CA, USA) in combination with the MX3005P light cycler (Stratagene, Santa Clara, CA, USA). The initial template concentration of each sample was calculated by comparison with serial dilutions of a calibrated standard. Primer sequences can be found in the Supplemental Methods section.

2.8 Western blot

Heart tissue was rapidly homogenized in a buffer containing 4 M urea, 140 mM Tris (pH 6.8), 1% SDS, 2% NP-40 and protease inhibitors (Roche, Grenzach, Germany). For immunoblot analysis, protein samples were resolved by SDS-PAGE and transferred onto nitrocellulose membranes (Amersham Biosciences, München, Germany) by semi-dry blotting (PeqLab, Erlangen, Germany). Membranes were probed with specific antibodies (see Supplemental Methods).

2.9 Isolation of cardiomyocytes and measurement of cardiomyocyte shortening and intracellular Ca²⁺

Hearts were excised from mice that were anaesthetized in an anaesthetic induction chamber with isoflurane and mounted on a Langendorff perfusion apparatus. The ventricular tissue was digested enzymatically, and single myocytes were isolated. After Ca²⁺ reintroduction (stepwise increase to 0.8 mM), myocytes were then plated onto superfusion chambers and used for immediate measurements. Myocytes were loaded with fluo-3. The dye was excited and emitted fluorescence measured. From the raw fluorescence, $\Delta F/F_0$ (increase in fluorescence compared to baseline) was calculated. Myocytes were field stimulated (voltage 25% above threshold) at 0.5, 1, 2, and 4 Hz at 37°C until a steady state was achieved; only those cells exhibiting stable steady-state contractions were included in the study. At least 25 myocytes from four mice per group were studied. For the measurements of cardiomyocyte shortening and Ca²⁺ transients, the investigator was blinded regarding genotypes. For additional details see Supplemental Methods.

2.10 Flow cytometry analysis

Seven days after sham surgery or TAC surgery, left ventricles were isolated and sliced into small pieces. Tissue digestion, staining procedure, and subsequent flow cytometry analysis are described in the Supplemental Methods.

2.11 Human myocardial tissue

Failing left ventricular (LV) tissues were obtained from patients with end-stage heart failure [dilated cardiomyopathy (DCM, $n = 9$) and ischaemic cardiomyopathy (ICM, $n = 10$)] undergoing heart transplantation. The LV ejection fraction was <30%, cardiac index 1.5–3.0 L/min \times m². Eight non-failing LV tissues (NF) from organ donors that could not be

transplanted for technical reasons were used as controls. Donor patient histories or echocardiography revealed no signs of heart disease. Details have been published previously.¹⁷ The study conforms to the principles outlined in the Declaration of Helsinki and was reviewed and approved by the Ethical Committee of the University Hospital Hamburg (Az. 532/116/9.7.1991).

2.12 Statistical analyses

Data are presented as means \pm SEM. We determined statistical differences by two-tailed Student's *t*-test (Figures 1B, C, and G; 2A, C, and D; 3A, B, D, and E; 4A, D, and I; and 5B; see Supplementary material online, Figure S2C–E and S3), one-way ANOVA (see Supplementary material online, Figure S2A and B; and Figure 5H) and two-way ANOVA (Figures 4F–H; 5A; and 5C–G). ANOVAs were followed by Bonferroni *post hoc* tests. A *P*-value less than 0.05 was considered statistically significant.

3. Results

3.1 Cardiomyopathy is associated with increased protein levels of HIF-1 α

In acute ischaemia, HIF-1 α is stabilized in the heart.¹⁸ To determine whether the HIF system is still affected in prolonged heart failure, we analysed HIF-1 α protein levels in ventricular tissue samples of patients with ICM and DCM and samples of non-failing hearts. In DCM samples, we found increased HIF-1 α protein levels compared with NF heart samples. In ICM samples, the increase was subtle and not significant (Figure 1A and B). Taken together with the previously described increased HIF-1 α protein levels in HCM patients,¹⁹ these data indicate a chronic activation of the HIF pathway in some heart failure patients.

3.2 Cardiac-specific *Hif-1 α ^{tg}* mice have normal heart function in the resting state

To dissect the impact of elevated HIF-1 α expression in the heart, we analysed the consequences of transgenic cardiac overexpression of HIF-1 α in a mouse model. *Hif-1 α ^{tg}* mice demonstrate significantly increased HIF-1 α RNA and protein levels in the heart, as demonstrated by quantitative real-time RT-PCR, western blot and immunohistochemistry analyses (Figure 1C–E). Transverse Masson's Trichrome- and Sirius Red stained heart sections of 2-month-old *Hif-1 α ^{tg}* mice did not reveal any obvious signs of gross malformation or fibrosis (Figure 1F and Supplementary material online, Figure S1). Likewise, heart weight related to body weight did not show any difference when *Hif-1 α ^{tg}* mice were compared with their wild-type littermates (Figure 1G). This was also verified by the analysis of septum thickness and posterior wall thickness by echocardiography. In addition, there was no significant change in fractional shortening, heart rate (see Supplementary material online, Figure S2A), or blood pressure (see Supplementary material online, Figure S2B).

3.3 Cardiac-specific *Hif-1 α ^{tg}* mice show differences in the expression of genes related to vasotonus, anaerobic metabolism and Ca²⁺ handling

HIF-1 affects diverse pathways associated with cellular and systemic adaptation to hypoxic conditions, including oxygen supply and metabolism, which are important for HIF-mediated tissue-protective

effects.⁹ Oxygen supply via the bloodstream is affected by vessel density and vessel diameter. Most interestingly, we found a significant up-regulation of the vascular endothelial growth factor in the hearts of the *Hif-1 α ^{tg}* mice only, whereas the expression of angiopoietin 1 and 2 was unaffected (Figure 2A). In contrast, we detected several HIF-1 target genes involved in regulating vascular tone, i.e. adrenomedullin, apelin, CD73, and inducible nitric oxide synthase to be up-regulated in the hearts of the *Hif-1 α ^{tg}* mice. Correspondingly, we found no change in the number of capillaries when analysing cryosections of left ventricles obtained from *Hif-1 α ^{tg}* and *Hif-1 α ^{w/t}* mice by CD31 staining (Figure 2B and C); however, when analysing capillary area we found a significant increase in the *Hif-1 α ^{tg}* mice (Figure 2D). The expected improvement in oxygen supply might be at least one reason for the cardioprotective effect following a myocardial infarction that was previously described in *Hif-1 α ^{tg}* mice.¹⁴

Cellular metabolism is changed dramatically in response to hypoxia, with the net effect of increased anaerobic glycolysis. This has been attributed partly to HIF-mediated transcription of glucose transporter-1 (*Glut-1*) and glycolytic genes accompanied by pH buffering through the hypoxia-inducible carboanhydrase IX (CAIX).³ In line with those findings, we observed an increased mRNA expression of *Glut-1*, phosphofructokinase I (*Pfk1*) and CAIX in the *Hif-1 α ^{tg}* hearts (Figure 3A). To determine whether this was accompanied by changes in the metabolic footprint, we performed cardiac [¹⁸F]FDG PET analysis. Compared with their wild-type littermates, hearts of *Hif-1 α ^{tg}* mice used more glucose (Figure 3B), without changes in blood glucose and insulin levels (see Supplementary material online, Figure S2C and D). When exposing tumour cells to hypoxia, increased anaerobic glucose metabolism is paradoxically associated with increased glycogen storage.²⁰ Unlike the situation in tumour tissue, we could not find an increased expression of glycogen synthase 1 (*Gys1*) and only a 1.5-fold increase in glycogen branching enzyme 1 (*GBE1*; Figure 3A). Moreover, there were no signs of increased glycogen storage in the hearts of *Hif-1 α ^{tg}* animals (Figure 3C). When analysing lipid metabolism as determined by quantifying the expression of peroxisome proliferator-activated receptor α (*PPAR α*) and *PPAR γ* and the expression of the *PPAR γ* target gene product, fatty acid translocase (*FAT*), we found a weak yet significant down-regulation of *PPAR α* , but no transcriptional changes in *PPAR γ* and *FAT* (Figure 3D). A slight down-regulation in fatty acid metabolism in *Hif-1 α ^{tg}* mice was seen when performing cardiac [¹⁸F]FTHA PET analysis (Figure 3E). This was not significant and exhibited much lower standard uptake values (SUV) than [¹⁸F]FDG PET images of the myocardium. Sudan III staining revealed no signs of lipid accumulation in *Hif-1 α ^{tg}* mice (Figure 3F). Taking these results together, the *Hif-1 α ^{tg}* hearts demonstrate metabolic remodelling with an increase in glucose utilization.

Heart function relies critically on proper calcium handling. There is a recent report demonstrating that HIF-1 α impairs the promoter activity of the sarcoplasmic calcium pump, sarcoplasmic/endoplasmic reticulum calcium ATPase 2a (*SERCA2a*).²¹ These *in vitro* data were verified in our *in vivo* mouse model, because we observed a reduction of RNA and protein levels of *SERCA2a* in the *Hif-1 α ^{tg}* hearts when compared with their littermates (Figure 4A, B and D). Besides *SERCA2a*, calcium handling critically involves the function of ryanodine receptor 2 (*RyR2*) and phospholamban (*PLB*); thus, we also investigated possible changes of these calcium handling

proteins. RyR2 expression (Figure 4B) and PLB protein levels (Figure 4C) were unchanged. However, the phosphorylation level of PLB at the protein kinase A (PKA) phosphorylation site (Ser16) and the Ca^{2+} /calmodulin-dependent protein kinase II (CaMKII) phosphorylation site (Thr17) was elevated in the *Hif-1 α^{tg}* hearts by 60 and 61%, respectively (Figure 4C and D). These changes were not associated with increased CaMKII protein levels or increased CaMKII activity as determined by analysing the phosphorylation state of CaMKII (Figure 4E).

To investigate whether the observed changes in SERCA2a protein level and PLB activity result in abnormal Ca^{2+} handling, we determined Ca^{2+} dynamics of isolated cardiomyocytes. *Hif-1 α^{tg}* cells demonstrated significantly increased intracellular

Ca^{2+} transients when stimulated at 0.5–4 Hz (Figure 4F). Twitch relaxation and intracellular $[\text{Ca}^{2+}]$ decline, which are approximately 90% dependent on SERCA function in mice,²² were significantly increased and thus faster in cardiomyocytes isolated from transgenic vs. wild-type mice (Figure 4G and H). Yet, the sarcoplasmic reticulum Ca^{2+} load did not differ ($P > 0.05$) when comparing isolated cardiomyocytes from both genotypes (Figure 4I). Overall, these data indicate that chronic overexpression of HIF-1 α alters Ca^{2+} handling properties of the myocardium, and that alterations in PLB phosphorylation may functionally override a reduction in SERCA2a protein levels.

3.4 *Hif-1 α^{tg}* transgenic mice develop heart failure with advanced age, or at a young age when challenged by increased mechanical load

The alterations identified in the *Hif-1 α^{tg}* mice regarding vessel area, metabolism, and calcium handling are at least partly protective adaptive mechanisms, which can be interpreted as improved oxygen supply and energy-saving mechanisms in response to ischaemia. Indeed, similar mechanisms do occur as compensatory mechanisms during the development of ischaemic heart failure.^{23,24} Despite those changes, *Hif-1 α^{tg}* mice demonstrated no decrease in heart function at the age of 3 months, as described above. To determine whether chronic activation of the HIF-induced adaptive pathways alters heart function over time, we followed *Hif-1 α^{tg}* and *Hif-1 α^{wt}* littermates over a period of 8 months (Figure 5A). With age, *Hif-1 α^{tg}* mice developed a spontaneous increase in septum wall thickness and a decrease in fractional shortening, indicating that over time the HIF-1 α -mediated changes result in cardiomyopathy.

Cardiac decompensation can be triggered by increased mechanical load. Initially, pressure overload leads to a compensatory response and myocardial remodelling, with a development of cardiac hypertrophy and ventricular dilatation. Ultimately, these changes have a det-

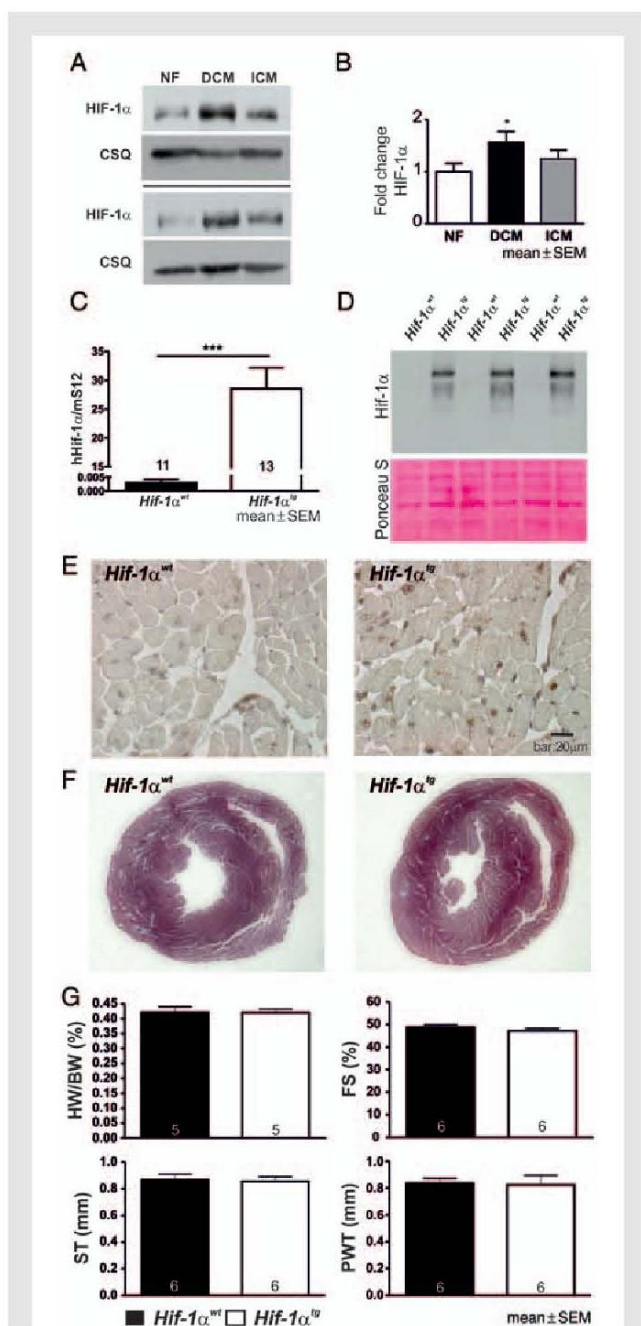
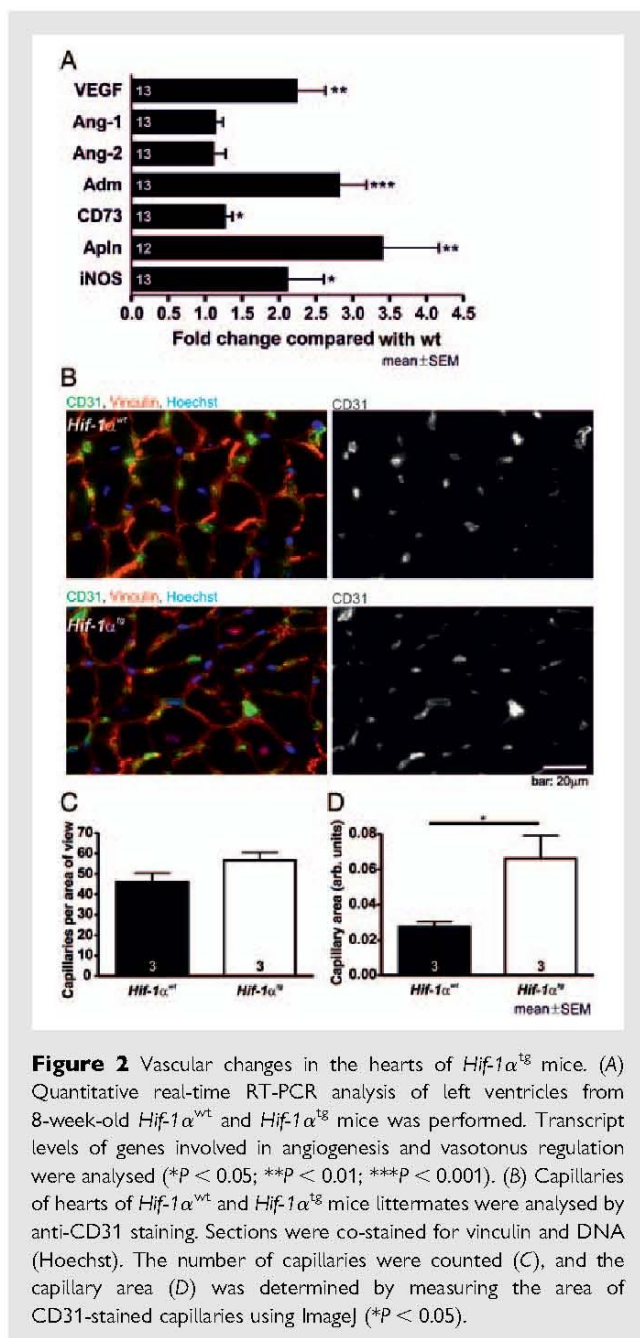


Figure 1 HIF-1 α accumulates in human DCM samples. Cardiac-specific HIF-1 α transgenic mice show no gross structural changes and have normal heart function in the resting state. (A) HIF-1 α protein was detected by western blot analysis. Tissue homogenates were prepared from normal, non-failing hearts (NF), and hearts of patients with end-stage dilated cardiomyopathy (DCM) and ischaemic cardiomyopathy (ICM). Samples were probed for HIF-1 α and calsequestrin (CSQ). (B) Bar graph shows mean values (\pm SEM) from densitometric analysis of all hearts analysed in A. Protein levels in DCM and ICM hearts are expressed as fold change relative to protein levels in NF, which was set to 1 ($*P < 0.05$). (C) RT-PCR analysis confirmed the significant increase of HIF-1 α mRNA transcripts in the left ventricles of *Hif-1 α^{tg}* mice compared with *Hif-1 α^{wt}* littermates ($***P < 0.001$). (D) Protein extracts prepared from left ventricles of *Hif-1 α^{wt}* and *Hif-1 α^{tg}* mice were analysed with anti-HIF-1 α antibodies, confirming stabilization of HIF-1 α protein in transgenic animals. (E) Immunohistochemical analyses of hearts from *Hif-1 α^{wt}* and *Hif-1 α^{tg}* mice. (F) Paraffin-embedded tissue sections of *Hif-1 α^{wt}* and *Hif-1 α^{tg}* hearts stained with Trichrome. (G) Hearts of 8-week-old female *Hif-1 α^{wt}* and *Hif-1 α^{tg}* mice were excised, and the ratios of heart weight (HW) to body weight (BW) were determined. Septum thickness (ST), posterior wall thickness (PWT) and fractional shortening (FS) were analysed by echocardiography.



perimental effect on ventricular function, resulting in heart failure. We investigated the response of 2-month-old *Hif-1 α^{ts}* mice and *Hif-1 α^{wt}* littermates to increased mechanical load after TAC. Constriction of the aorta resulted in a significantly increased pressure afterload, which was not different between *Hif-1 α^{ts}* mice and *Hif-1 α^{wt}* groups (Figure 5B). Cardiac HIF-1 α protein levels were not obviously changed 8 weeks after TAC treatment in *Hif-1 α^{ts}* mice and *Hif-1 α^{wt}* , as detected by western blotting (see Supplementary material online, Figure S3A). Myocardial inflammation in sham-operated and TAC-treated animals did not show any differences when *Hif-1 α^{ts}* mice were compared with their wild-type littermates, as determined by quantifying the number of CD45-positive cells (see

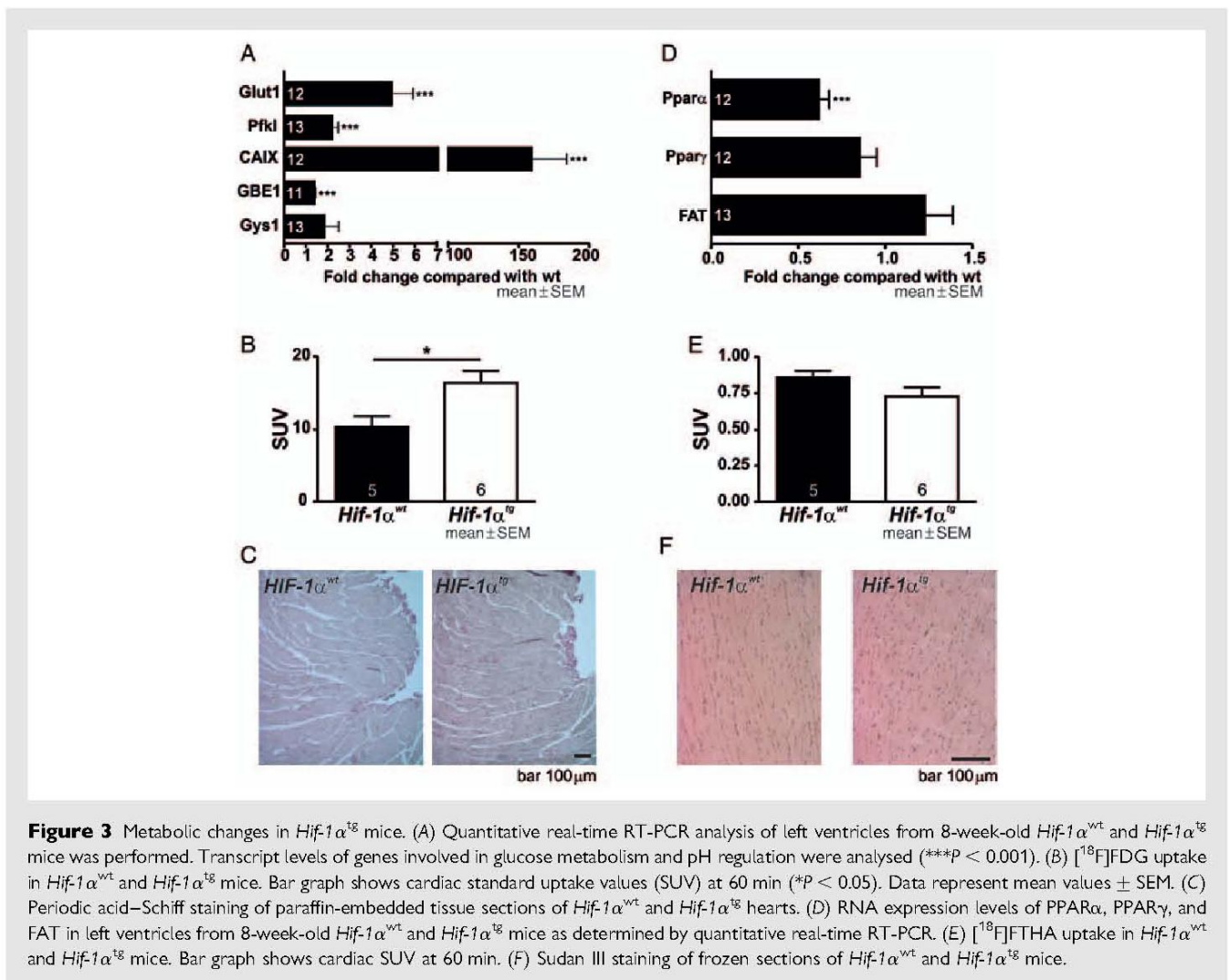
Supplementary material online, Figure S3B). Left ventricular hypertrophy was indicated by a significant increase in ST and PWT in TAC-treated *Hif-1 α^{ts}* mice (Figure 5C and D) 2 weeks after surgery, as determined by echocardiography. While *Hif-1 α^{wt}* mice did not show any signs of decompensation compared with sham-treated mice, the *Hif-1 α^{ts}* mice demonstrated a significant increase in LVESD 4 and 8 weeks after surgery (Figure 5E), together with a decrease in FAS (Figure 5F). The LVEDD (Figure 5G) was not significantly affected in TAC-treated transgenic mice compared with wild-type animals. In support of the TAC-induced hypertrophy and heart failure in *Hif-1 α^{ts}* mice, the heart-to-tibia length ratio was also increased (Figure 5H). Taking these results together, chronic activation of HIF-1 triggers intrinsic pathways in the cardiomyocytes, which impair long-term preservation of heart function and weaken adaption to increased mechanical load.

4. Discussion

There is ample evidence that HIF-1 protects the heart from an acute ischaemic insult. Based on the characterization of the *Hif-1 α^{ts}* hearts, as demonstrated in our study, this may be attributed to an increased capillary area in the heart and metabolic preconditioning via increasing gene expression and glucose metabolism that is necessary for the anaerobic metabolic switch. Moreover, the changes in calcium handling in *Hif-1 α^{ts}* hearts demonstrate energy-saving mechanisms regarding the depressed SERCA2a expression. The decrease in SERCA2a might be counter-regulated by an increased PLB phosphorylation and thus, a net increase in calcium release and shorter relaxation time. Although the HIF-mediated adaptation pathways regarding metabolic reprogramming and altered calcium handling are beneficial to withstand acute ischaemia, these same pathways are indicative of defective cardiac homeostasis in the failing heart.^{11,24,25} Accordingly, the tissue-protective properties of HIF-1 in the young *Hif-1 α^{ts}* mice were accompanied by development of heart failure with ageing or after increased mechanical load. Thus, it is tempting to speculate that chronic activation of HIF-1 and its associated adaptive pathways alone are sufficient to induce cardiomyopathy. We found increased protein levels of HIF-1 α in heart samples of cardiomyopathy patients, indicating that the HIF pathway is activated during disease progression. According to the data obtained with our mouse model, induction of this regulatory pathway may be beneficial initially; however, if sustained it may actively contribute to heart failure.

Bao *et al.*²⁶ showed in a rat model that treatment with GSK360A, and thus chronic stabilization of HIF-1 α signalling, after myocardial infarction improved cardiac remodelling and ventricular performance in the ischaemic myocardium without affecting infarct size. This is contrary to the observed cardioprotective effect in the *Hif-1 α^{ts}* mice, which goes along with a decreased infarct size. In the study of Bao *et al.* no long-term maladaptive effects were observed 3 months after treatment. Nevertheless, it should be noted that the animals were treated systemically, whereas in the *Hif-1 α^{ts}* mice HIF-1 α is stabilized in cardiomyocytes only. Furthermore, treatment with the PHD-inhibiting compound GSK360A lasted for only 4 weeks, after which the compound was withdrawn and washed out.

Likewise, the cardiac short hairpin RNA PHD2 knockdown after myocardial infarction mediates HIF-1 α up-regulation and improved cardiac function²⁷ without any chronic adverse effects. Again, however, in that mouse model the HIF-1 α protein levels returned to baseline only 4 weeks after short hairpin RNA injection, whereas



in the present *Hif-1α^{tg}* mice we saw the first signs of cardiomyopathy at 3 months of age.

A detrimental effect associated with long-term stabilization of HIF-1α is similar to ventricular dysfunction of the heart in cardiac-specific pVHL^{-/-} mice.²⁸ It is important to note that a detrimental cardiac effect was also reported in tetracycline-inducible cardiac-specific HIF-1α transgenic mice and cardiac-specific HIF-2α transgenic mice.^{29,30} In both mouse models, the authors demonstrated a spontaneous cardiac decompensation of the mice at a young age, whereas the animals in our mouse model demonstrated normal heart function in non-challenged conditions but aggravated myocardial dysfunction over time and after TAC. This development of cardiomyopathy over time enabled us to determine the HIF-dependent adaptive changes in the heart, as described above, which occur before the onset of heart failure. While Bekeredjian *et al.* have created tetracycline-inducible HIF-1α overexpressing mice, we analysed an unregulated HIF-1α transgenic mouse model, which most probably presents a lower transgenic HIF-1α expression compared with the acutely inducible model.²⁹ This assumption is additionally supported by the fact that in the tetracycline-inducible model, an HIF-1α variant was used that substituted amino acids critical to HIF-1α

degradation (i.e. Pro402Ala, Pro564Ala, and Asn803Ala), whereas in the present model the wild-type HIF-1α protein was overexpressed. Likewise, Moslehi *et al.* have created a cardiac-specific HIF-2α transgenic mouse model, which overexpresses a non-hydroxylatable HIF-2α variant.³⁰ The different degrees of HIFα levels over time may explain the varying onset of heart failure in our model compared with the tetracycline-inducible HIF-1α model and the HIF-2α transgenic mice. Interestingly, we previously showed that mice with reduced HIF-1α levels (HIF-1α^{+/-} mice) also develop heart failure after TAC.¹⁵ This might imply that HIF-1α protein levels need to be tightly regulated, whereby neither decreased nor elevated HIF-1α protein levels can be tolerated.

While ischaemia develops rapidly in myocardial infarction, tissue hypoxia supposedly develops over a longer period of time during cardiac hypertrophy. The heart is particularly susceptible to hypoxia/ischaemia, because only limited reserves of high-energy phosphates are maintained.³¹ Quick metabolic reprogramming to anaerobic metabolism is therefore of critical importance to the heart's survival of an acute ischaemic insult.³² The *Hif-1α^{tg}* hearts demonstrated signs of energy metabolism remodelling, with a shift towards glucose consumption. The ratio of ATP synthesis compared with

3. Original Publications

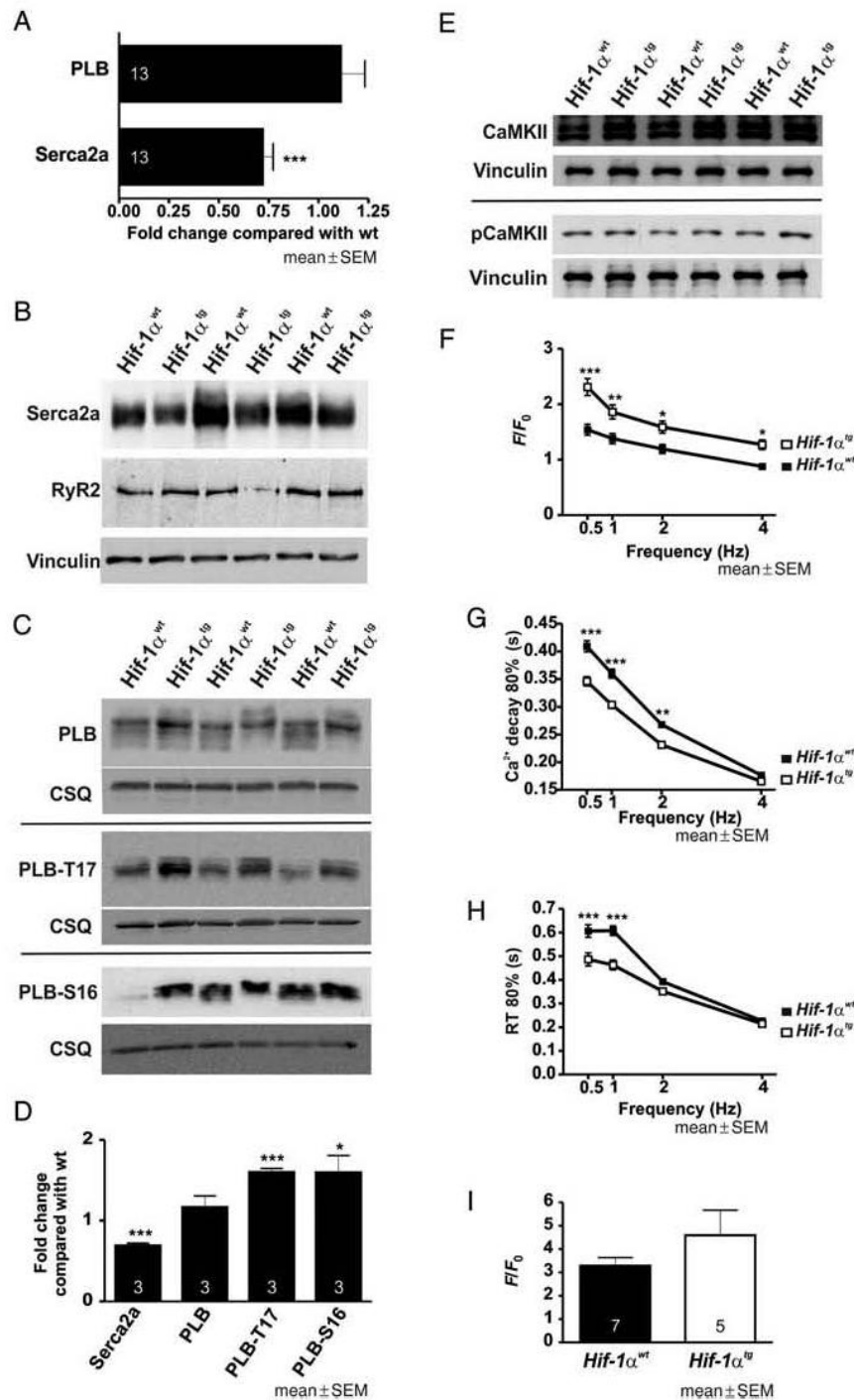


Figure 4 Changes in calcium handling in cardiomyocytes of *Hif1 α^{tg}* mice. (A) RNA expression of SERCA2a and phospholamban (PLB) in left ventricles of 8-week-old *Hif1 α^{wt}* and *Hif1 α^{tg}* mice was determined in quantitative real-time RT-PCR analysis (***) $P < 0.001$). (B) SERCA2a protein levels were decreased and RyR2 protein levels unchanged in the left ventricles of *Hif-1 α^{tg}* mice compared with *Hif-1 α^{wt}* mice, as determined by western blot analysis. (C) Protein expression of calcium handling proteins was detected by western blot analysis of protein extracts from left ventricles of *Hif1 α^{wt}* and *Hif1 α^{tg}* mice. (D) Quantification of SERCA2a, PLB, PLB T-17 and PLB-S16 protein levels as shown in A, B and C was determined by western blot analysis. (E) CaMKII and phosphorylated CaMKII protein levels were determined by western blot analysis. (F–I) Ca^{2+} homeostasis in isolated *Hif1 α^{wt}* and *Hif1 α^{tg}* cardiomyocytes. Cells were stimulated at 0.5–4 Hz and analysed for Ca^{2+} transient amplitude (F; ***) $P < 0.01$, ***) $P < 0.001$; data represent mean values \pm SEM), RT 80% intracellular $[Ca^{2+}]$ decline (G; ***) $P < 0.001$; data represent mean values \pm SEM), and RT 80% twitch relaxation (H; ***) $P < 0.01$, ***) $P < 0.001$). (I) The sarcoplasmic reticulum Ca^{2+} content is unaltered in cardiomyocytes from *Hif1 α^{tg}* mice measured by caffeine-induced Ca^{2+} transients.

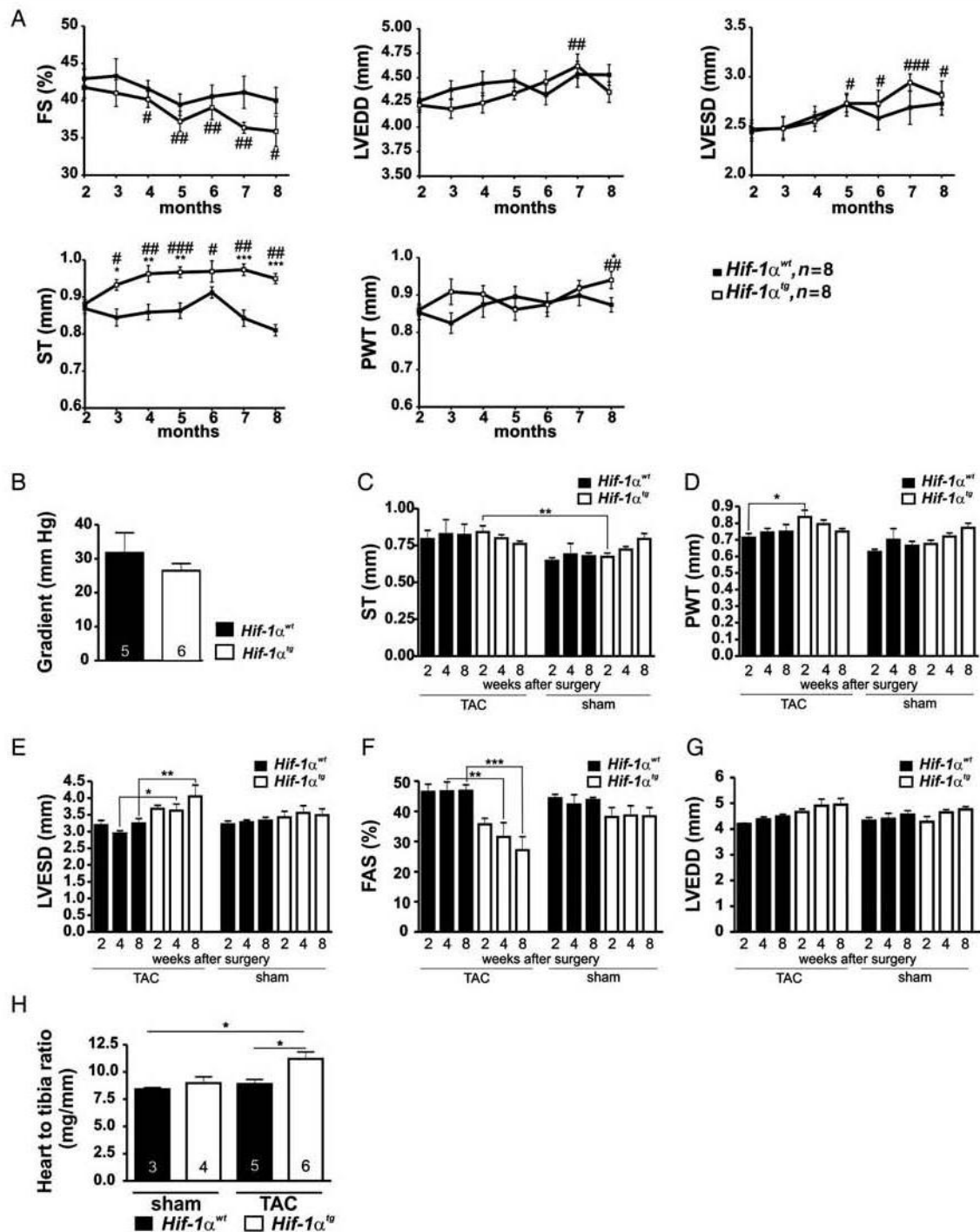
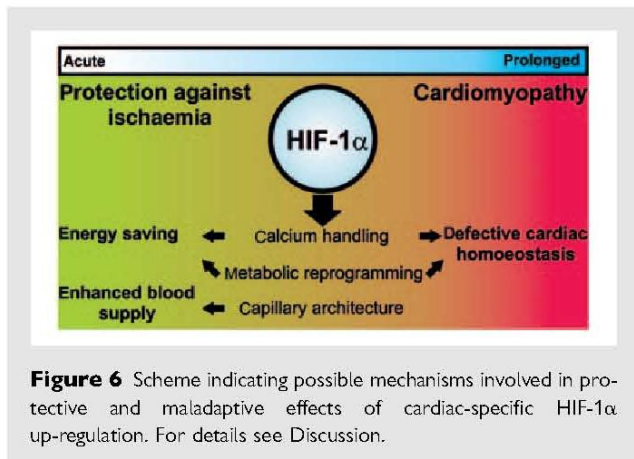


Figure 5 *Hif-1α^{tg}* mice develop signs of heart failure with ageing and after transverse aortic constriction. (A) Echocardiographic measurements were performed serially on a cohort of male *Hif-1α^{wt}* ($n = 8$) and *Hif-1α^{tg}* mice ($n = 8$) between the age of 2 and 8 months. Fractional shortening (FS), septum thickness (ST), posterior wall thickness (PWT), left ventricular end-diastolic diameter (LVEDD), and left ventricular end-systolic diameter (LVESD) were analysed ($*P < 0.05$, $**P < 0.01$, $***P < 0.001$, *Hif-1α^{tg}* mice vs. *Hif-1α^{wt}* control mice; $\#P < 0.05$, $\#\#\#P < 0.001$, aged *Hif-1α^{tg}* mice vs. 2-month-old *Hif-1α^{tg}* mice). Sustained pressure overload was induced in female *Hif-1α^{wt}* and *Hif-1α^{tg}* mice by TAC [TAC treatment, *Hif-1α^{wt}* ($n = 5$) and *Hif-1α^{tg}* ($n = 6$); sham treatment, *Hif-1α^{wt}* ($n = 3$) and *Hif-1α^{tg}* ($n = 4$)]. (B) The TAC-induced pressure gradient was measured 1 day after surgery. Numbers in the bars indicate the number of animals in each group. ST (C), PWT (D), LVESD (E), fractional area shortening (FAS; F), and LVEDD (G) were analysed 2, 4, and 8 weeks after TAC by echocardiography. (H) The heart weight-to-tibia length ratios were determined 8 weeks after TAC ($*P < 0.05$).



the spent O₂ is lower when glucose vs. fatty acids is consumed. This mechanism is used by the heart in the case of severe ischaemia and, based on our results demonstrated here, is transcriptionally controlled at least in part by HIF-1. On the molar basis over the long term, however, much more ATP is produced from fatty acid oxidation than from anaerobic glucose utilization.³³ In uncompensated hypertrophy and in other forms of heart failure as a consequence of high energy demand, a sole increase in glucose uptake and utilization is therefore not sufficient to compensate for the overall energy demand.³⁴ Thus, the HIF-1 α overexpressing heart seems to be well prepared to face an acute ischaemic insult via expression of anaerobic metabolism-related genes and adapting calcium handling. In line with our results, a previous study has shown that constitutive HIF-1 α overexpression protects the heart from diabetic-induced glucose metabolism impairment, partly by up-regulation of Glut-1.³⁵ The metabolic preconditioning in HIF-1 α transgenic mice, however, seems not to be sufficient for the adaptation towards increased mechanical load, because energy supply may be a limiting factor in this hypertrophy-inducing and energy-wasting setting.

In summary, the cardiac stabilization of HIF-1 α results in tissue protection in the case of myocardial infarction.¹⁴ HIF-mediated pathways involved may include changes in vascular tone, energy metabolism, and calcium handling (Figure 6). According to our results, long-term activation of HIF-1 and its associated adaptive pathways is detrimental. Although short-term activation of HIF-1 is beneficial and may be used in therapeutic strategies, prolonged activation of HIF-1 over time drives the development of cardiomyopathy.

Supplementary material

Supplementary material is available at *Cardiovascular Research* online.

Acknowledgements

We would like to acknowledge the technical support of Annette Hillemann, Anika Hunold, Felicia Steuer, and Thomas Sowa. Mareike Lehnhoff, Maren König, and Daniel Bukala were of valuable help in PET measurements. The radiopharmacy group, Gerald Reischl, Denis Lamparter, and Walter Ehrlichmann, of the Department of Pre-clinical Imaging and Radiopharmacy at the University Hospital of Tübingen, is acknowledged for radiotracer production. We also

thank Samantha Whitman (University of Arizona, Tucson, AZ, USA) for her help preparing this manuscript.

Conflict of interest: none declared.

Funding

This work was supported by grants from the Else Kröner-Fresenius-Stiftung (P25/10/A12/10 to A.Z.); and the Deutsche Forschungsgemeinschaft (Ka1269/11-1 to D.M.K.).

References

- Mudd JO, Kass DA. Tackling heart failure in the twenty-first century. *Nature* 2008;**451**: 919–928.
- Giordano FJ. Oxygen, oxidative stress, hypoxia, and heart failure. *J Clin Invest* 2005; **115**:500–508.
- Majmundar AJ, Wong WJ, Simon MC. Hypoxia-inducible factors and the response to hypoxic stress. *Mol Cell* 2010;**40**:294–309.
- Jewell UR, Kvietkova I, Scheid A, Bauer C, Wenger RH, Gassmann M. Induction of HIF-1 α in response to hypoxia is instantaneous. *FASEB J* 2001;**15**:1312–1314.
- Ivan M, Kondo K, Yang H, Kim W, Valiando J, Ohh M *et al*. HIF α targeted for VHL-mediated destruction by proline hydroxylation: implications for O₂ sensing. *Science* 2001;**292**:464–468.
- Jaakkola P, Mole DR, Tian YM, Wilson MI, Gielbert J, Gaskell SJ *et al*. Targeting of HIF- α to the von Hippel-Lindau ubiquitylation complex by O₂-regulated prolyl hydroxylation. *Science* 2001;**292**:468–472.
- Hon WC, Wilson MI, Hartos K, Claridge TD, Schofield CJ, Pugh CW *et al*. Structural basis for the recognition of hydroxyproline in HIF-1 α by pVHL. *Nature* 2002;**417**: 975–978.
- Min JH, Yang H, Ivan M, Gertler F, Kaelin WG Jr, Pavletich NP. Structure of an HIF-1 α -pVHL complex: hydroxyproline recognition in signaling. *Science* 2002;**296**: 1886–1889.
- Wenger RH, Stiehl DP, Camenisch G. Integration of oxygen signaling at the consensus HRE. *Sci STKE* 2005;**2005**:re12.
- Eckle T, Kohler D, Lehmann R, El Kasmi K, Eitzschig HK. Hypoxia-inducible factor-1 is central to cardioprotection: a new paradigm for ischemic preconditioning. *Circulation* 2008;**118**:166–175.
- Hölscher M, Silter M, Krull S, von Ahlen M, Hesse A, Schwartz P *et al*. Cardiomyocyte-specific prolyl-4-hydroxylase domain 2 knock out protects from acute myocardial ischemic injury. *J Biol Chem* 2011;**286**:11185–11194.
- Hyvarinen J, Hassinen IE, Sormunen R, Maki JM, Kivirikko KI, Koivunen P *et al*. Hearts of hypoxia-inducible factor prolyl 4-hydroxylase-2 hypomorphic mice show protection against acute ischemia-reperfusion injury. *J Biol Chem* 2010;**285**:13646–13657.
- Myylyharju J. HIF prolyl 4-hydroxylases and their potential as drug targets. *Curr Pharm Des* 2009;**15**:3878–3885.
- Kido M, Du L, Sullivan CC, Li X, Deutsch R, Jamieson SW *et al*. Hypoxia-inducible factor 1 α reduces infarction and attenuates progression of cardiac dysfunction after myocardial infarction in the mouse. *J Am Coll Cardiol* 2005;**46**:2116–2124.
- Silter M, Kögler H, Ziesenis A, Wiltung J, Schäfer K, Toischer K *et al*. Impaired Ca²⁺-handling in HIF-1 α ^{+/−} mice as a consequence of pressure overload. *Pflügers Arch* 2010;**459**:569–577.
- Ziesenis A, Schroeder U, Buchmeier S, Schoenenberger CA, van den Heuvel J, Jockusch BM *et al*. Raver1 is an integral component of muscle contractile elements. *Cell Tissue Res* 2007;**327**:583–594.
- El-Armouche A, Ouchi N, Tanaka K, Doros G, Wittköpper K, Schulte T *et al*. Follistatin-like 1 in chronic systolic heart failure: a marker of left ventricular remodeling. *Circ Heart Fail* 2011;**4**:621–627.
- Lee SH, Wolf PL, Escudero R, Deutsch R, Jamieson SW, Thistlethwaite PA. Early expression of angiogenesis factors in acute myocardial ischemia and infarction. *N Engl J Med* 2000;**342**:626–633.
- Krishnan J, Suter M, Windak R, Krebs T, Felley A, Montessuit C *et al*. Activation of a HIF-1 α -PPAR γ axis underlies the integration of glycolytic and lipid anabolic pathways in pathologic cardiac hypertrophy. *Cell Metab* 2009;**9**:512–524.
- Pescador N, Villar D, Cifuentes D, Garcia-Rocha M, Ortiz-Barahona A, Vazquez S *et al*. Hypoxia promotes glycogen accumulation through hypoxia inducible factor (HIF)-mediated induction of glycogen synthase 1. *PLoS One* 2010;**5**:e9644.
- Ronkainen VP, Skoumal R, Tavi P. Hypoxia and HIF-1 suppress SERCA2a expression in embryonic cardiac myocytes through two interdependent hypoxia response elements. *J Mol Cell Cardiol* 2011;**50**:1008–1016.
- Li L, Chu G, Kranias EG, Bers DM. Cardiac myocyte calcium transport in phospholamban knockout mouse: relaxation and endogenous CaMKII effects. *Am J Physiol* 1998;**274**:H1335–H1347.
- Knuuti J, Tuunanen H. Metabolic imaging in myocardial ischemia and heart failure. *Q J Nucl Med Mol Imaging* 2010;**54**:168–176.

3. Original Publications

24. Hasenfuss G, Schillinger W, Lehnart SE, Preuss M, Pieske B, Maier LS et al. Relationship between Na^+ - Ca^{2+} -exchanger protein levels and diastolic function of failing human myocardium. *Circulation* 1999;**99**:641–648.
25. Taegtmeyer H, Dilsizian V. Imaging myocardial metabolism and ischemic memory. *Nat Clin Pract Cardiovasc Med* 2008;**5**:S42–S48.
26. Bao W, Qin P, Needle S, Erickson-Miller CL, Duffy KJ, Ariazi JL et al. Chronic inhibition of hypoxia-inducible factor (HIF) prolyl 4-hydroxylase improves ventricular performance, remodeling and vascularity following myocardial infarction in the rat. *J Cardiovasc Pharmacol* 2010;**56**:147–155.
27. Huang M, Chan DA, Jia F, Xie X, Li Z, Hoyt G et al. Short hairpin RNA interference therapy for ischemic heart disease. *Circulation* 2008;**118**:S226–S233.
28. Lei L, Mason S, Liu D, Huang Y, Marks C, Hickey R et al. Hypoxia-inducible factor-dependent degeneration, failure, and malignant transformation of the heart in the absence of the von Hippel-Lindau protein. *Mol Cell Biol* 2008;**28**:3790–3803.
29. Bekeredjian R, Walton CB, MacCannell KA, Ecker J, Kruse F, Outten JT et al. Conditional HIF-1 α expression produces a reversible cardiomyopathy. *PLoS One* 2010;**5**: e11693.
30. Mostlehi J, Minamishima YA, Shi J, Neuberger D, Charytan DM, Padera RF et al. Loss of hypoxia-inducible factor prolyl hydroxylase activity in cardiomyocytes phenocopies ischemic cardiomyopathy. *Circulation* 2010;**122**:1004–1016.
31. Taegtmeyer H, Wilson CR, Razeghi P, Sharma S. Metabolic energetics and genetics in the heart. *Ann N Y Acad Sci* 2005;**1047**:208–218.
32. Jennings RB, Reimer KA. The cell biology of acute myocardial ischemia. *Annu Rev Med* 1991;**42**:225–246.
33. Ingwall JS. Energy metabolism in heart failure and remodelling. *Cardiovasc Res* 2009;**81**: 412–419.
34. Neglia D, De Caterina A, Marraccini P, Natali A, Giardetti M, Vecoli C et al. Impaired myocardial metabolic reserve and substrate selection flexibility during stress in patients with idiopathic dilated cardiomyopathy. *Am J Physiol Heart Circ Physiol* 2007;**293**:H3270–H3278.
35. Xue W, Cai L, Tan Y, Thistlethwaite P, Kang YJ, Li X et al. Cardiac-specific over-expression of HIF-1 α prevents deterioration of glycolytic pathway and cardiac remodeling in streptozotocin-induced diabetic mice. *Am J Pathol* 2010;**177**: 97–105.

3. Original Publications

Supplemental figures

Fig.1

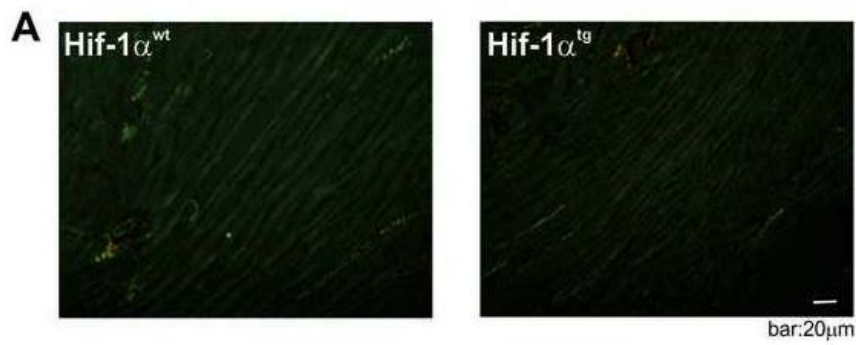
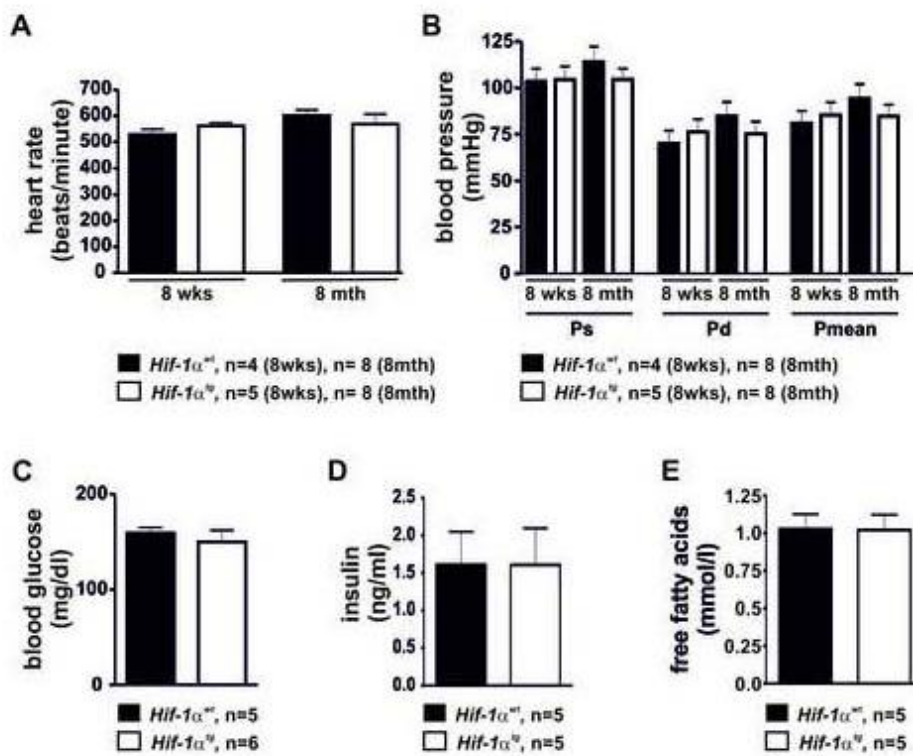
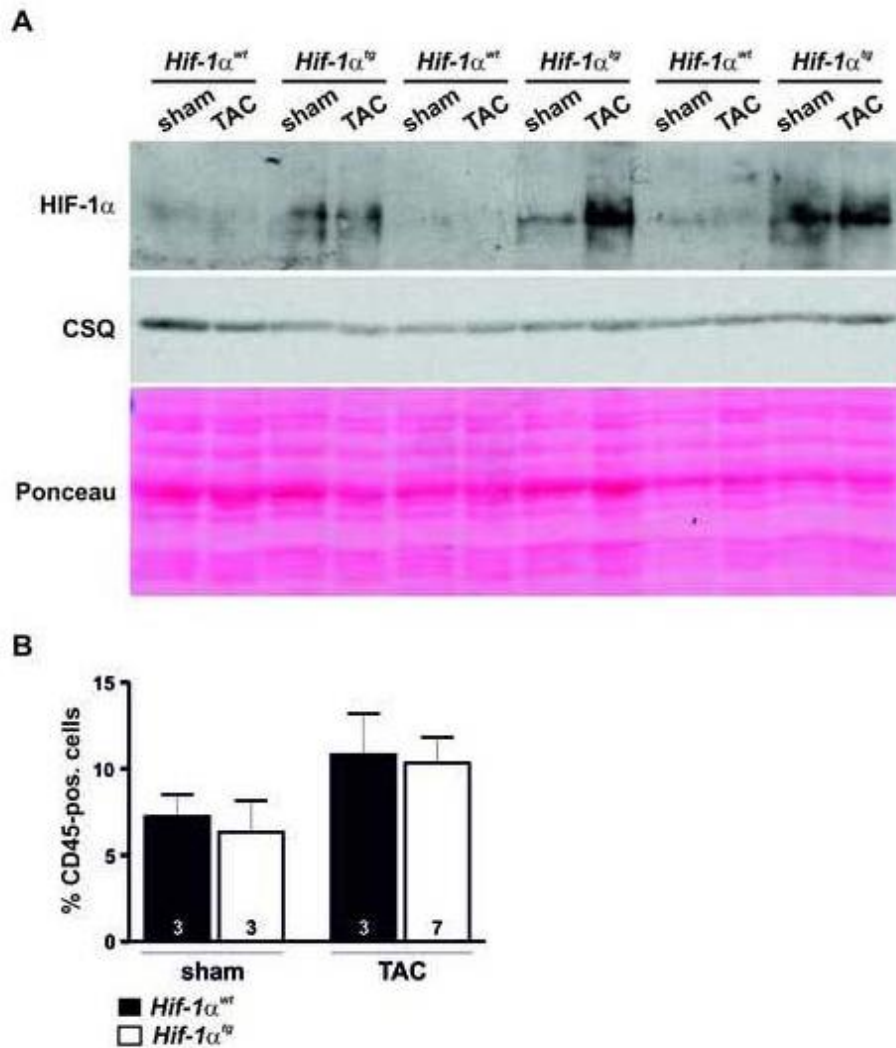


Fig.2



3. Original Publications

Fig.3



Supp. Fig. 1. Histological staining for collagen (Sirius Red) on *Hif-1 α^{wt}* and *Hif-1 α^{tg}* hearts.

Supp. Fig. 2. Heart rate (A), blood pressure (B) analyzed in 8 weeks and 8 month old mice, blood glucose (C), insulin (D) and free fatty acids (E) do not differ between *Hif-1 α^{wt}* and *Hif-1 α^{tg}* hearts.

Supp. Fig. 3. (A) HIF-1 α protein was detected by Western blot analysis of protein extracts from left ventricles of *Hif-1 α^{wt}* and *Hif-1 α^{tg}* mice 8 weeks after sham- and TAC-treatment. (B) Myocardial inflammation was analyzed in sham and TAC treated *Hif-1 α^{wt}* and *Hif-1 α^{tg}* hearts by CD45 flow cytometry.

3. Original Publications

Supplemental Methods

Primer sequences

mS12 forward, 5'-GAAGCTGCCAAGGCCTTAGA-3' and mS12 reverse, 5'-AACTGCAACCAACCACCTTC-3'; HIF-1 α forward, 5'-TGCATCTCCATCTCCTACCC -3' and HIF-1 α reverse, 5'-GTAGCTGCATGATCGTCTGG-3'; Glut1 forward, 5'-TGGCCTTGCTGGAACGGCTG-3' and Glut1 reverse, 5'-TCCTTGGGCTGCAGGGAGCA-3'; phosphofruktokinase 1 (Pfk1) forward, 5'-ACGAGGCCATCCAGCTCCGT-3' and Pfk1 reverse, 5'-TGGGGCTTGGGCAGTGTCT-3'; carbonic anhydrase IX (CA IX) forward, 5'-GGGGTTCATCTGGACTGTGTT-3' and CA IX reverse, 5'-CCCCTTCTGTGCCTGTGCT-3'; Glucan (1,4-alpha) branching enzyme (GBE1) forward, 5'-GCTTTCAGCTCCACAGGCCTACG -3' and GBE1 reverse, 5'-TGAGGGGGATCAGCGGCAACA-3'; Glycogen synthase 1 (Gys1) forward, 5'- CCCTGGGACACCCGCTAACTCTAC-3' and Gys1 reverse, 5'- CCCCTGTCACCTTCGCCTTCG -3'; adrenomedullin (Adm) forward, 5'-TGGCCCCCTACAAGCCAGCAAT-3' and adrenomedullin reverse, 5'-GCCAACGGGATACTCGCCCG-3'; apelin forward, 5'-TGCAGTTTGTGGAGTGCCACTG-3' and apelin reverse, 5'-GCACCGGGAGGCACT-3'; VEGFa forward, 5'-CACGACAGAAGGAGAGCAGAAGT-3' and VEGFa reverse, 5'- TTCGCTGGTAGACATCCATGAA-3'; angiopoietin (Ang)-1 forward, 5'-CGCTCTCATGCTAACAGGAGGTTGG-3' and Ang-1 reverse, 5'-GCATTCTCTGGACCCAAGTGGCG-3'; Ang-2 forward, 5'-CACCCAACCTCCAAGAGCTCGG-3' and Ang-2 reverse, 5'-CACGTAGCGGTGCTGACCGG-3'; Phospholamban (PLB) forward 5'-CCGAAGCCAAGACAGAAGCAGGTG-3' and PLB reverse, 5'-CCCATGACGGA GTGCTCGGC-3'; SERCA2a forward, 5'-AGATGGTCCTGGCAGATGAC-3' and SERCA2a reverse, 5'-CCAGGTCTGGAGGATTGAAC -3', PPAR α forward 5'-CACGGCGTGGTGC ATTTGGG-3' and PPAR α reverse 5'- TGACAGAGCCCTCGGAGCCC-3'; PPAR γ forward 5'-ACGGGTCTCGGTTGAGGGG-3' and PPAR γ reverse 5'-TCCGCCAAACCTGATGGCATT-3'; CD36 forward 5'-AATCCCTTGGCAACCAACCACA-3' and CD36 reverse 5'-GTGGCCCGTTCTACTAATTCATGA-3'; iNOS forward 5'-CCTCACTGGGACAGCACAGAATGT-3' and iNOS reverse 5'-CCGATGCAGCGAGGGGCATT-3'.

Antibodies used for Western blots

Membranes were probed with anti-HIF-1 α (Novus), anti-Vinculin (Sigma), anti-Calsequestrin (Affinity Bioreagents), anti-Serca2a (Dianova), anti-RyR2 (Acris), anti-CaMKII (a gift from D. M. Bers, University of California, Davis, Calif, to L.S. Maier), anti-pospho-CaMKII (Thermo

3. Original Publications

Scientific), anti-Phospholamban (Badrilla), anti-Phospho-Thr17 (Badrilla) anti-Phospho-S16 (Badrilla) followed by a goat HRP (horseradish peroxidase)-labelled anti-mouse or anti-rabbit antibody (Santa Cruz Biotechnology).

TAC surgery

Pressure overload was induced by TAC in 5-7 week old female mice. Mice were anesthetized by 1.5% isoflurane inhalation. Pain management of the mice comprised treatment with buprenorphine (0.06 mg/kg body weight i.p. before surgery) and 1.33 mg/ml metamizole (for 7 days in the drinking water). Once anesthesia was administered the anesthetic plane was assessed by the reaction to pinching the toe, determining the respiration rate and close clinical supervision. The aorta was constricted with polyviolene non-absorbable braided nylon strings (5-0 USP) using blunted 25-gauge needles as placeholders that were removed after ligation.

Echocardiography

For transthoracic echocardiography after TAC a Vevo2100 (VisualSonics, Toronto, Canada) system with a 30 MHz center frequency transducer was used. Two-dimensional cine loops with frame rates of 200 frames/s of a long axis view and a short-axis with at mid-level of the papillary muscles as well as M-mode loops of the short axis view were recorded. Thickness of the septum (ST), the posterior myocardial wall (PWT), and the area of the left ventricular cavity were measured in systole and diastole from the short-axis view. Fractional area shortening was calculated: % FAS = (LV end-diastolic area – LV end-systolic area)/ (LV end-diastolic areas x 100).

Mouse heart rate and blood pressure measurements

Heart rate and blood pressure were measured in 8 week and 8 month old mice using a CODA non-invasive blood pressure system (Kent Scientific Corporation, Connecticut, USA).

Radiotracer production

Fluorine-18 was produced as [¹⁸F]fluoride at the PETtrace cyclotron (General Electric Healthcare, Uppsala, Sweden) using the $^{18}\text{O}(p,n)^{18}\text{F}$ nuclear reaction. [¹⁸F]Fluoro-2deoxyglucose ([¹⁸F]FDG) was synthesized in a FDG MicroLab module (GE Healthcare,

3. Original Publications

Münster, Germany) as published ¹. Radiochemical purity was >95%. [¹⁸F]FTHA was synthesized using the method from DeGrado ² with modifications on a modified TRACERlab FFX-N PET tracer Synthesizer (GE Healthcare, Münster, Germany). Briefly, 2 µL of the precursor benzyl-14-(R,S)-tosyloxy-6-thiaheptadecanoate (ABX, Germany) in 1 mL of acetonitrile were reacted with a mixture of azeotropically dried [¹⁸F]fluoride, 15 mg of Kryptofix 2.2.2. and 3.5 mg K₂CO₃ at 110°C for 5 min. After hydrolysis with 350 µL of 0.14 N KOH (110 °C, 5 min) 0.3 mL of 6.5% sulfuric acid were added for neutralization. The product was purified using HPLC chromatography (Supelcosil ABZ+; 10 x 250 mm; H₂O/MeOH 80/20 with 1% H₃PO₄; 5 ml/min; detection: UV 216 nm and NaI(Tl)). The product was obtained in uncorrected yields of 15 ± 5% (n = 13), corresponding to 9.3 ± 3.3 GBq of isolated [¹⁸F]FTHA, after irradiations using 35 to 60 µA for 40 to 60 min. Radiochemical purity as determined by TLC was > 90%. Specific activities were > 50 GBq/µmol at end of synthesis.

1. Hamacher K, Coenen HH, Stocklin G. Efficient stereospecific synthesis of no-carrier-added 2-[¹⁸F]-fluoro-2-deoxy-d-glucose using aminopolyether supported nucleophilic substitution. *J Nucl Med* 1986;27:235-238.
2. DeGrado TR, Coenen HH, Stocklin G. 14(r,s)-[¹⁸F]fluoro-6-thia-heptadecanoic acid (ftha): Evaluation in mouse of a new probe of myocardial utilization of long chain fatty acids. *J Nucl Med* 1991;32:1888-1896.

PET analysis

Before each scan day the mice were fasted for at least 14 hr. For anesthesia 1.5% isoflurane was evaporated in medical oxygen using a dedicated vaporizer for rodents (Vetland, Louisville, KY, USA). After the tail vein i.v. injection of [¹⁸F]FTHA (13±1.03 MBq) or [¹⁸F]FDG (13±0.3 MBq) and a 55 min uptake time under anesthesia, a 15 min emission scan was obtained. This PET measurement was followed by 13 min transmission scan based on a rotating ⁵⁷Co source for photon attenuation correction. The PET images were reconstructed using an ordered subset expectation maximization (OSEM) 2D algorithm with attenuation correction (matrix: 128x128; voxel size: 0.776x0.776x0.796 mm³). For image analysis regions of interests (ROIs) were placed on 3 consecutive slices of the middle left myocardium in short axis view to avoid the spillover effect from liver to the heart apex region. The counts of left ventricle cavity were subtracted. The myocardial [¹⁸F]FTHA and [¹⁸F]FDG uptake was reported as standardized uptake value (SUV, SUV = tissue radioactivity concentration

3. Original Publications

[Bq/ml]/ (injection dose [Bq]/ body weight [g])). One mouse of the transgenic group was excluded from [¹⁸F]FDG SUV evaluation because it was not anesthetized properly during the PET scan.

Sirius Red Polarization Method for Collagen Staining

Interstitial collagen was detected by Sirius red polarization microscopy. Paraffin sections were stained with 0.1% Sirius red in saturated picric acid for 1h. Sections were rinsed with acidified water for 1 minute twice and then dehydrated with 100% ethanol, sections were coverslipped. The stained sections were observed under polarized light and photographed with the same exposure time for each section.

Cryosections and immunofluorescence labelling

Hearts were sectioned (5-10 μm) in a cryostat, mounted on glass slides and dried for at least 30 min. After being washed with PBS, the sections were briefly incubated with 1% Triton X-100 and then fixed with 4% formaldehyde and permeabilized with 0.2% Triton X-100. Non-specific binding of antibodies was blocked by incubation with 1% bovine serum albumin for 1 h. The sections were then incubated with the polyclonal anti-CD31 antibodies (Dianova, DIA 310) and anti-vinculin antibodies (Sigma, hVin-1) at room temperature for 1 h, washed three times in PBS and then incubated with anti-mouse TR (diluted 1:200; SantaCruz) and anti-rat FITC (1:200, SantaCruz). Samples were counterstained for DNA (Hoechst). Finally, samples were extensively washed in PBS, mounted in Mowiol, and examined by fluorescence microscopy (Axio Observer D1, Carl Zeiss, Göttingen, Germany). Capillary area was determined by analyzing CD31 positive pixels using ImageJ (NIH Bethesda, MD). In addition, numbers of capillaries were counted per view of field.

Isolation of cardiomyocytes, cardiomyocyte shortening and intracellular Ca^{2+} -measurements

Isolated hearts were mounted on a Langendorff-perfusion apparatus driven by gravity and perfused with nominally Ca^{2+} -free Tyrode's solution containing (in mM) NaCl 115, KCl 4.7, KH_2PO_4 0.6, Na_2HPO_4 0.32, MgSO_4 1.2, NaHCO_3 12, KHCO_3 10, HEPES 10, taurine 30, 2,3-butanedioneminoxime 10, glucose 5.5 (pH 7.46) for 2-4 min at 37°C. Perfusion was then switched to the same solution containing Liberase blendzyme 1 (Roche) 0.25 mg/ml and

3. Original Publications

Trypsin 0.14 mg/ml with perfusion continuing until the heart became flaccid (7-12 min). Ventricular tissue was removed, dispersed, filtered and suspensions were rinsed several times. After Ca^{2+} reintroduction (stepwise increase to 0.8 mM), isolated myocytes were then plated onto superfusion chambers, with the glass bottoms treated with laminin to allow cell adhesion and used for immediate measurements. Myocytes were loaded with fluo-3 by incubation with 10 μM of the acetoxymethyl ester (AM) form of the dye (Molecular Probes, Eugene, OR) for 15 min at room temperature in darkness. The dye was excited with a wavelength at 480 ± 15 nm using a 75 W xenon arc lamp (Ushio, Japan) on the stage of a Nikon Eclipse TE200-U inverted microscope. Emitted fluorescence was measured using a photomultiplier (at 535 ± 20 nm; IonOptix Corp., Milton, MA).

Flow cytometry analysis of CD45 inflammatory cells

The tissue was treated with 1.2 U/mL DispaseII (PAN), 150 U/mL Collagenase IV (Biochrom) and 2 mM CaCl_2 in PBS for 45 min at 37°C . Digestion was stopped using DMEM supplemented with 15% FCS and remaining connective tissues and fibers were removed using 70 μm and 40 μm nylon cell strainers (BD). Cells were spun down at 400 g and 4°C and resuspended in erythrocyte lysis buffer containing 10 mM KHCO_3 , 155 mM NH_4Cl and 126 μM EDTA. Lysis was stopped after 5 min with DMEM + 15% FCS and cells were again centrifuged at 400 g and 4°C . Cells were resuspended in PBS and stained with PerCPCy5.5-conjugated CD45 antibody or respective isotype control (BD) and measured on a Becton Dickinson FACSCalibur. Cells were gated according to size (FCS-A) and granularity (SSC-A) as well as SSC-W to exclude cell debris and duplets. Using FACSdiva software percentage of CD45-positive cells within the gated population was analyzed. It should be noted that the analysis is suitable for detecting changes in the percentage of CD45 positive immune cells among different treatment groups but does not allow to quantify absolute CD45-positive cell numbers since disruption and digestion might release more small non-integrated cells (like leukocytes and endothelial cells) while dissociation of fibroblasts and the myocyte network can be less efficient.

3. Original Publications

Insulin measurements

Insulin concentrations in serum of 8 month old mice were determined using the Ultra Sensitive Mouse Insulin ELISA kit (Crystal Chem, Inc.) according to manufacturer's instructions.

Measurements of free fatty acids

Free fatty acids in mouse serum of 8 month old animals were analyzed using assay kits from Wako (Osaka, Japan) and a clinical analyzer (Hitachi 917).

Blood glucose level analysis

5 μ l whole blood was drawn from retrobulbar by a capillary when the mice were under 1.5% isoflurane anesthesia. After the blood was collected, the blood glucose level was measured immediately by a glucose analyzer (Hemocue, Ängelholm, Sweden).

4. Unpublished Data

4. Unpublished Data

The following chapter contains additional data of the cardiomyocyte-specific PHD2 knock-out mice (*cPhd2*^{-/-}) that were not published at the submission date of this thesis and furthermore unpublished data of cardiomyocyte-specific PHD2/PHD3 double knock-out mice (*cPhd2/3*^{-/-}).

4.1 Detrimental consequences of a cardiomyocyte-specific knock-out of PHD2

Marion Hölscher¹, Yun Lin², Bernd J. Pichler², Ben Wielockx³, Georg Breier³, Dörthe M. Katschinski^{1*}, Anke Ziesenis^{1*} (*both authors contributed equally)

(1) From the Department of Cardiovascular Physiology, Universitätsmedizin Göttingen, Georg-August University Göttingen, **(2)** from the Department of Preclinical Imaging and Imaging Technology of the Werner Siemens-Foundation, University of Tübingen and **(3)** from the Department of Pathology, TU Dresden

Introduction

Cardiomyocyte-specific PHD2 knock-out (*cPhd2*^{-/-}) mice are protected from acute myocardial infarction as shown earlier by our group (Hölscher *et al.*, 2011). However we did not analyze the long-term consequences of cardiomyocyte-specific PHD2 knock-out. Therefore, we followed a cohort of *cPhd2*^{-/-} and *wt* littermates over a time period of eight months. *cPhd2*^{-/-} mice developed a hypertrophy with aging. Furthermore the metabolism of eight months old *cPhd2*^{-/-} mice was shifted towards glycolysis with an increased uptake of glucose and a diminished uptake of fatty acid as shown by PET analysis which was not detectable in eight week old mice.

Material and methods

Mice- Cardiomyocyte-specific PHD2 knock-out mice (*cPhd2*^{-/-}) (described in Hölscher *et al.*, 2011) were further analyzed.

Echocardiography- Two-dimensional images and M-mode tracings were recorded from the parasternal long axis view at midpapillary level (Vevo 660™, VS-0 M-VE660 version 3.1, Visual Sonics). Posterior wall thickness (PWT) and fractional shortening (FS) were determined. FS was calculated as (systolic diameter-diastolic diameter/diastolic diameter x 100). FS was used as marker for cardiac contractile function.

Pet analysis- The PET analysis was done as described previously in Hölscher *et al.*, 2012.

4. Unpublished Data

Results

Cardiomyocyte-specific PHD2 knock-out animals develop cardiac hypertrophy with aging but without impairment of the heart function (fig. 1).

Fig.1

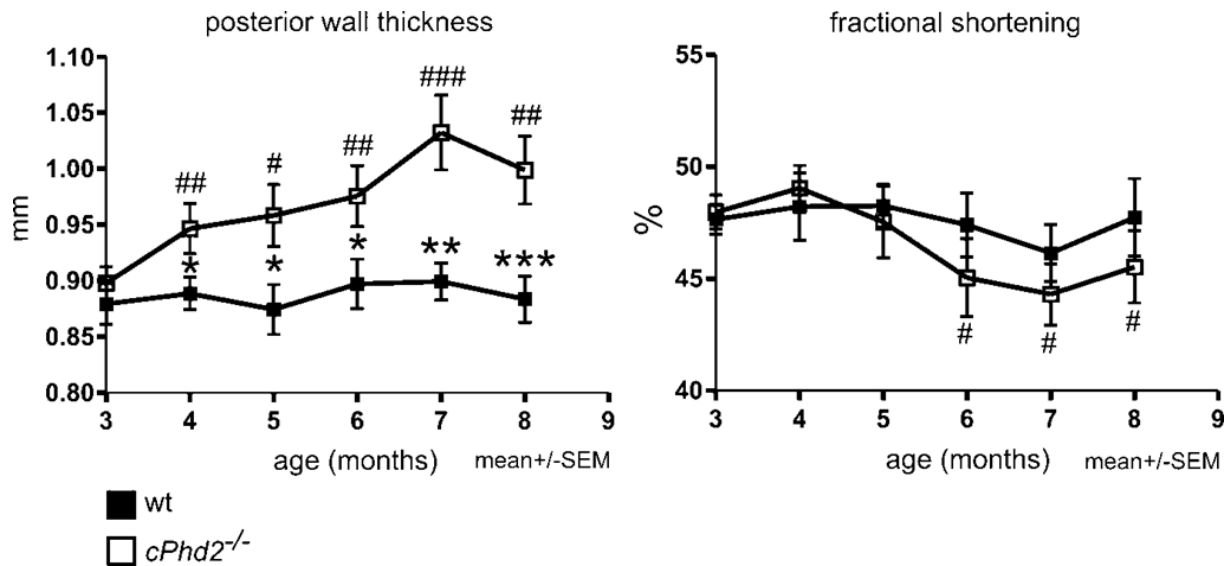


Fig.1 *cPhd2*^{-/-} mice develop a hypertrophy with aging. A cohort of wt (n=13) and *cPhd2*^{-/-} (n=13) mice was followed over a time period of 8 months to determine long-term consequences of a PHD2 knock-out.

*, p < 0.05; **, p < 0.01; ***, p < 0.001 compared to wt; #, p < 0.05; ##, p < 0.01; ###, p < 0.001 compared to 3 months

When analyzing the metabolism of 8 week and 8 month old *cPhd2*^{-/-} and wt littermates by PET analysis we could detect a shift towards glycolysis in 8 month old *cPhd2*^{-/-} mice but not in 8 week old animals (fig. 2).

4. Unpublished Data

Fig.2

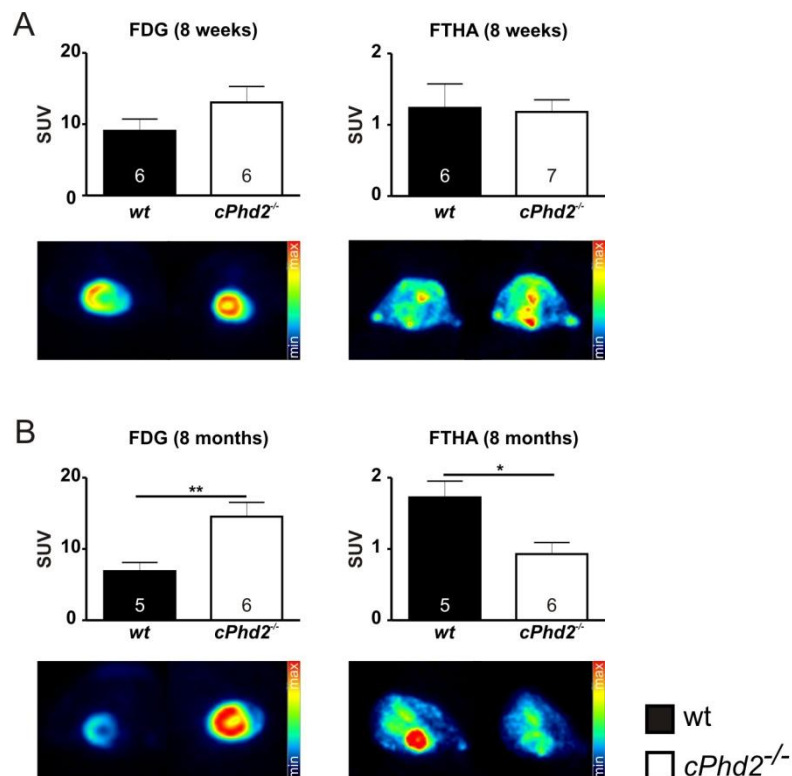


Fig. 2 The metabolism of 8 month old *cPhd2*^{-/-} mice is shifted towards glycolysis. [¹⁸F]FDG uptake and [¹⁸F]FTHA uptake in **(A)** 8 week old and **(B)** 8 month old *cPhd2*^{-/-} and wt mice. Bar diagram shows cardiac SUV at 60 min. *, $p < 0.05$; **, $p < 0.01$. Data represent mean \pm SEM. The number in the bars indicate the number of analyzed animals.

Discussion

Earlier on, we could show that *cPhd2*^{-/-} mice show a mild cardiac HIF-1 α stabilization with subsequent up-regulation of several HIF target genes. Amongst other genes, genes involved in metabolism were significantly up-regulated. Furthermore the capillary diameter was increased in hearts of *cPhd2*^{-/-} mice. Due to these changes *cPhd2*^{-/-} mice are primed to withstand acute ischemic insults. This could be shown by a smaller area at risk and a better preserved heart function three weeks after the ligation of the *left anterior descending artery*. Although these changes are beneficial on a short-term basis they have a detrimental outcome on a long-term basis. *cPhd2*^{-/-} mice develop a hypertrophy with aging (fig. 1) which can be partly explained by the observed in shift in metabolism towards glycolysis (fig. 2). As this same result (shift towards glycolysis and hypertrophy) can be also observed in *HIF-1 α ^{tg}* mice (Hölscher *et al.*, 2012) it can be assumed that the effects are HIF-mediated.

4. Unpublished Data

4.2 Cardiomyocyte-specific double knock-out of PHD2 and PHD3 leads to dilated cardiomyopathy and a premature death

Marion Hölscher¹, Ben Wielockx², Georg Breier², Dörthe M. Katschinski^{1*}, Anke Ziesenis^{1*}
(*both authors contributed equally)

(1) From the Department of Cardiovascular Physiology, Universitätsmedizin Göttingen, Georg-August University Göttingen and (2) from the Department of Pathology, TU Dresden

Abstract

Prolyl-4-hydroxylase domain enzymes (PHDs) are the most important enzymes that sense changes in oxygen concentration and directly control the cellular response by destabilizing the α -subunit of the hypoxia-inducible factor (HIF), the master transcriptional regulator of the hypoxic response. Beforehand we have generated cardiomyocyte-specific PHD2 knock-out mice (*cPhd2*^{-/-}) that showed a HIF-1 α stabilization with subsequent up-regulation of several HIF target genes. As PHD3 is a HIF target gene itself it was also up-regulated. To repress this regulatory feedback loop, we created cardiomyocyte-specific PHD2/PHD3 double knock-out mice (*cPHD2/3*^{-/-}) (*Phd2*^{flox/flox} x *Phd3*^{flox/flox} x *MLCvCre*). These mice show signs of dilated cardiomyopathy that is already detectable at the age of eight weeks. This leads to premature death of the mice at the age of four to six months.

Introduction

The maintenance of oxygen homeostasis is critical to all aerobic organisms. In animals, complex systems have evolved to sense and to adapt to changes in cellular oxygen availability. The most important factor in response to low oxygen concentrations is the Hypoxia-Inducible Factor (HIF). HIF is a heterodimeric transcription factor consisting of one of three oxygen-sensitive α -subunits (HIF-1 α , HIF-2 α or HIF-3 α) and the common oxygen-independently regulated β -subunit. Under normoxic conditions two proline residues (Pro⁴⁰² and Pro⁵⁶⁴) of the α -subunit of HIF-1 are hydroxylated by prolyl-4-hydroxylase domain enzymes (PHDs). This hydroxylation marks HIF-1 α for ubiquitination by the VHL E3 Ligase which then leads to rapid degradation by the proteasome (Maxwell *et al.*, 1999).

Up to now three PHD isoforms with known physiological functions have been identified, PHD1, PHD2 and PHD3. Based on its ubiquitous expression pattern and its dominant effect in normoxia, PHD2 seems to be the most important isoform. This assumption was further affirmed by the finding that PHD2 knock-out mice are not viable, as they die early between

4. Unpublished Data

embryonic day 12.5 and 14.5, whereas PHD1 as well as PHD3 knock-out mice are viable (Takeda *et al.*, 2006).

To gain further insight into the function of PHD2 *in vivo* two independent inducible PHD2 knock-out mice were generated (Minamishima *et al.*, 2007; Takeda *et al.*, 2007). These mice show, amongst other symptoms, signs of a dilated cardiomyopathy. However, these mice also have an increased hematocrit, thus it is not clear if the observed cardiac phenotype is a primary effect or if it is due to the hyperviscosity.

Therefore we have previously generated cardiomyocyte-specific PHD2 knock-out mice (*cPhd2^{-/-}*) (Hölscher *et al.*, 2011). These mice show slightly stabilized HIF-1 α protein levels with subsequent up-regulation of HIF target genes. These mice are protected from acute myocardial infarction which can be displayed by a smaller area of necrosis (AON) and a smaller area at risk (AAR) six hours after ligation of the *left anterior descending artery*. Furthermore the heart function of these mice is better preserved three weeks after the infarction. The response to an elevated afterload, as induced by *transverse aortic constriction*, however did not differ in *cPhd2^{-/-}* mice compared to *wt* mice. As PHD3 is a HIF target gene itself, it is also significantly up-regulated (about 8-fold on mRNA level compared to *wt* littermates).

Minamishima *et al.* (2009) could show that PHD2 and PHD3 are partially redundant *in vivo* with PHD3 to some extent compensating when PHD2 is inactive. Thus the effects caused by the PHD2 knock-out in the *cPhd2^{-/-}* mice are attenuated by the compensatory up-regulation of PHD3. To analyze the cardiac function of a double knock-out of PHD2 and PHD3 we generated cardiomyocyte-specific knock-out mice by crossing *Phd2^{flox/flox}* x *Phd3^{flox/flox}* mice with *MLCVvCre/+* mice. These mice show a significant down-regulation of PHD2 and PHD3 and a subsequent up-regulation of several HIF target genes. Furthermore, the PHD2/PHD3 double knock-out mice develop a dilated cardiomyopathy that leads to premature death.

Material and Methods

Animal Experimentation and Echocardiography—Animal experimentation was performed with *cPhd2/3^{-/-}* mice and littermate *Phd2/3 wt* control mice. All protocols regarding animal experimentation were conducted according to the German animal protection laws and approved by the responsible governmental authority (Niedersächsisches Landesamt für Verbraucherschutz und Lebensmittelsicherheit in Oldenburg; animal experimentation

4. Unpublished Data

numbers 33.942502-04-10/0024 and 33.9-42502-04-10/0069). Echocardiography and measurement of left ventricular end systolic diameter (LVESD), left ventricular end diastolic diameter (LVEDD) and fractional shortening (FS) were performed as described by Silter *et al.* (2009).

Mice- All animals in this study were backcrossed to C57BL/6 mice at least five times. *Phd2*^{fl^{ox}/fl^{ox}} x *MLCvCre*/+ mice were crossed with *Phd3*^{fl^{ox}/fl^{ox}} x *MLCv*/+ (or *vice versa*) to obtain *Phd2*^{fl^{ox}/fl^{ox}} x *PHD3*^{fl^{ox}/fl^{ox}} x *MLCvCre*/+ and littermate *wt* control mice (*Phd2*^{fl^{ox}/fl^{ox}} x *Phd3*^{fl^{ox}/fl^{ox}} x *MLCv*/+) within two generations.

Mice were genotyped by PCR using the following primers: Cre forward, 5'-CGTACTGACGGTGGGAGAAT-3' and Cre reverse, 5'-CGGCAAAACAGGTAGTTA-3'; PHD2 forward, 5'-CTCACTGACCTACGCCGTGT-3' and PHD2 reverse, 5'-CGCATCTTCCATCTCCATTT-3'; PHD3 forward, 5'-ATGGCCGCTGTATCACCTGTAT-3' and PHD3 reverse, 5'-CCACGTAACTCTAGAGCCACTGA-3'.

The successful deletion of PHD2 and PHD3 in the floxed mice was verified by qRT-PCR analysis.

Protein Extraction and Immunoblot Analyses- Protein extraction and immunoblot analyses were performed as previously described by Hölscher *et al.* (2011).

qRT-PCR Analyses—After RNA extraction reverse transcription (RT) was performed with 2 µg (left ventricle) or 1 µg (atrium) of RNA and a first strand cDNA synthesis kit (Fermentas, St. Leon-Rot). mRNA levels were quantified by using 0.5 µl of the cDNA reaction and a SYBR Green qPCR reaction kit (Clontech) in combination with a MX3000P light cycler (Stratagene). The initial template concentration of each sample was calculated by comparison with serial dilutions of a calibrated standard in reference to mS12. Primers were as follows: mS12 forward, 5'-GAAGCTGCCAAGGCCTTAGA-3' and mS12 reverse, 5'-AACTGCAACCAACCACCTTC-3'; PHD1 forward, 5'-GCTAGGCTGAGGGAGGAAGT-3' and PHD1 reverse, 5'-TCTACCCAGGCAATCTGGTC-3'; PHD2 forward, 5'-TCTATTTTGCCAGACCTGTCACC-3' and PHD2 reverse, 5'-GAAGCAACACGTCGTCACCTACT-3'; PHD3 forward, 5'-GGCCGCTGTATCACCTGTAT-3' and PHD3 reverse, 5'-TTCTGCCCTTTCTTCAGCAT-3'; HIF-1α forward, 5'-TCAAGTCAGCAACGTGGAAG-3' and HIF-1α reverse, 5'-TATCGAGGCTGTGTCGACTG-3'; phosphofruktokinase 1 (Pfk1) forward, 5'-ACGAGGCCATCCAGCTCCGT-3' and Pfk1 reverse, 5'-TGGGGCTTGGGCAGTGTCT-3'; glucose transporter-1 (Glut1) forward, 5'-TGGCCTTGCTGGAACGGCTG-3' and Glut1 reverse,

4. Unpublished Data

5'-TCCTTGGGCTGCAGGGAGCA-3'; CA IX (Carbonic anhydrase 9) forward, 5'-GGGTGTCATCTGGACTGTGTT-3' and CA IX reverse, 5'-CTTCTGTGCTGCCTTCTCATC-3'; α -skeletal actin forward, 5'-GGCACCCAGGGCCAGAGTCA-3' and α -skeletal actin reverse, 5'-CACGATGCCGGTGGTACGGC-3'.

Statistical analysis- Data were analysed by 2-tailed Student's unpaired *t* test or in case of repeated echocardiography analysis of aging mice as paired *t* test and presented as mean \pm SEM. A *P* value less than 0.05 was considered statistically significant.

Kaplan-Meier survival curves have been made using GraphPad Prism 4 (GraphPad Software, San Diego, CA) and analyzed using log-rank test: **, $p < 0.01$

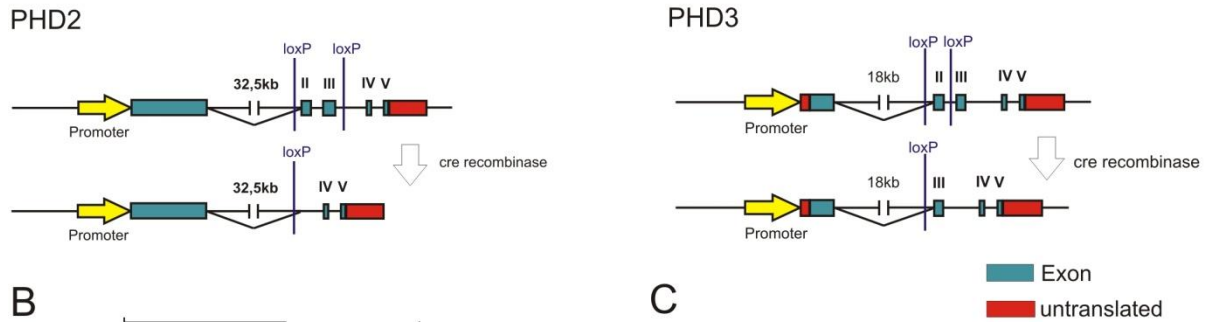
Results

Generation of cardiomyocyte-specific PHD2/PHD3 knock-out mice- For generating cardiomyocyte-specific PHD2/PHD3 knock-out mice (*cPhd2/3*^{-/-}) *Phd2*^{flox/flox} x *MLCvCre*^{+/+} mice were crossed with *Phd3*^{flox/flox} x *MLCv*^{+/+} to obtain *cPhd2/3*^{-/-} mice within two generations. The expression of the *MLCvCre* starts at embryonic day E7.5 which coincides with the earliest stages of ventricular specification (Chen *et al.*, 1998). Exons 2 and 3 of the *Phd2* gene and Exon 2 of the *Phd3* gene are flanked by loxP-sites. The *MLCv*-driven Cre recombinase allows the recombination of the floxed exons only in ventricular cardiomyocytes (fig. 1A). Analyzing the mRNA levels of PHD1, PHD2 and PHD3 it could be shown that the levels of PHD2 and PHD3 are significantly reduced in the ventricle but not in the atrium (fig. 1B). As the mRNA is isolated from whole tissues, *i.e.* ventricles and atria, and not from isolated cardiomyocytes the knock-out is not 100% in the sample but within an expected dimension. The mRNA-levels of the non-hypoxia inducible PHD1 remain unchanged. Intriguingly, HIF-1 α is significantly down-regulated on mRNA level (fig. 1C). Despite this down-regulation, HIF-1 α protein levels show a stabilization of HIF-1 α in the left ventricle. This stabilization is in a similar range as in *cPhd2*^{-/-} mice but seemingly less than in *Hif-1 α ^{tg}* mice (fig. 1D). Representative HIF target genes were analyzed on mRNA level. Genes involved in glucose metabolism (Glut1, Pfk1), pH control (CA IX) and a constituent of the contractile apparatus (α -skeletal actin) are significantly up-regulated (fig. 1E). This demonstrates that the HIF pathway is activated in the cardiomyocytes of *cPhd2/3*^{-/-} mice in spite of the reduction of HIF-1 α on mRNA level.

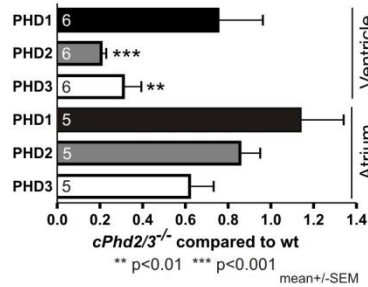
4. Unpublished Data

Fig.1

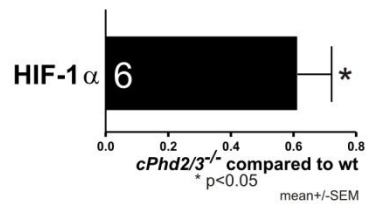
A



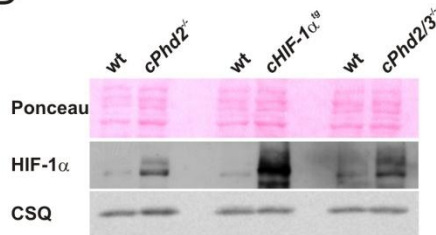
B



C



D



E

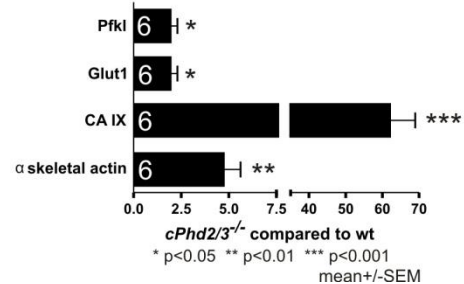


Fig.1 Generation and analyses of *cPhd2/3*^{-/-} mice. (A) Schematic description of the gene targeting strategy is shown. In the targeted *Phd2* locus exons 2 and 3 and in the targeted *Phd3* locus exon 2 are flanked by two *loxP* sites. These flanked exons of *Phd2* and *Phd3* are deleted by Cre-mediated recombination by crossing *Phd2*^{fllox/fllox} x *Phd3*^{fllox/fllox} mice with MLCvCre mice. (B) qRT-PCR analysis confirmed the significant reduction of PHD2 and PHD3 mRNA transcripts in the left ventricles but not in the atria of 8 week old *cPhd2/3*^{-/-} mice compared with *wt* littermates. PHD1 mRNA levels were unchanged in the ventricle and in the atrium. In total, 6 (atrium: 5) *wt* and 6 (atrium: 5) *cPhd2/3*^{-/-} mice were analyzed. **, *p* < 0.01; ***, *p* < 0.001. Data represent mean ± SEM. (C) HIF-1α mRNA levels in left ventricle were determined by qRT-PCR analysis and showed a significant down-regulation. *, *p* < 0.05. Data represent mean ± SEM. (D) HIF-1α protein was detected by Western blot analysis. Protein extracts prepared from left ventricles of 8 week old *Phd2* *wt* and *cPhd2*^{-/-}, *Hif-1α*^{wt} and *Hif-1α*^{tg} and *cPhd2/3* *wt* and *cPhd2/3*^{-/-} mice were analyzed with anti-HIF-1α and anti-calsequestrin (CSQ) antibodies, confirming that HIF-1α is stabilized in the left ventricles. Ponceau staining and CSQ show equal loading. (E) Representative HIF target genes were analyzed by qRT-PCR. Pfk1, Glut1, α-skeletal actin and CA IX showed a significant up-regulation on mRNA level in left ventricles of 8 week old *cPhd2/3*^{-/-} mice in comparison to *wt* littermates. *, *p* < 0.05; **, *p* < 0.01; ***, *p* < 0.001. Data represent mean ± SEM. The number in the bars indicate the number of analyzed animals.

4. Unpublished Data

cPhd2/3^{-/-} mice develop dilated cardiomyopathy with aging which leads to a premature death. I was able to show earlier (Hölscher *et al.*, 2012) that cardiac-specific HIF-1 α transgenic mice develop heart failure with aging or when challenged by increased mechanical load. *cPhd2^{-/-}* mice, which show only mild levels of HIF-1 α stabilization did not respond differently to elevated mechanical load than their *wt* littermates (Hölscher *et al.*, 2011). However these mice also develop cardiac hypertrophy with aging, though, without a loss in heart function (see chapter 4.1, fig. 1). To determine the consequences of a double knock-out of PHD2 and PHD3 in cardiomyocytes on the cardiac function *cPhd2/3^{-/-}* mice underwent echocardiography every two weeks between the age of eight and eighteen weeks. Representative echocardiographic recordings are shown in figure 2B (B-mode; brightness mode) and in figure 2C (M-mode; motion mode). *cPhd2/3^{-/-}* mice already show an inferior heart function at the age of eight weeks that worsens over time (fig. 2A). At the age of 4.5 months, *cPhd2/3^{-/-}* mice show an enlargement of the heart (fig. 2D), which is also shown by an increased end-diastolic diameter (fig. 2A). *Wt* littermates on the contrary, did not show any signs of a weakened heart function, an increase in heart size or premature death. *cPhd2/3^{-/-}* mice die significantly earlier than *wt* mice with a median survival of 21 weeks (fig. 2E).

4. Unpublished Data

Fig.2

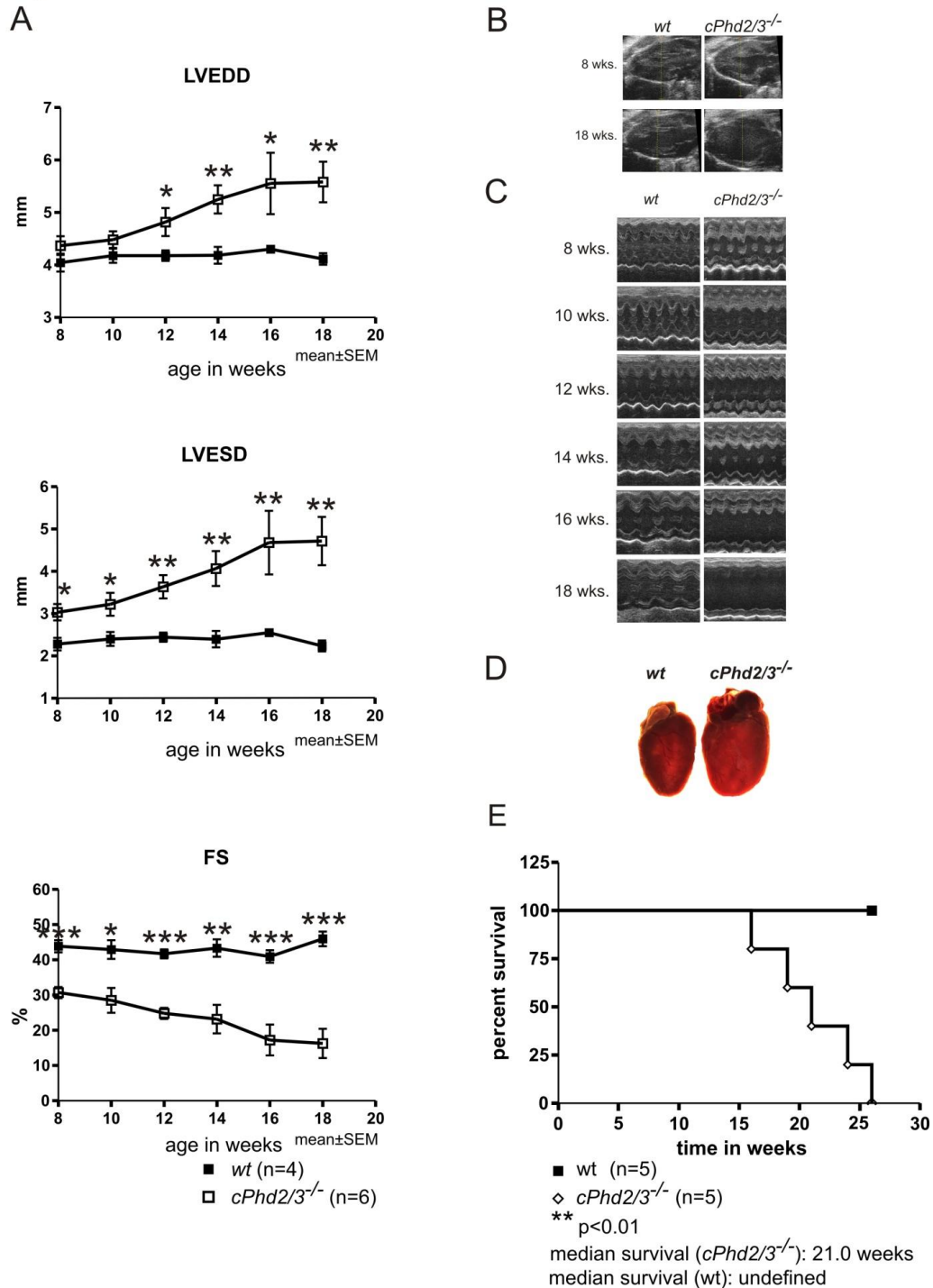


Fig. 2 Cardiomyocyte-specific deficiency of PHD2 and PHD3 leads to dilated cardiomyopathy. *cPhd2/3^{-/-}* (n=6) and *wt* littermates (n=4) were analyzed by echocardiography every two weeks between the age of eight and eighteen weeks. **(A)** Left ventricular end-diastolic diameter (LVEDD) and left ventricular end-systolic diameter (LVESD) were determined. Fractional shortening (FS) of the left ventricle as a marker for heart function was defined as $(FS = \frac{LVEDD - LVESD}{LVEDD} \times 100)$. Graphs represent mean \pm SEM. *, p<0.05; **, p<0.01; ***, p<0.001. Echocardiographic images recorded from parasternal long axis view of a *cPhd2/3^{-/-}* and a *wt* mice; **(B)** B-Mode, **(C)** M-Mode. **(D)** Explanted hearts of a *cPhd2/3^{-/-}* and a *wt* mouse at the age of eighteen weeks; **(E)** Kaplan-Meier survival curve for *cPhd2/3^{-/-}* and *wt* littermates. *Wt* mice live significantly longer than *cPhd2/3^{-/-}* mice which die around the age of 21 weeks.

4. Unpublished Data

Discussion

HIF-1 α was shown to be critically involved in cardioprotection (Cai *et al.*, 2003; Date *et al.* 2005). Previously it has been shown by our group (Hölscher *et al.*, 2011) and others (e.g. Hyvärinen *et al.*, 2010) that stabilization of HIF-1 α mediated by a knock-out of PHD2 is beneficial in the setting of acute myocardial infarction. Currently small molecule inhibitors are being developed to stabilize HIF-1 α in order to treat diseases related to hypoxia like anemia, stroke, or myocardial infarction (Katschinski, 2009; Myllyharju, 2009; Yan *et al.*, 2010).

To gain insight into the outcome of a double knock-out of PHD2 and PHD3 in the heart, *cPhd2/3*^{-/-} mice were created. These mice show a significant down-regulation of PHD2 and PHD3 in the ventricular cardiomyocytes compared to *wt* animals but unchanged levels of PHD1. Interestingly, *cPhd2/3*^{-/-} show a significant down-regulation of HIF-1 α mRNA levels. In a recent report it was shown that in HMEC-1 cells sustained hypoxia progressively decreases HIF-1 α mRNA while HIF-1 α protein levels rapidly peak after 3h and then slowly decay (Chamboredon *et al.*, 2011). Therefore it can be speculated that in *cPhd2/3*^{-/-} hearts an extreme hypoxic environment is mimicked so that the HIF-1 α mRNA levels are decreased. Representatively analyzed HIF target genes show a significant up-regulation to a similar extent as in *cPhd2*^{-/-} mice (e.g. Glut1 2.5-fold up-regulated in *cPhd2*^{-/-} and *cPhd2/3*^{-/-} mice) but less than in *Hif-1 α* ^{tg} mice (e.g. Glut1 5-fold up-regulated).

cPhd2/3^{-/-} mice show already at a very young age (eight weeks) signs of cardiomyopathy and a constriction of their heart function. The impairment of the heart function of *cPhd2/3*^{-/-} mice finally leads to a premature death at the age of maximal six months.

HIF-1 α transgenic mice (either over-expressing the wild-type HIF-1 α isoform or a modified form which cannot be hydroxylated as amino acids critical to HIF-1 α degradation (*i.e.* Pro⁴⁰²Ala, Pro⁵⁶⁴Ala and Asn⁸⁰³Ala) were substituted) (Hölscher *et al.*, 2012; Bekeredjian *et al.*, 2010) develop a hypertrophy with aging or when challenged by elevated mechanical load. As *cPhd2/3*^{-/-} mice unexpectedly do not show a more profound HIF-1 α stabilization than *Hif-1 α* ^{tg} mice the HIF-1 stabilization could still be a contributing factor for the premature death but might not be the main reason. This will be analyzed in follow-up studies by creating cardiomyocyte-specific PHD2/PHD3/HIF-1 α triple knock-out mice. If the HIF-1 α stabilization is causative for the premature death of the *cPhd2/3*^{-/-} mice the *cPhd2/3/HIF-1 α* ^{-/-} triple knock-out mice should show a normal life span.

4. Unpublished Data

Despite the promising perspective in developing drugs to mediate the cardioprotective effect of HIF-1 α , it is indispensable to gain deeper insight into the specific functions of the PHD isoforms to create isoform specific PHD inhibitors as at least a double knock-out of PHD2 and PHD3 in cardiomyocytes has a detrimental outcome. Furthermore other pathways than the HIF pathway that are regulated by the PHDs need to be studied to further elucidate the consequences of this inhibition.

Acknowledgments—We thank Sabine Krull and Annette Hillemann for expert technical assistance.

References

- Chamboredon S, Ciais D, Desroches-Castan A, Savi P, Bono F, Feige JJ, Cherradi N. Hypoxia-inducible factor-1 α mRNA: a new target for destabilization by tristetraprolin in endothelial cells. *Mol Biol Cell* 18:3366-78.
- Chen J, Kubalak SW and Chien KR (1998). Ventricular muscle-restricted targeting of the RXR α gene reveals a non-cell autonomous requirement in cardiac chamber morphogenesis. *Development* 125:1943-1949
- Bekeredjian R, Walton CB, MacCannell KA, Ecker J, Kruse F, et al. 2010 Conditional HIF-1 α Expression Produces a Reversible Cardiomyopathy. *PLoS ONE* 5(7): e11693
- Hölscher M, Silter M, Krull S, von Ahlen M, Hesse A, Schwartz P, Wielockx B, Breier G, Katschinski DM, Ziesenis A (2011). Cardiomyocyte-specific prolyl-4-hydroxylase domain 2 knock out protects from acute myocardial ischemic injury. *J. Biol. Chem.* 286:11185-11194
- Hölscher M, Schäfer K, Krull S, Farhat K, Hesse A, Silter M, Lin Y, Pichler BJ, Patricia Thistlethwaite P, El Armouche A, Maier LS, Katschinski DM, Ziesenis A (2012) Unfavourable consequences of chronic cardiac HIF-1 α stabilization. *Cardiovasc Res* 94:77-86
- Hyvärinen J, Hassinen IE, Sormunen R, Mäki JM, Kivirikko KI, Koivunen P, and Myllyharju, J (2010). Hearts of hypoxia-inducible factor prolyl 4-hydroxylase-2 hypomorphic mice show protection against acute ischemia-reperfusion injury. *J Biol Chem* 285:13646-13657
- Katschinski DM (2009). In vivo functions of the prolyl-4-hydroxylase domain oxygen sensors: direct route to the treatment of anaemia and the protection of ischaemic tissues. *Acta Physiol* 195:407-414
- Maxwell PH, Wiesener MS, Chang GW, Clifford SC, Vaux EC, Cockman ME, Wykoff CC, Pugh CW, Maher ER, and Ratcliffe PJ (1999). The tumour suppressor protein VHL targets hypoxia-inducible factors for oxygen-dependent proteolysis. *Nature* 399:271-275.

4. Unpublished Data

Minamishima YA, Moslehi J, Bardeesy N, Cullen D, Bronson RT, Kaelin WG Jr (2007). Somatic inactivation of the PHD2 prolyl hydroxylase causes polycythemia and congestive heart failure; *Blood* 111:3236-44.

Minamishima YA, Moslehi J, Padera RF, Bronson RT, Liao R and Kaelin Jr WG (2009). A Feedback Loop Involving the Phd3 Prolyl Hydroxylase Tunes the Mammalian Hypoxic Response In Vivo. *Mol Cell Biol* 29:5729-5741

Myllyharju J. (2009). HIF Prolyl 4-Hydroxylases and their Potential as Drug Targets. *Curr Pharm Des* 15:3878-3885

Takeda K, Cowan A, Fong GH (2007). Essential role for prolyl hydroxylase domain protein 2 in oxygen homeostasis of the adult vascular system. *Circulation* 116:774-81

Takeda K, Ho V, Takeda H, Duan L, Nagy A, and Fong G (2006). Placental but Not Heart Defects Are Associated with Elevated Hypoxia-Inducible Factor α Levels in Mice Lacking Prolyl Hydroxylase Domain Protein 2. *MCB* 22:8336-8346

Silter M, Kögler H, Zieseniss A, Wilting J., Schäfer K, Toischer K, Rokita AG, Breves G, Maier LS, Katschinski DM (2010). Impaired Ca²⁺-handling in HIF-1 α +/- mice as a consequence of pressure overload. *Pflugers Arch - Eur J Physiol* 459:569-577

Yan L, Colandrea VJ, and Hale JJ (2010). Prolyl hydroxylase domain-containing protein inhibitors as stabilizers of hypoxia-inducible factor: small molecule-based therapeutics for anemia. *Expert Opin Ther Pat* 20:1219-1245

5. Discussion

5. Discussion

The maintenance of cellular oxygen homeostasis is critical to all aerobic organisms in order to produce energy for cell survival and reproduction. The master regulator in response to decreased oxygen availability is HIF. HIF is a heterodimeric transcription factor consisting of one of three oxygen-sensitive α -subunits and an oxygen-stable β -subunit. The molecular basis for the oxygen-dependent regulation of the α -subunit is the hydroxylation of two distinct proline residues. This hydroxylation is committed by a family of oxygen-, iron- and 2-oxoglutarate dependent PHD enzymes that have been first described in 2001 (Bruick and McKnight, 2001; Epstein *et al.*, 2001; Ivan *et al.*, 2002). So far three members of this family with known physiological functions have been identified- PHD1, PHD2 and PHD3. The PHDs have many features in common but they show some differences in expression pattern, catalytic properties and physiological role (see table 1). PHD inhibition has been proven to activate the HIF pathway *in vitro* and *in vivo* (Warnecke *et al.*, 2003). The knowledge about PHD isoform specific functions is important for the ongoing development of small molecule PHD inhibitors. The first PHD inhibitors are currently tested in preclinical and clinical trials for the treatment of anemia and for cytoprotection (Yan *et al.*, 2010).

HIF-1 has been attributed a central role in a variety of cell functions by transcriptional regulation of a multitude of genes involved in *e.g.* angiogenesis, vasotonus regulation, glucose metabolism, viability and pH control.

In the course of time HIF-1 became a promising candidate in mediating cardioprotection. Cai *et al.* demonstrated a positive effect of hypoxia in the setting of acute myocardial infarction for the first time in 2003. Rats were exposed to intermittent hypoxia (5 cycles: 6 minutes of 6% O₂ followed by room air for 6 minutes); control rats did not undergo this procedure. Afterwards explanted hearts perfused in Langendorff mode showed a smaller infarction area compared to control hearts. Since then several studies followed that could show that HIF-1 is critical involved in regulation of cellular heart functions (for review see: Tekin *et al.*, 2010).

Despite the fact that PHD inhibitors are already currently being designed in order to treat or attenuate the outcome of acute myocardial infarction (and other diseases like stroke, anemia, cancer, etc.) in the nearby future a lot of open questions regarding HIF-1 α stabilization still remain.

The aims of this thesis were to analyze the cardiomyocyte-specific functions of PHD2 and PHD3 and to address the effects of cardiac HIF-1 α stabilization.

5. Discussion

5.1 Beneficial effects of PHD2 knock-out, respectively HIF-1 α stabilization

Myocardial infarction is the death of heart muscle caused by sudden blockage of a coronary artery perfusion. If blood flow is not restored to the heart muscle within 20 to 40 minutes, irreversible death of the heart muscle will begin to occur. In the last couple of years evidence thickened that HIF-1 is an important mediator of cardioprotection. This was beforehand also shown by Kido *et al.* (2005) for the HIF-1 α transgenic mice (*Hif-1 α ^{tg}*) that were further analyzed in this thesis.

In this thesis I could show that cardiomyocyte-specific PHD2 knock-out mice (*cPhd2^{-/-}*) mice, which show elevated cardiac HIF-1 α protein levels, had significantly smaller areas at risk and areas of necrosis as well as a better preserved heart function after a permanent ligation of the *left anterior descending artery* (LAD) (Hölscher *et al.*, 2011, fig. 8). Furthermore I could demonstrate a better cell survival in the infarcted myocardium of *cPhd2^{-/-}* mice compared to *wt* mice with significant less apoptotic cells in *cPhd2^{-/-}* mice (Hölscher *et al.*, 2011, fig. 8).

In *Hif-1 α ^{tg}* mice I could show a significant up-regulation of several vasotonus regulating genes. When determining the area and the number of capillaries via CD31 staining I could show that the number of capillaries is the same in *Hif-1 α ^{tg}* and *wt* littermates, the area of the capillaries in *Hif-1 α ^{tg}* mice, however, is significantly increased which allows a better blood flow into the heart (Hölscher *et al.*, 2012, fig. 2). The same effect could be shown for *cPhd2^{-/-}* mice despite the non-changed expression of vasotonus regulating genes (Hölscher *et al.*, 2011, fig. 6). The increase of capillary diameter and therefore an expected improvement in oxygen supply might be at least one reason for the cardioprotective effect following a myocardial infarction.

The heart can use different metabolic fuels, including fatty acids, glucose, lactate, ketones, and amino acids. In healthy condition fatty acids are the preferred fuel, accounting for up to 90% of the total acetyl-CoA provided to cardiac mitochondria. Comparing fatty acids (*e.g.* palmitate) and glucose the complete oxidation of one mol palmitate generates 105 molecules of ATP and consumes 46 atoms of oxygen. Oxidation of one mol glucose in contrast generates 31 molecules of ATP and consumes twelve atoms of oxygen. Thus the oxidation of fatty acids generates more ATP but it comes at the cost of higher O₂ consumption (Lopaschuk *et al.*, 2010).

During fetal stages glucose is used as the primary energy substrate whereas rates of fatty acid oxidation are low. After birth a switch towards fatty acid oxidation occurs. If the

5. Discussion

newborn heart is exposed to volume overload hypertrophy this switch fails to appear (Stanley *et al.*, 2005).

Glucose is central for energy production in the ischemic heart when the lack of oxygen induces a shift to anaerobic metabolism with subsequent stimulation of glucose uptake. There is evidence from animal studies that stimulation of carbohydrate oxidation with simultaneous inhibition of fatty acid oxidation can improve the heart function (Stanley *et al.*, 2004). In hearts of *cPhd2*^{-/-} and *Hif-1α*^{tg} mice genes regulating glycolysis are significantly up-regulated (*e.g.* Glut1, Pfk1) which goes along with higher rates of glucose uptake and lower fatty acid uptake as determined by PET analysis (Hölscher *et al.*, 2012, fig. 3; chapter 4.1, fig. 2). In addition to the changes in capillary structure, this change in metabolism most likely also contributes to the cardioprotective effect after myocardial infarction. The hearts of these mice are likely pre-conditioned to resist ischemic conditions.

Furthermore, the calcium handling of cells is a critical component for proper heart function. Despite the decrease of SERCA2a in hearts of *Hif-1α*^{tg} mice we observed changes in calcium handling with increased intracellular Ca²⁺-transients and a faster Ca²⁺-decline. This leads to the assumption that the down-regulation of SERCA2a might be counter-regulated by the observed increased PLB-phosphorylation (Hölscher *et al.*, 2012, fig. 4).

Taken together the changes in metabolism, apoptosis, calcium handling and capillary area in *cPhd2*^{-/-} and *Hif-1α*^{tg} mice can be interpreted as improved oxygen supply and energy saving mechanisms which protects the heart in case of an acute ischemic insult.

5.2 Detrimental effects of PHD2 knock-out, respectively HIF stabilization

An important parameter for the application of potential PHD inhibitory drugs in order to treat ischemic diseases will be the duration of the treatment. As shown in this thesis develop *Hif-1α*^{tg} (Hölscher *et al.*, 2012, fig. 5) as well as *cPhd2*^{-/-} mice (Chapter 4.1, fig. 1) a cardiac hypertrophy with aging which goes along with non-lethal heart failure up to the age of eight months.

Cardiac hypertrophy is a thickening of the heart muscle which results in decreased size of the chamber of the heart, including the left and right ventricle. Hypertrophy can occur pathologically in response to diverse stimuli including hypertension, valve disease, myocardial infarction and genetic mutations, or it can occur physiological in response to regular physical activity or chronic exercise training (McMullen and Jennings, 2007). While

5. Discussion

the remodeling of the heart during developing pathological hypertrophy is irreversible it is fully reversible in the setting of physiological hypertrophy (Mihl *et al.*, 2008).

Pathologic cardiac hypertrophy is associated with an increased risk of angina, heart attack or even heart failure. In a mouse model, pathological cardiac hypertrophy can be triggered by *transverse aortic constriction*. Consequences of this hypertrophy can be a dilatation of the ventricle which finally leads to heart failure. A developing mismatch between the number of capillaries and the size of cardiomyocytes which leads to myocardial hypoxia goes along with cardiac hypertrophy. The impact of HIF-1 on cardiac hypertrophy is discussed controversially in the literature. Several studies revealed a critical involvement of HIF-1 in the regulation of cardiac hypertrophy and cardiac function occurring in response to an elevated workload. Silter *et al.* (2009) could show that HIF-1 α ^{+/-} mice developed severe heart failure after TAC as revealed by a significantly reduced fractional shortening whereas HIF-1 α ^{+/+} mice did not. The extent of cardiac hypertrophy on the contrary was similar in both genotypes. As the calcium handling of cardiomyocytes is critically important for heart function it was analyzed in the mice. On the single cell level, cells from HIF^{+/-} mice showed reduced myocyte shortening, decreased intracellular Ca²⁺-transients and SR-Ca²⁺ content in myocytes in comparison to HIF^{+/+} mice.

Huang *et al.* (2004) demonstrated a mild hypertrophy with increased wall thickness and heart to body weight ratio in resting constitutive cardiac-specific Hif-1 α knock-out mice despite of cardiac hypovascularization.

Bekeredjian *et al.* (2010) showed that mice carrying an oxygen-stable, inducible HIF-1 α (tet-off system) show an increased heart to body weight ratio after removal of doxycycline. Most interestingly this effect was fully reversible by restoring doxycycline to the drinking water and thus, restoring low HIF-1 α protein levels so that the heart to body weight ratio gradually decreased back to basal level.

The definite reasons for the induction of cardiomyopathy by HIF-1 remain still unclear. But it is very likely that it is a multifactorial process. The HIF-mediated metabolic switch to glycolysis can drive the detrimental outcome of long-term HIF-1 α stabilization. Taegtmeyer *et al.* (1988) described that an adaptive metabolic switching from fatty acid to glucose metabolism can precede the development of hypertrophy (Taegtmeyer *et al.*, 1988). The observed glycolytic switch in *cPhd2*^{-/-} and *Hif-1 α* ^{tg} mice might therefore drive the observed cardiac hypertrophy observed in aging mice.

5. Discussion

After triggering cardiac hypertrophy by TAC surgery *cPhd2*^{-/-} mice did not react differently than *wt* littermates (Hölscher *et al.*, 2011, fig. 7), while *Hif-1α*^{tg} mice showed severe signs of a dilated cardiomyopathy (Hölscher *et al.*, 2012, fig. 5). The different results of *cPhd2*^{-/-} and *Hif-1α*^{tg} to the pressure induced overload suggest that the severity of cardiomyopathy might be determined by the level of HIF-1α stabilization.

These findings indicate that HIF-1 is indeed critically involved in the adaptation towards an increased mechanical load. In contrast to an acute ischemic insult, where HIF-mediated changes seem beneficial to withstand this situation, HIF-1α stabilization seems to be inadequate in order to treat diseases related to elevated load.

In summary we can conclude that HIF-mediated changes in metabolism, apoptosis, calcium handling and capillary area are beneficial to withstand acute ischemia but that long-term stabilization of HIF-1α has detrimental effects which are likely to be caused by various factors that have to be further elucidated. Thereby it seems that the severity of cardiomyopathy is determined by the level of HIF-1α stabilization.

However, it remains possible that the threshold of HIF activity required for therapeutic effects (e.g. attenuation of outcome of myocardial infarction; red blood cell production in severe anemia) is lower than the threshold required for deleterious effects.

5.3 *cPhd2/3*^{-/-} mice

Using the *cPhd2*^{-/-} mice we showed that PHD3 is significantly up-regulated as a consequence of a PHD2 knock-out (Hölscher *et al.*, 2011, fig. 1). As PHD2 and PHD3 have partially redundant functions it is likely that the effects seen by the PHD2 knock-out are attenuated by the regulatory feedback up-regulation of PHD3. Subsequently we created cardiomyocyte-specific PHD2/PHD3 double knock-out mice (*cPhd2/3*^{-/-}) in order to see if the changes in e.g. metabolism and cardioprotection are more profound. *cPhd2/3*^{-/-} mice were expected to have high levels of HIF-1α protein as HIF-1α does not get hydroxylated by PHD2 and PHD3 in these mice. Surprisingly these mice do only show modestly elevated HIF-1α protein levels that do not exceed those of *Hif-1α*^{tg} mice. The HIF-1α mRNA levels are even diminished (chapter 4.2, fig. 1). Therefore, it is somewhat unlikely that the slightly elevated HIF-1α protein levels are the main reason for the cardiomyopathy and the premature death of the knock-out mice. In further studies cardiomyocyte-specific PHD2/PHD3/HIF-1α triple knock-out mice will be studied to determine the contribution of HIF-1α to this phenotype.

5. Discussion

Besides HIF-1 α the PHDs can also hydroxylate other substrates. A recently published paper (Yan *et al.*, 2011) showed an activation of 5'adenosine-monophosphate-activated protein kinase (AMPK) by activation of the prolyl-hydroxylase oxygen-sensing signal cascade through inhibition of the PHDs by PHD2-RNAi or dimethyloxaloylglycine (DMOG), a cell-permeable 2-OG (2-oxoglutarate) analog that is expected to act as a competitive inhibitor against all 2-OG-dependent dioxygenases, in cardiomyocytes. AMPK plays an important role in cellular energy homeostasis; it can increase cellular energy levels by inhibiting anabolic energy consuming pathways (e.g. fatty acid synthesis) and stimulate energy producing, catabolic pathways (e.g. glucose transport).

One might speculate that AMPK might be activated in cardiomyocytes of *cPhd2/3*^{-/-} mice. In the cardiac hypertrophy associated with glycogen overload, both activating and inactivating mutations of AMPK in mice are associated with a marked cardiac hypertrophy (Dyck and Lopaschuk, 2006). Therefore it is tempting to speculate that besides HIF-1 α AMPK contributes to the observed phenotype in *cPhd2/3*^{-/-} mice. However it is likely that there will be a multitude of other factors that have to be determined in order to fully understand the molecular basis for the detrimental outcome of the double knock-out of PHD2 and PHD3 in cardiomyocytes of mice.

5.4 PHD inhibitors as a therapeutic approach in acute myocardial infarction

Patients with myocardial infarction (MI) are treated with stents or fibrolytic therapy to enable tissue reperfusion (Andersen *et al.*, 2003). Patients that have survived an MI are still endangered to suffer from heart failure as their hearts are scarred and became enlarged as the heart tries to compensate for the insufficient pump function.

So far no therapy has been developed that directly aims to protect the heart muscle during the ischemic infarct. While the condition of the cells in the main area of the infarct region is not improvable it is of great interest to improve the situation for the cells in the hypoxic region surrounding the infarct area.

Since the discovery of HIF and the PHDs the HIF pathway has been exploited for therapeutic purposes. The use of PHD inhibitors is a promising new therapeutic option in treating diseases like myocardial infarction but also stroke, renal or liver injury or severe anemia.

Earlier it was shown by Natarajan *et al.* (2006) that normoxic activation of HIF-1 in the heart by PHD2 siRNA administration attenuates reperfusion injury via an iNOS-dependent

5. Discussion

pathway. Since then, two novel orally active HIF-PHD inhibitors, GSK360A (Toronto Research Chemicals) and FG2216 (Fibrogen), were developed and are now being tested.

In a rat model of LAD ligation it has been shown that chronic treatment with GSK360A for 28 days prevented the progressive reduction in ejection fraction (Bao *et al.*, 2010). In a different study (Philipp *et al.*, 2006) it could be shown that treatment with FG2216 induces a significantly reduced heart and lung weight, improved left ventricular contractility and left ventricular ejection fraction without affecting infarct size in rats 30 days after myocardial infarction.

Despite these promising results further studies need to be conducted in order to determine the long-term consequences of these inhibitors. So far the effects of chronic PHD inhibition are largely unknown and existing data are only obtained from genetically modified knock-out mice. Furthermore the up to now available PHD inhibitors are not suitable to test PHD isoform-specific effects. Based on our results of the detrimental outcome of a cardiomyocyte-specific PHD2/PHD3 double knock-out mouse it seems indispensable to develop PHD inhibitors that inhibit specifically one isoform.

In rat heart-derived H9c2 cells PHD3 silencing substantially ameliorates doxorubicin-induced apoptosis, whereas PHD1 or PHD2 knockdown did not significantly influence apoptosis. Thus, PHD3 is likely to be cardioprotective by reducing apoptosis in some heart disorders (Liu *et al.*, 2010). Therefore it would be interesting to design a PHD3 specific inhibitor to determine if the apoptosis can be limited after an ischemic infarct.

Furthermore it would be interesting to design a PHD1 specific inhibitor as PHD1 knock-out mice show significant protection in a myocardial ischemia/reperfusion model (Adluri *et al.*, 2011). But in contrast to cardiomyocyte-specific PHD2 knock-out mice which develop cardiomyopathy over time in the here presented study do PHD1 knockout mice survive without any cardiac defects until adulthood (Takeda *et al.*, 2007). The reason for this difference might be that PHD1 loss induces HIF-1 α to a lesser extent than the loss of PHD2, so that there might be sufficient HIF to provide protection from ischemia but without activating other detrimental pathways.

Besides treatment of myocardial infarction PHD inhibitors are currently being tested for the treatment of anemia. Whereas treatment for tissue protection is based on short term application the treatment of anemia is designed to be a chronic treatment. Furthermore in tissue protection the treatment is based on the diversity of HIF target genes and their

5. Discussion

potential to protect cells against consequences of hypoxia whereas in anemia treatment is based on a single target gene, erythropoietin. Phase 2 clinical trials in patients with chronic kidney disease are currently under way, studying the effect of oral PHD inhibitors as potential substitutes to EPO injection (Fibrogen, Press release 17.03.2011: Fibrogen announces initiation of phase 2B studies of FG-4592, an oral HIF proly hydroxylase inhibitor, for treatment of anemia in chronic kidney disease).

As the long-term stabilization of HIF-1 α seems to have detrimental long-term effects (Hölscher *et al.*, 2012; Bekeredjian *et al.*, 2010) PHD inhibitors will have to be carefully titrated to achieve beneficial effects without doing more harm than good.

5.5 Summary and Outlook

In this thesis several mouse models with different levels of HIF-1 α protein stabilization in cardiomyocytes were analyzed. It could be shown that HIF-1 α stabilization has a beneficial outcome in the setting of acute myocardial infarction. *cPhd2*^{-/-} and *Hif-1 α* ^{tg} mice have a smaller area at risk six hours after the ligation of the *left anterior descending artery* and a better preserved heart function three, respectively four weeks after surgery (Hölscher *et al.*, 2011; Kido *et al.*, 2005). Likely due to the stabilization of HIF-1 α the vascular tone, cardiac metabolism, and the calcium handling of the cells are changed. The metabolism of *cPhd2*^{-/-} and *Hif-1 α* ^{tg} mice is shifted towards glycolysis with a net increase in glucose uptake. Furthermore the calcium handling of isolated cardiomyocytes is, at least in *Hif-1 α* ^{tg} mice, changed, leading to increased intracellular Ca²⁺-transients when stimulated at 0.5-4Hz. Although being beneficial in the setting of acute myocardial infarction, these changes lead in the long term to hypertrophy that goes along with heart failure. Still unclear is, however, if hypoxia is reason for or outcome of cardiac hypertrophy. To analyze if in a developing hypertrophy hypoxia leads to hypertrophy or if hypertrophy subsequently leads to hypoxia mice carrying the oxygen-dependent degradation domain in fusion with the *firefly luciferase* will be analyzed (Safran *et al.*, 2005) in further studies. This fusion protein makes it possible to determine the bioluminescence which correlates with the stabilization of HIF-1 α . In ODD-luciferase mice the luciferase is continuously transcribed and translated in all cells, but is also rapidly degraded under normoxic conditions. Only in hypoxia does luciferase accumulate and, thus, by providing the substrate luciferin, regions of hypoxia within these

5. Discussion

mice may be imaged. With the help of this mouse model the question what comes first- hypertrophy or hypoxia- can hopefully be answered.

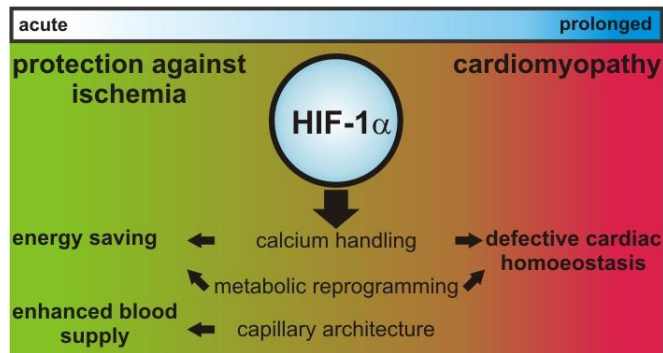
In the future it will be worthwhile to look deeper into the consequences of cardiomyocyte-specific HIF-1 α up-regulation. It will be interesting to know if the mitochondrial function is affected, and if so, if this leads to an improved or an impaired cellular respiration. Furthermore, it will be interesting to develop fibroblast-specific PHD2 knock-out mice to elaborate the differences and the similarities between cardiomyocyte- and fibroblast-specific PHD2 knock-out mice.

In this thesis the first unpublished results of cardiomyocyte-specific PHD2/PHD3 knock-out mice were described. These mice show a significant down-regulation of PHD2 and PHD3. Unexpectedly, these mice do not show excessively elevated HIF-1 α levels but instead they show a significant down-regulation of HIF-1 α mRNA and only a modest stabilization of HIF-1 α protein levels. *cPhd2/3*^{-/-} mice develop a dilated cardiomyopathy already at a young age that finally leads to premature death. The main cause for this phenotype has to be further elucidated. Besides the HIF-1 α stabilization HIF-independent but PHD-dependent pathways are likely to be involved.

In summary, we could show that cardiomyocyte-specific HIF-1 α stabilization, mediated by a knock-out of PHD2, protects against acute myocardial infarction. Via the stabilization of HIF-1 α HIF target genes are transcriptional activated and thereby the calcium handling, the cell metabolism and the capillary structure are altered. These changes seem to cause cardiac hypertrophy over time.

In figure 3 a schematic overview demonstrating possible mechanisms involved in beneficial and detrimental effects of cardiac-specific HIF-1 α up-regulation are shown.

5. Discussion



Hölscher et al., 2012

Fig.3 Schematical illustration of possible mechanisms that are involved in beneficial and detrimental effects of cardiac-specific HIF-1 α up-regulation.

Recapitulatory, it can be concluded from the here presented data that the HIF-mediated changes in metabolism, apoptosis, calcium handling and capillary area are on the one hand beneficial to withstand acute ischemia but are on the other hand, however, indicative for defective cardiac homeostasis in the failing heart. This has to be considered when designing PHD inhibiting drugs in the nearby future.

6. References

6. References

- Adluri RS, Thirunavukkarasu M, Dunna NR, Zhan L, Oriowo B, Takeda K, Sanchez JA, Otani H, Maulik G, Fong GH, Maulik N (2011). Disruption of Hypoxia-Inducible Transcription Factor-Prolyl Hydroxylase Domain-1 (PHD-1^{-/-}) Attenuates *Ex Vivo* Myocardial Ischemia/Reperfusion Injury Through Hypoxia-Inducible Factor-1 α Transcription Factor and Its Target Genes in Mice. *Antioxidants & Redox Signaling* 15:1789-1797
- Andersen HR, Nielsen TT, Rasmussen K, Thuesen L, Kelbaek H, Thayssen P, Abildgaard U, Pedersen F, Madsen JK, Grande P, Villadsen AB, Krusell LR, Haghfelt T, Lomholt P, Husted SE, Vigholt E, Kjaergard HK, Mortensen LS (2003). A Comparison of Coronary Angioplasty with Fibrinolytic Therapy in Acute Myocardial Infarction *N Engl J Med* 349:733-742
- Appelhoff RJ, Tian YM, Raval RR, Turley H, Harris AL, Pugh CW, Ratcliffe PJ, Gleadle JM (2004). Differential Function of the Prolyl Hydroxylases PHD1, PHD2, and PHD3 in the Regulation of Hypoxia-inducible Factor. *J Biol Chem.* 279:38458-38465
- Asikainen TM and White CW (2007). HIF stabilizing agents: shotgun or scalpel? *Am J Physiol Lung Cell Mol Physiol.* 293:555-556
- Bekeredjian R, Walton CB, MacCannell KA, Ecker J, Kruse F, Outten JT, Sutcliffe D, Gerard RD, Bruick RK, Shoheit RV (2010). Conditional HIF-1 α Expression Produces a Reversible Cardiomyopathy. *PLoS ONE* 5(7):e11693
- Benita Y, Kikuchi H, Smith AD, Zhang MQ, Chung DC, Xavier RJ (2009). An integrative genomics approach identifies Hypoxia Inducible Factor-1 (HIF-1)-target genes that form the core response to hypoxia. *Nucleic Acids Research* 37:4587-4602
- Berra E, Benizri E, Ginouves A, Volmat V, Roux D, and Pouyssegur J (2003) HIF prolyl-hydroxylase 2 is the key oxygen sensor setting low steady-state levels of HIF-1 α in normoxia. *EMBO* 22:4082-4090
- Bohl S, Medway DJ, Schulz-Menger J, Schneider JE, Neubauer S, Lygate C (2009). Refined approach for quantification of in vivo ischemia-reperfusion injury in the mouse heart. *Am J Physiol Heart Circ Physiol* 297:H2054-2058.
- Bruick RK and McKnight SLA (2001). Conserved Family of Prolyl-4-Hydroxylases That Modify HIF. *Science* 294:1337-1340
- Cai Z, Manalo DJ, Wei G, Rodriguez ER, Fox-Talbot K, Lu H, Zweier JL, Semenza GL (2003). Hearts from rodents exposed to intermittent hypoxia or erythropoietin are protected against ischemia-reperfusion injury. *Circulation* 108:79-85
- Chamboredon S, Ciais D, Desroches-Castan A, Savid P, Bonod F, Feige JJ, Cherradia N (2011). Hypoxia-inducible factor-1 α mRNA: a new target for destabilization by tristetraprolin in endothelial cells. *Mol Biol Cell* 18:3366-78

6. References

- Chan DA, Kawahara TLA, Sutphin PD, Chang HY, Chi JT, Giaccia AJ (2009). Tumor Vasculature Is Regulated by PHD2-Mediated Angiogenesis and Bone Marrow-Derived Cell Recruitment. *Cancer Cell* 15:527-538
- Compernelle V, Brusselmans K, Acker T, Hoet P, Tjwa M, Beck H, Plaisance S, Dor Y, Keshet E, Lupu F, Nemery B, Dewerchin M, Van Veldhoven P, Plate K, Moons L, Collen D, Carmeliet P (2002). Loss of HIF-2 α and inhibition of VEGF impair fetal lung maturation, whereas treatment with VEGF prevents fatal respiratory distress in premature mice. *Nat Med* 8:1329.
- Cummins EP, Berra E, Comerford KM, Ginouves A, Fitzgerald KT, Seeballuck F, Godson C, Nielsen JE, Moynagh P, Pouyssegur J, Taylor CT (2006). Prolyl hydroxylase-1 negatively regulates I κ B kinase- β , giving insight into hypoxia-induced NF κ B activity. *Proc Natl Acad Sci U S A*. 103:18154-18159
- Date T, Mochizuki S, Belanger AJ, Yamakawa M, Luo Z, Vincent KA, Cheng SH, Gregory RJ, Jiang C (2005). Expression of constitutively stable hybrid hypoxia-inducible factor-1 α protects cultured rat cardiomyocytes against simulated ischemia-reperfusion injury. *Am J Physiol Cell Physiol* 288:C314-C320
- Dyck JRB and Lopaschuk GD (2006). AMPK alterations in cardiac physiology and pathology: enemy or ally? *J Physiol* 574:95-112
- Ema M, Taya S, Yokotani N, Sogawa K, Matsuda Y, Fujii-Kuriyama Y (1997). A novel bHLH-PAS factor with close sequence similarity to hypoxia-inducible factor 1 α regulates the VEGF expression and is potentially involved in lung and vascular development. *Proc Natl Acad Sci USA* 94:4273–4278
- Erbel PJA, Card PB, Karakuzu O, Bruick RK, and Gardner KH (2003). Structural basis for PAS domain heterodimerization in the basic helix–loop–helix-PAS transcription factor hypoxia-inducible factor. *PNAS* 100:15504-15509
- Epstein ACR, Gleadle JM, McNeill LA, Hewitson KS, O'Rourke J, Mole DV, Mukherji M, Metzen E, Wilson MI, Dhanda A, Tian YM, Masson N, Hamilton DL, Jaakkola P, Barstead R, Hodgkin J, Maxwell PH, Pugh CW, Schofield J, Ratcliffe PJ (2011). *C. elegans* EGL-9 and Mammalian Homologs Define a Family of Dioxygenases that Regulate HIF by Prolyl Hydroxylation. *Cell* 107:43-54
- Fibrogen press release (2011). FibroGen Announces Initiation of Phase 2b Studies of FG-4592, an Oral HIF Prolyl Hydroxylase Inhibitor, for Treatment of Anemia in Chronic Kidney Disease
- Flamme I, Frohlich T, von Reutern M, Kappel A, Damert A, and Risau W (1997). HRF, a putative basic helix-loop-helix-PAS-domain transcription factor is closely related to hypoxia-inducible factor-1 α and developmentally expressed in blood vessels. *Mech Dev* 63:51-60
- Goldberg MA, Dunning SP and Bunn HF (1988). Regulation of the erythropoietin gene: evidence that the oxygen sensor is a heme protein. *Science* 242:1412-1415

6. References

- Gu YZ, Moran SM, Hogenesch JB, Wartman L, Bradfield CA (1998). Molecular characterization and chromosomal localization of a third alpha-class hypoxia inducible factor subunit, HIF3alpha. *Gene Expr* 7:205-213
- Hackett PH and Roach RC (2001). High-altitude illness. *N Engl J Med.* 345:107-114
- Hara S, Hamada J, Kobayashi C, Kondo Y, Imura N (2001). Expression and Characterization of Hypoxia-Inducible Factor (HIF)-3 α in Human Kidney: Suppression of HIF-Mediated Gene Expression by HIF-3 α . *Biochem Biophys Res Commun* 287:808–813
- Hirsilä M, Koivunen P, Günzler V, Kivirikko KI, Myllyharju J (2003). Characterization of the Human Prolyl 4-Hydroxylases That Modify the Hypoxia-inducible Factor. *J Biol Chem* 278:30772-30780.
- Hogenesch JB, Chan WK, Jackiw VH, Brown RC, Gu YZ, Pray-Grant M, Perdeu GH, Bradfield CA (1997). Characterization of a subset of the basic-helix-loop-helix-PAS superfamily that interacts with components of the dioxin signaling pathway. *J Biol Chem* 272:8581-8593
- Hölscher M, Schäfer K, Krull S, Farhat K, Hesse A, Silter M, Lin Y, Pichler BJ, Thistlethwaite P, El-Armouche A, Maier LS, Katschinski DM, Anke Zieseniss A (2012). Unfavourable consequences of chronic cardiac HIF-1 α stabilization. *Cardiovasc Res.* 94:77-86
- Hölscher M, Silter M, Krull S, von Ahlen M, Hesse A, Schwartz P, Wielockx B, Breier G, Katschinski DM, Anke Zieseniss (2011). Cardiomyocyte-specific Prolyl-4-hydroxylase Domain 2 Knock Out Protects from Acute Myocardial Ischemic Injury. *J Biol Chem* 286:11185-11194
- Hu CJ, Wang LY, Chodosh LA, Keith B, Simon MC (2003). Differential Roles of Hypoxia-Inducible Factor 1 α (HIF-1 α) and HIF-2 α in Hypoxic Gene Regulation. *Mol Cell Biol* 23:9361-9374
- Iyer NV, Kotch LE, Agani F, Leung SW, Laughner E, Wenger RH, Gassmann M, Gearhart JD, Lawler AM, Yu AY, Semenza GL (1998). Cellular and developmental control of O₂ homeostasis by hypoxia-inducible factor 1 α . *Genes Dev* 12:149-162
- Kido M, Du L, Sullivan CC, Li X, Deutsch R, Jamieson SW, Thistlethwaite PA (2005). Hypoxia-inducible factor 1 α reduces infarction and attenuates progression of cardiac dysfunction after myocardial infarction in the mouse. *J Am Coll Cardiol* 46:2116-2124
- Koivunen P, Tiainen P, Hyvärinen J, Williams KE, Sormunen R, Klaus SJ, Kivirikko KI, and Myllyharju J (2007). An Endoplasmic Reticulum Transmembrane Prolyl 4-Hydroxylase Is Induced by Hypoxia and Acts on Hypoxia-inducible Factor α . *J Biol Chem* 282:30544-30552
- Laufs U, Maack C Und Böhm M (2008). Signaltransduktion bei adaptiven und maladaptiven kardialen Remodeling-Prozessen. *Magazin Forschung* 1/2008
- Lieb ME, Menzies K, Moschella MC, Ni R, Taubman MB (2002) Mammalian *EGLN* genes have distinct patterns of mRNA expression and regulation. *Biochem Cell Biol* 80:421-426

6. References

- Liu Y, Huo Z, Yan B, Lin X, Zhou ZN, Liang X, Zhu W, Liang D, Li L, Liu Y, Zhao H, Sun Y, Chen YH (2010). Prolyl hydroxylase 3 interacts with Bcl-2 to regulate doxorubicin-induced apoptosis in H9c2 cells. *Biochem Biophys Res Commun* 401:231-237
- Loenarz C, Coleman ML, Boleininger A, Schierwater B, Holland PW, Ratcliffe PJ, Schofield CJ (2011). The hypoxia-inducible transcription factor pathway regulates oxygen sensing in the simplest animal, *Trichoplax adhaerens*. *EMBO Rep* 12:63-70
- Lopaschuk GD, Ussher JR, Folmes CDL, Jaswal JS, Stanley WC (2010). Myocardial Fatty Acid Metabolism in Health and Disease. *Physiol Rev* 90:207-258
- Mahon PC, Hirota K, and Semenza GL (2001). FIH-1: a novel protein that interacts with HIF-1 α and VHL to mediate repression of HIF-1 transcriptional activity. *Genes & Dev* 15:2675-2686
- Maron BJ (2006). The 2006 American Heart Association Classification of Cardiomyopathies Is the GoldStandard. *Circ Heart Fail* 1:72-76
- Maxwell PH, Wiesener MS, Chang GW, Clifford SC, Vaux EC, Cockman ME, Wykoff CC, Pugh CW, Maher ER, Ratcliffe PJ (199). The tumour suppressor protein VHL targets hypoxia-inducible factors for oxygen-dependent proteolysis. *Nature* 399:271-275
- McDonough MA, Li V, Flashman E, Chowdhury R, Mohr C, Liénard BMR, Zondlo J, Oldham NJ, Clifton IJ, Lewis J, McNeill LA, Kurzeja RJM, Hewitson KS, Yang E, Jordan S, Syed RS, Schofield CJ (2006). Cellular oxygen sensing: Crystal structure of hypoxia-inducible factor prolyl hydroxylase (PHD2). *PNAS* 103: 9814-9819
- McMullen JR and Jennings GL (2007). Differences between pathological and physiological cardiac hypertrophy: novel therapeutic strategies to treat heart failure. *Clin Exp Pharmacol Physiol* 34:255–262
- Metzen E, Berchner-Pfannschmidt U, Stengel P, Marxsen JH, Stolze I, Klinger M, Qi Huang W, Wotzlaw C, Hellwig-Bürgel T, Jelkmann W, Acker H, Fandrey J (2003). Intracellular localisation of human HIF-1 α hydroxylases: implications for oxygen sensing. *J Cell Sci* 116:1319-26.
- Metzen E, Stiehl DP, Doege K, Marxsen JH, Hellwig-Bürgel T, Jelkmann W (2005). Regulation of the Prolyl Hydroxylase Domain Protein 2 (phd2/egln-1) gene: Identification of a functional hypoxia-responsive element. *Biochem J* 387:711-717
- Mihl C, Dassen WRM, Kuipers H (2008). Cardiac remodelling: concentric versus eccentric hypertrophy in strength and endurance athletes. *Neth Heart J* 16:129-133.
- Minamishima YA, Moslehi J, Bardeesy N, Cullen D, Bronson RT, Kaelin WG Jr (2008). Somatic inactivation of the PHD2 prolyl hydroxylase causes polycythemia and congestive heart failure. *Blood* 111:3236-44

6. References

- Natarajan R, Salloum FN, Fisher BJ, Kukreja RC, Fowler AA (2006). HIF-1 activation by prolyl 4-hydroxylase-2 gene silencing attenuates myocardial ischemia-reperfusion injury. *Circ Res* 98:133-140.
- Oehme F, Ellinghaus P, Kolkhof P, Smith TJ, Ramakrishnan S, Hütter J, Schramm M, Flamme I (2002). Overexpression of PH-4, a novel putative proline 4-hydroxylase, modulates activity of hypoxia-inducible transcription factors. *Biochem Biophys Res Commun* 296:343-349
- Ortiz-Barahona A, Villar D, Pescador N, Amigo J, del Peso L (2010). Genome-wide identification of hypoxia-inducible factor binding sites and target genes by a probabilistic model integrating transcription-profiling data and in silico binding site prediction. *Nuc Acids Res* 38:2332-2345
- Paralikaar SJ and Paralikaar JH (2010). High-altitude medicine. *JH Indian J Occup Environ Med* 14:6-12
- Pescador N, Cuevas Y, Naranjo S, Alcaide M, Villar D, Land'Azuri MO, del Peso L (2005). Identification of a functional hypoxia-responsive element that regulates the expression of the egl nine homologue 3 (egl3/phd3) gene. *Biochem J* 390:189-197
- Philipp S, Jürgensen JS, Fielitz J, Bernhardt WM, Weidemann A, Schiche A, Bernhard Pilz b, Dietz R, Regitz-Zagrosek V, Eckardt KU, Willenbrock R (2006). Stabilization of hypoxia inducible factor rather than modulation of collagen metabolism improves cardiac function after acute myocardial infarction in rats. *Eur J Heart Fail* 8:347-354
- Reyes H, Reisz-Porszasz S, Hankinson O (1992). Identification of the Ah receptor nuclear translocator protein (Arnt) as a component of the DNA binding form of the Ah receptor. *Science* 256:1193-5.
- Semenza GL. (1998). Hypoxia-inducible factor 1: master regulator of O₂ homeostasis. *Curr Opin Genet Dev* 8:588-594
- Sharp FR and Bernaudin M (2004). HIF1 and Oxygen Sensing in the Brain. *Nat Rev Neurosci*. 5:437-48.
- Siliter M, Kögler H, Zieseniss A, Wilting J, Schafer K, Toischer K, Rokita AG, Breves G, Maier LS, Katschinski DM (2010). Impaired Ca²⁺-handling in HIF-1 $\alpha^{+/-}$ mice as a consequence of pressure overload. *Pflugers Arch* 459:569-577.
- Patten RD, Aronovitz MJ, Deras-Mejia L, Pandian NG, Hanak GG, Smith JJ, Mendelsohn ME, Kosntam MA (1998). Ventricular remodeling in a mouse model of myocardial infarction. *Am J Phys* 274:H1812-1820.
- Safran M, Kim WY, O'Connell F, Flippin L, GünzlerV, Horner JW, DePinho RA, Kaelin, Jr. WG (2006). Mouse model for noninvasive imaging of HIF prolyl hydroxylase activity: Assessment of an oral agent that stimulates erythropoietin production. *PNAS* 103:105-110

6. References

- Sano M, Minamino T, Toko H, Miyauchi H, Orimo M, Qin Y, Akazawa H, Tateno K, Kayama Y, Harada M, Shimizu I, Asahara T, Hamada H, Tomita S, Molckentin JD, Zou Y, Komuro I (2007). p53-induced inhibition of Hif-1 causes cardiac dysfunction during pressure overload. *Nature* 446:444-448
- Stanley WC, Recchia FA, Lopaschuk GD (2005). Myocardial Substrate Metabolism in the Normal and Failing Heart. *Physiol Rev* 85:1093-1129
- Taegtmeyer H and Overturn ML (1988). Effects of moderate hypertension on cardiac function and metabolism in the rabbit. *Hypertension* 11:416-26
- Takeda K, Cowan A, Fong GH (2007). Essential Role for Prolyl Hydroxylase Domain Protein 2 in Oxygen Homeostasis of the Adult Vascular System. *Circulation* 116:774-781
- Takeda K, Ho VC, Takeda H, Duan LJ, Nagy A, Fong GH (2006). Placental but Not Heart Defects Are Associated with Elevated Hypoxia-Inducible Factor α Levels in Mice Lacking Prolyl Hydroxylase Domain Protein 2. *Mol Cell Biol* 26:8336-8346
- Tekin S, Dursun D, Xi L (2010). Hypoxia inducible factor 1 (HIF-1) and cardioprotection. *Acta Pharm Sinic* 31: 1085-1094
- Tian H, Hammer RE, Matsumoto AM, Russell DW, McKnight SL (1998). The hypoxia-responsive transcription factor EPAS1 is essential for catecholamine homeostasis and protection against heart failure during embryonic development. *Genes Dev* 12:3320-3324
- Tian H, McKnight SL, Russell DW (1997). Endothelial PAS domain protein 1 (EPAS1), a transcription factor selectively expressed in endothelial cells. *Genes Dev* 11:72-82
- Tian J, Yan Z, Wu Y, Zhang SL, Wang K, Ma XR, Guo L, Wang J, Zuo L, Liu JY, Quan L, Liu HR (2010). Inhibition of iNOS protects endothelial-dependent vasodilation in aged rats. *Acta Pharm Sinic* 31:1324-1328
- Toischer K, Rokita AG, Unsöld B, Zhu W, MD, Kararigas G, Sossalla S, Reuter SP, Becker A, Teucher N, Seidler T, Grebe C, Preuß L, Gupta SN, Schmidt K, Lehnart SE, Krüger M, Linke WA, Backs J, Regitz-Zagrosek V, Schäfer K, Field LJ, Maier LS, Hasenfuss G (2010). Differential Cardiac Remodeling in Preload Versus Afterload. *Circulation* 122: 993-1003
- Warnecke C, Griethe W, Weidemann A, Jürgensen JS, Willam C, Bachmann S, Ivashchenko Y, Wagner I, Frei U, Wiesener M, Eckardt KU (2003). Activation of the hypoxia-inducible factor-pathway and stimulation of angiogenesis by application of prolyl hydroxylase inhibitors. *Faseb J* 17:1186-8.
- Yan L, Colandrea VJ, Hale JJ (2010). Prolyl hydroxylase domain-containing protein inhibitors as stabilizers of hypoxia-inducible factor: small molecule-based therapeutics for anemia. *Expert Opin Ther Pat* 20:1219-1245

6. References

Yan H, Zhang DX, Shi X, Zhang Q, Huang YS (2011). Activation of the Prolyl-hydroxylase oxygen-sensing signal cascade leads to AMPK activation in cardiomyocytes. *J Cell Mol Med* doi: 10.1111/j.1582-4934.2011.01500.x

Zhang H, Bosch-Marce M, Shimoda LA, Tan YS, Baek JH, Wesley JB, Gonzalez FJ, and Gregg L. Semenza GL (2008). Mitochondrial Autophagy Is an HIF-1-dependent Adaptive Metabolic Response to Hypoxia. *J Biol Chem* 283:10892-10903

Acknowledgments

DANKE sagen möchte ich an dieser Stelle...

... allen, die zum Gelingen dieser Arbeit beigetragen haben.

... Frau Prof. Dr. Dörthe M. Katschinski, die mir die Möglichkeit gab an diesem spannenden Thema zu arbeiten und mich mit vielen fachlichen Ratschlägen unterstützt hat. Zudem gab sie mir die Möglichkeit, meine Forschungsergebnisse auf mehreren nationalen und internationalen Tagungen präsentieren zu können.

... Dr. Anke Zieseniß. Danke für die tolle Betreuung und die wertvollen Tipps, die zum guten Gelingen dieser Arbeit beigetragen haben.

... Frau Prof. Dr. F. Alves und Frau Prof. Dr. S. Pöggeler für die freundliche Übernahme des Referates und Koreferates dieser Arbeit und ihre stets wertvollen Anregungen bei meinen Thesis Committees.

... Frau Prof. Dr. B. Schwappach, Frau Prof. Dr. Dr. H. Ehrenreich und Herrn Dr. V. Nikolaev für die sofortige Bereitschaft als Prüfer zur Verfügung zu stehen.

...Sabine für etliche qPCRs, Gewebeschnitte, Färbungen, etc...

...Monique, die mich geduldig in die mir bis dahin unbekannte Welt der „Mausarbeit“ eingearbeitet hat.

...Annette für unzählige Genotypisierungen.

...allen aktuellen und ehemaligen Mitarbeitern der AG Katschinski... Katja, Marieke, Sabine, Amke, Anke, Sabine, Melanie, Monique, Pia, Liza, Cordula, Ulrike, Jaco, Moritz und Annette für die tolle Atmosphäre und eure stete Hilfsbereitschaft und wertvollen Tipps. Ohne euch wäre die Laborzeit nur halb so toll gewesen...

... Frau Dr. Sarah Kimmina sowie den Mitarbeitern der Zentralen Tierexperimentellen Einrichtung der UMG für die freundliche Zusammenarbeit.

... allen, die mit mir die ein oder andere Stunde im OP3 zugebracht haben.

... AG Schäfer, insbesondere Frau Prof. Dr. K. Schäfer und Anika für die tolle Kooperation bei den *Hif-1 α ^{tg}* Mäusen.

... AG Maier, insbesondere Felicia, für die Calciummessungen.

... meiner Familie, die mich immer unterstützt hat.

... Sven. Einfach danke für alles...

Curriculum vitae

Name	Marion Hölscher
Date of birth	22.09.1982
Place of birth	Paderborn, Germany
August 1993-July 2002	Pelizaeus Secondary School, Paderborn
July 2002-August 2003	Au pair in Park City, Utah, USA
October 2003-July 2008	Diploma Biology, Justus-Liebig University, Gießen, Germany Thesis title: "Kleine nicht-codierende RNAs in <i>S.meliloti</i> 1021"
June 2009-June 2012	PhD student at the Department of Cardiovascular Physiology, Georg-August University, Göttingen, Germany Thesis title: "Cardiac functions of the cellular oxygen sensors prolyl-4-hydroxylase domain enzymes 2 and 3"

Publications

Björn Voss, **Marion Hölscher**, Birgit Baumgarth, Andreas Kalbfleisch, Ceren Kaya, Wolfgang R. Hess, Anke Becker, Elena Evguenieva-Hackenberg (2009)

Expression of small RNAs in Rhizobiales and protection of a small RNA and its degradation products by Hfq in *Sinorhizobium meliloti*

Biochem Biophys Res Commun 390:331-336

Marion Hölscher, Monique Silter, Sabine Krull, Melanie von Ahlen, Amke Hesse, Peter Schwartz, Ben Wielockx, Georg Breier, Dörthe M. Katschinski, Anke Zieseniss (2011)

Cardiomyocyte-specific Prolyl-4-hydroxylase domain 2 knock out protects from acute myocardial ischaemic injury

J Biol Chem 286:11185-11194

Marion Hölscher, Katrin Schäfer, Sabine Krull, Katja Farhat, Amke Hesse, Monique Silter, Yun Lin, Bernd J. Pichler, Patricia Thistlethwaite, Ali El Armouche, Lars S. Maier, Dörthe M. Katschinski*, Anke Zieseniss* (*both authors contributed equally) (2012)

Unfavourable consequences of chronic cardiac HIF-1 α stabilization

Cardiovasc Res 94:77-86

Conferences

- 18.-19.10.2010 **2nd EUGENEHEART PhD Student Exchange Meeting**
London, England
poster presentation
- 08.-12.01.2011 **Oxygen 2011**
Davos, Switzerland
poster presentation
- 12.-17.02.2012 **Advances in Hypoxic Signaling: From Bench to Bedside**
Banff, Alberta, Canada
poster presentation
- 22.-25.03.2012 **91st Annual Meeting of the Deutsche Physiologische Gesellschaft**
Dresden, Germany
poster presentation (poster prize award)